CRANFIELD UNIVERSITY

Mohamed Ali Elforjani

Condition Monitoring of Slow Speed Rotating Machinery Using Acoustic Emission Technology

SCHOOL OF ENGINEERING

PhD THESIS
Academic Year: 2009 - 2010

Supervisor: Dr. David Mba
June 2010

CRANFIELD UNIVERSITY

SCHOOL OF ENGINEERING

PhD THESIS

Academic Year: 2009 - 2010

Mohamed Ali Elforjani

Condition Monitoring of Slow Speed Rotating Machinery Using Acoustic Emission Technology

Supervisor: Dr. David Mba

June 2010

ABSTRACT

Slow speed rotating machines are the mainstay of several industrial applications worldwide. They can be found in paper and steel mills, rotating biological contractors, wind turbines etc. Operational experience of such machinery has not only revealed the early design problems but has also presented opportunities for further significant improvements in the technology and economics of the machines. Slow speed rotating machinery maintenance, mostly related to bearings, shafts and gearbox problems, represents the cause of extended outages. Rotating machinery components such as gearboxes, shafts and bearings degrade slowly with operating time. Such a slow degradation process can be identified if a robust on-line monitoring and predictive maintenance technology is used to detect impending problems and allow repairs to be scheduled. To keep machines functioning at optimal levels, failure detection of such vital components is important as any mechanical degradation or wear, if is not impeded in time, will often progress to more serious damage affecting the operational performance of the machine. This requires far more costly repairs than simply replacing a part.

Over the last few years there have been many developments in the use of Acoustic Emission (AE) technology and its analysis for monitoring the condition of rotating machinery whilst in operation, particularly on slow speed rotating machinery. Unlike conventional technologies such as thermography, oil analysis, strain measurements and vibration, AE has been introduced due to its increased sensitivity in detecting the earliest stages of loss of mechanical integrity.

This programme of research involves laboratory tests for monitoring slow speed rotating machinery components (shafts and bearings) using AE technology. To implement this objective, two test rigs have been designed to assess the capability of AE as an effective tool for detection of incipient defects within low speed machine components (e.g. shafts and bearings). The focus of the experimental work will be on the initiation and growth of natural defects. Further,

this research work investigates the source characterizations of AE signals associated with such bearings whilst in operation. It is also hoped that at the end of this research program, a reliable on-line monitoring scheme used for slow speed rotating machinery components can be developed.

Keywords: Acoustic Emission, Condition Monitoring, Natural Cracks, Source Characterizations, Slow Speed Rotating Machinery.

DEDICATION

There are not enough words in the world to tell people how much I love my mother Kheria Daw and my father Ali Elforjani, how much I appreciate them, or how much I want to thank them. Without their knowledge, wisdom, and guidance I would not have the goals I have to strive and be the best to reach my dreams. For all the times they have taught me the true meaning of education and for all the sacrifices, my work is dedicated to them.

ACKNOWLEDGEMENTS

My ultimate thanks are to ALLAH almighty that created me and gave me strength and knowledge.

I would deeply like to express my appreciation and gratitude to my supervisor Dr. David Mba for his superb guidelines and the fruitful discussion with him on which this thesis is based.

I also wish a warm thank to my brother Fathi Forjani for his support and assistance in doing this work.

A very special appreciation is due to my wife Eman Elmodham not only for her constant encouragement but also for her patience and understanding throughout my study period. May ALLAH bless her in all her endeavours because without her unreserved support, completion of this study would not have been possible.

I am deeply indebted to all the members of my family; Amna, Ahmed, Rabyah, Ezdeen, Fatma and Salma for their support, prayer, love and encouragement.

Special thanks should be given to the Libyan Government. Without its support and dedication this work would not have been possible.

I would also like to express my gratitude to the many people for their help. Particular mention goes to those individuals and bodies listed below:

Mr. Josh Redmond (Cranfield University, UK)

Mrs Kay Roly (Housing Manager, Cranfield University, UK)

Mr. Aymen El-Namy

Mr. Makalowf Al-Twer

Mr. Abo-Jareeda Salme (Elfornaj Communications, Tripoli-Libya)

Dr. Ghaith Beshish (Faculty of Engineering, Tripoli-Libya)

Dr. Ahmed Al-Gady (Faculty of Engineering, Tripoli-Libya)

Mr. Scott Booden (Cranfield University, UK)

Mrs. Deborah Hiscock (Cranfield University, UK)

Many individuals and institutions have contributed information that was used to do this work. Their contributions are gratefully acknowledged.

Last, but not least, I would like to express my thanks to the staff members of the Department of Power and Propulsion and my colleagues for their help.

TABLE OF CONTENTS

ABSTRACT i
DEDICATION iii
ACKNOWLEDGEMENTS iv
LIST OF FIGURES viii
LIST OF TABLES x
NOTATIONS xi
LIST OF EQUATIONS xii
1 Introduction 1
1.1 Background and Motivation 1
1.2 Project Scope 2
1.3 Thesis Outline 3
1.4 Scientific Contribution 3
1.5 Publications 4
1.5.1 Journal Publications 4
1.5.2 Conference Publications 5
2 Literature Review 6
2.1 Failure Modes and Their Causes in Rotating Machinery 6
2.1.1 Shafts 6
2.1.2 Bearings 8
2.2 Condition Monitoring 10
2.2.1 Condition Monitoring Technologies 11
2.2.2 Viabilities and Drawbacks of Technologies 15
2.3 Signal Processing Techniques and Fault Index Extraction 18
2.4 Previous Work 26
2.4.1 Vibration Analysis 26
2.4.2 Acoustic Emission Technology 29
3 Acoustic Emission Technology 34
3.1 Introduction 34
3.2 Definition of Acoustic Emission (AE) 35
3.3 Applications of Acoustic Emission Technology 38
3.4 Acoustic Emission Sensors 39
3.5 Calibration and Attenuation Test 40
3.6 Acoustic Emission Measurements 43
3.6.1 Hit Driven Data Measurements 44
3.6.2 Time Driven Data Measurements 45
3.6.3 Acoustic Emission Source Location 47
3.7 Advantages and Disadvantages of AE Technology 49
4 Bearing Condition Monitoring 51
4.1 Test-Rig Design and Layout 52
4.2 Instrumentation and Acquisition System Calibration 55
4.3 Bearing Tests 60
4.3.1 Case I 63
4.3.2 Case II 70
4.3.3 Case III 75
4.3.4 Formation of Grooved Pathway on the flat Bearing Race 81

4.3.5 Defect Size 84
4.3.6 Case IV 85
5 AE Source Location Analysis 89
5.1 Bearing Tests 89
5.1.1 Case I 91
5.1.2 Case II 93
5.1.3 Case III 96
6 Shaft Condition Monitoring 99
6.1 Test-Rig Design and Layout 100
6.2 Instrumentation and Acquisition System Calibration 101
6.3 Shaft Tests 102
6.3.1 Case I 103
6.3.2 Case II 109
7 Discussion 115
7.1 On Existing Knowledge 115
7.2 On Results of This Research 118
8 Conclusion 124
9 Recommendations 128
REFERENCES 129
APPENDICES 141
Appendix A Bearing Test Rig Design 141
Appendix B Shaft Test Rig Design 145

LIST OF FIGURES

Figure 3—1 Example of Kaiser Effect 37
Figure 3—2 Basic setup of an AE sensor..... 40
Figure 3—3 Example of AE sensor calibration certificate..... 41
Figure 3—4 Hsu-Nielsen source 43
Figure 3—5 Common measured parameters of AE signals 44
Figure 3—6 Example of Acoustic Emission waveforms 46
Figure 3—7 Principle of AE localization and the arrival time differences..... 48
Figure 3—8 Cluster analysis for spherical storage tank for natural gas 49
Figure 4—1 Steps of bearing test from basic design to the results interpretation 51
Figure 4—2 Test bearing arrangement for accelerated failure on the flat race 53
Figure 4—3 Test bearing run under starvation of grease 53
Figure 4—4 Test-Rig layout..... 54
Figure 4—5 Schematic of the data acquisition systems 56
Figure 4—6 Breaking lead pencil at four different positions (Program I) 57
Figure 4—7 Relative attenuation at four different positions (Program I)..... 57
Figure 4—8 Breaking lead pencil at three different positions (Program II) 59
Figure 4—9 Relative attenuation at four different positions (Program II)..... 59
Figure 4—10 General trend of AE energy throughout the bearing tests (Approach I & Approach II)..... 62
Figure 4—11 Test conditions run until visually observable surface damage 64
Figure 4—12 Classical AE parameters 65
Figure 4—13 Typical AE waveforms associated with case-I 65
Figure 4—14 Crack zones on flat ring 66
Figure 4—15 IE, KU, EI and KS-test results..... 67
Figure 4—16 AE waveform, enveloping and FFT after 4-hrs 68
Figure 4—17 AE waveform, enveloping and FFT after 10-hrs 69
Figure 4—18 AE waveform, enveloping and FFT after 16-hrs 69
Figure 4—19 Test conditions run until visually observable surface damage 70
Figure 4—20 Classical AE parameters 71
Figure 4—21 Typical AE waveforms associated with case-II 71
Figure 4—22 Crack zones on flat ring 72
Figure 4—23 IE, KU, EI and KS-test results..... 73
Figure 4—24 AE waveform, enveloping and FFT after 6-hrs 74
Figure 4—25 AE waveform, enveloping and FFT after 14-hrs 74
Figure 4—26 AE waveform, enveloping and FFT after 20-hrs 75
Figure 4—27 Test conditions run until visually observable surface damage 76
Figure 4—28 Classical AE parameters 77
Figure 4—29 Typical AE waveforms associated with case-III 77
Figure 4—30 Crack zone on flat ring..... 78
Figure 4—31 IE, KU, EI and KS-test results..... 79
Figure 4—32 AE waveform, enveloping and FFT after 15-hrs 80
Figure 4—33 AE waveform, enveloping and FFT after 45-hrs 80
Figure 4—34 AE waveform, enveloping and FFT after 50-hrs 81

Figure 4—35 Phenomenon of an increase in AE levels between 2- and 7 hrs of operation 82
Figure 4—36 Bearing test operated to 7-hrs only 83
Figure 4—37 AE waveforms at 2-, 3- and 5-hrs 83
Figure 4—38 Grooved pathway on the flat bearing race after 7-hrs 84
Figure 4—39 Defect size measurement 85
Figure 4—40 Bearing test results; run under grease starvation 86
Figure 4—41 Classical AE parameters 87
Figure 4—42 Typical AE waveforms associated with case-IV 87
Figure 4—43 Damage on the bearing cage 88
Figure 5—1 Dominant frequency content of AE's 90
Figure 5—2 Source location layout for linear detection 91
Figure 5—3 Source location estimates of AE events at 1-hr operation 92
Figure 5—4 Source location estimates of AE events at 4-hrs operation 92
Figure 5—5 Source location estimates of AE events at 10-hrs operation 93
Figure 5—6 Source location estimates of AE events at 16-hrs operation 93
Figure 5—7 Source location estimates of AE events at 1-hr operation 94
Figure 5—8 Source location estimates of AE events at 13-hrs operation 95
Figure 5—9 Source location estimates of AE events at 14-hrs operation 95
Figure 5—10 Source location estimates of AE events at 20-hrs operation 96
Figure 5—11 Source location estimates of AE events at 1-hr operation 97
Figure 5—12 Source location estimates of AE events at 15-hrs operation 97
Figure 5—13 Source location estimates of AE events at 45-hrs operation 98
Figure 5—14 Source location estimates of AE events at 50-hrs operation 98
Figure 6—1 Steps of shaft test from basic design to results interpretation 99
Figure 6—2 Test-Rig layout 101
Figure 6—3 Schematic of oil-filled cylinder 102
Figure 6—4 Observations of a run-to–failure shaft test 105
Figure 6—5 Classical AE parameters of counts, amplitude and ASL, ... 105
Figure 6—6 AE waveforms associated with results in figure (6-4), ... 106
Figure 6—7 AE waveforms associated with results in figure (6-4), ... 107
Figure 6—8 IE, KU, EI and KS-test results 108
Figure 6—9 Spectrogram results associated with Case I (highlighted region of waveform in figure (6-7), 500-mins of operation) 109
Figure 6—10 Observations of a run-to–failure shaft test 110
Figure 6—11 Classical AE parameters of counts, amplitude and ASL, ... 111
Figure 6—12 AE waveforms associated with results in figure (6-10), ... 111
Figure 6—13 AE waveforms associated with results in figure (6-10), ... 112
Figure 6—14 IE, KU, EI and KS-test results 113
Figure 6—15 Spectrogram results associated with Case II (highlighted region of waveform in figure (6-13), 120-mins of operation) 114
Figure 6—16 Observed fatigue associated with case I and case II 114

LIST OF TABLES

Table 2—1 Condition monitoring technologies available for slow speed rotating machinery..... 16
Table 3—1 Factors that affect the relative amplitude of AE response..... 37
Table 3—2 Advantages and disadvantages of AE technology..... 50
Table 4—1 Predicted and experimental life of test bearing races 55
Table 4—2 Results for the attenuation test (Program I). 58
Table 4—3 Results for the attenuation test (Program II). 60
Table 4—4 Results for the defect size measurements..... 85

NOTATIONS

Symbol	Definition	Unit
μ	Mean Value	-
ASL	Average Signal Level	dB (Decibel)
At	Attenuation	dB (Decibel)
At_P	Attenuation Using Signal Power	dB (Decibel)
At_V	Attenuation Using Signal Voltage	dB (Decibel)
CF	Crest Factor	-
r	Transmission Distance	cm
EI	Energy Index	-
f	Signal Frequency	Hz
FFT	Fast Fourier Transform	-
IE	Information Entropy	-
KS-test	Kolmogorov-Smirnov test	-
KU	Kurtosis	-
L	Defect Size	mm
N	Date Points (Sample Size)	-
N_e	Constant	-
Ø	Bearing Diameter	mm
P_i	Individual Probability Distribution	-
Prop ($D_{S(t)1S(t)2}$)	Similarity Probability	-
Q_{ks}	Constant	-
RMS	Root Mean Square Value	Volt
S	Bearing Speed	mm/sec
SA	Signal Amplitude	dB (Decibel)
SE	Signal Energy	Joule
SP	Signal Power	Watt
V_{max}	Maximum Amplitude	Volt
X_i	Individual Event	-
α	AE Signal	Volt
ζ	Duration	Second
λ	Constant	-
β	Medium Coefficient	dB/MHz.cm
σ	Standard Deviation	-
ω	Rotational Speed	rps (Revolution Per Second)

LIST OF EQUATIONS

$$\mu = \frac{\sum_{i=1}^{N} X_i}{N}$$ 18

$$\sigma = \sqrt{\frac{\sum_{i=1}^{N}(X_i-\mu)^2}{N}}$$ 18

$$RMS = \sqrt{\frac{X_1^2+X_2^2+.....+X_N^2}{N}}$$ 19

$$SE = \int_0^T \alpha^2(t)dt$$ 19

$$\text{Energy Index} = \left(\frac{RMS_{Segment}}{RMS_{overall}}\right)^2$$ 20

$$D = \max\left|S(t)_1 - S(t)_2\right|_{-\infty<t>\infty}$$ 20

$$\text{Prop}\,(D_{S(t)_1S(t)_2}) = Q_{ks}\left(\left[\sqrt{N_e}+0.12+\frac{0.11}{\sqrt{N_e}}\right]D_{S(t)_1S(t)_2}\right)$$ 20

$$N_e = \frac{(S(t)_1)(S(t)_2)}{(S(t)_1)+(S(t)_2)}$$ 20

$$Q_{ks}(\lambda) = 2\sum_{j=1}^{\lambda}(-1)^{j-1}e^{-2j^2\lambda^2}$$ 20

$$Q_{ks}(\lambda) = \begin{pmatrix} 1 & \text{as } \lambda \to 0 \\ 0 & \text{as } \lambda \to 1 \end{pmatrix}$$ 20

$$KU = \frac{1}{N}\sum_{i=1}^{N}\left(\frac{X_i-\mu}{\sigma}\right)^4$$ 21

$$CF = \frac{\text{Peak Value}}{RMS}$$ 21

$$IE = -\sum_{i=1}^{N} P_i * \log(P_i)$$ 22

$$At = \beta * r * f$$ 42

$$SA = 20\,Log_{10}\left(\frac{V_{max}}{10^{-6}}\right)$$ 42

$$SE = \int_0^{T(sec)} \alpha^2(t)dt$$ 42

$$SP = \frac{SE}{T(sec)} = \frac{1}{T(sec)}\int_0^{T(sec)} \alpha^2(t)dt$$ 42

$At_P = 10\ Log_{10}\left(\frac{P_s}{P_d}\right)$ 42

$At_V = 20\ Log_{10}\left(\frac{V_s}{V_d}\right)$ 42

$ASL=20\ Log_{10}(1.4 * RMS/100)$ 55

$S = 2\pi * \frac{\varnothing}{2} * \omega$ 84

$L = S * \zeta$ 84

1 Introduction

1.1 Background and Motivation

Condition monitoring is state of the art in many kinds of industrial processes. During long-ago decades, people have often used their ears or screwdrivers as a pick-up sensor of the vibration and noise while the machine was in operation. Typical modern condition monitoring systems consist of a number of sensors and a data acquisition system, integrated with a software program, which analyzes the signals.

Robust on-line monitoring and predictive maintenance technology is used to detect impending problems in machines and allow repairs to be scheduled. To keep machines functioning at optimal levels, detection of failures in their vital components (e.g. shafts and bearings) is important because any wear, if it is not detected in time, will often progress to more serious damage affecting the other parts of the machine.

Modern slow speed rotating machines are fatigue loaded machines (e.g. wind turbines) and operational experience with these machines manifested that their components are failing at abrupt high rates. Rotating machinery components that are subject to repeated bending may develop cracks which eventually make the component break. Metal fatigue is a well known problem in many industries. A historical example is the huge German Growian machine (100 m rotor diameter) which had to be taken out of service after less than three weeks of operation [1]. To run slow speed rotating machines at optimal levels in efficient industrial processes, enhancements of reliability and lifetime of the machines will be essential.

This has led engineers and scientists to develop online condition monitoring schemes and fault detection technologies for early forewarning of incipient mechanical and electrical faults. Reliable and robust monitoring systems can lead to planned corrective maintenance actions before complete component failure occurs, thereby minimizing collateral damage to adjacent components.

Planned maintenance can cover all preventive maintenance, including routine checks, periodic maintenance, periodic testing, and high voltage equipment maintenance. Hence, if a condition monitoring programme is successfully implemented it will allow the machine to operate to its full capacity without having to halt the machine at fixed periods for inspection.

1.2 Project Scope

In the past, machines were simply utilized until failure and then maintained. However, run-to failure has become a less-possible option if not impossible as machine sizes rapidly increase and their vital components (e.g. shafts and bearings) become more costly. These factors influence operating and maintenance economics. Thus, this program of research investigates the qualities of AE as a reliable, stable and viable monitoring technology that can be used in slow speed rotating machinery applications. Such technology may offer:

- Early warning of incipient failures.
- Scheduled proactive maintenance and intervention and increase the efficiency of slow speed rotating machinery by minimizing the stoppages.
- Establishment of a correlation between Acoustic Emission and natural initiation and propagation of defects in low speed bearings and shafts.
- Estimation of the location of the AE sources in real-time throughout the bearing test period and correlate the eventual surface defect to the identified sources of AE.
- Identification of the size of a natural defect on bearings using AE technology.
- Investigation of the effects on AE signals associated with the natural initiation and propagation of cracks on thrust bearing races whilst in operation by running bearing tests under conditions of grease starvation.

To achieve the final goal of this programme of research, several tasks have been accomplished. In addition to a comprehensive review of condition monitoring technologies, two test rigs to run full-scale experimental work were designed for bearing and shaft tests and the results were analyzed using the most representative techniques such as EI, KS-test, enveloping and FFT.

1.3 Thesis Outline

This thesis encompasses nine chapters. Chapter 2 summarises the literature study that included an overview of failure modes and their causes of rotating machinery components. Further, available condition monitoring technologies and their applicability in slow speed rotating machinery applications are investigated. In Chapter 3, Acoustic Emission technology is discussed in more detail. Chapter 4 presents the details of bearing test rig design, laboratory experiments, results and observations. The linear source location technique developed in this research program and used for all bearing tests is presented in Chapter 5. Details of shaft test rig design, laboratory experiments, results and observation are discussed in Chapter 6 to map the fault features to a shaft's health condition. The aim of Chapter 7 is to collate and discuss the material and the results presented in previous chapters. It draws together the findings of chapters 4 to 6, and explores some of the theoretical issues associated with machinery operation, for the purpose of determining machinery integrity. Lastly, Chapters 8 and Chapter 9 provide concluding remarks and recommendations for future research respectively.

1.4 Scientific Contribution

This work addresses the potential of identifying the natural cracks in operational slow speed rotating machinery with Acoustic Emission (AE) technology. To date this investigation is unique and offers a significant contribution to the exiting body of knowledge on AE. There are significant contributions of this work in the area of condition monitoring of slow speed rotating machinery. Firstly, the establishment of a correlation between acoustic emission activity and natural initiation and propagation of defects in low speed rotating machinery components (bearings and shafts); at the rotational speed on which these tests were employed, this is the first known attempt at correlating AE and natural defect generation in slow speed rotating shafts. Secondly, in addition to verifying the applicability of AE in detecting crack initiation and propagation on bearing races whilst in operation, an estimation of the location of the AE

sources was undertaken in real-time throughout the test period in an attempt to correlate the eventual surface defect to the identified sources of AE; this study is the first of its kind to date. Thirdly, this study also attempted to identify the size of a natural defect on bearings using AE technology. Fourthly, this research programme can be considered one of the few programmes that involved running bearing tests under conditions of grease starvation and investigated the effects of this on AE signals associated with the natural initiation and propagation of cracks on thrust bearing races whilst in operation. Finally, the results from this investigation show that whilst measurements on operational bearings and shafts cannot be achieved as described in this study, the method of identifying the onset of crack propagation can be employed as a quality control tool for bearing and shaft manufacturers, particularly for testing bearing and shaft materials homogeneity.

1.5 Publications

The findings of this study were published in several international journals and conferences.

1.5.1 Journal Publications

- M. Elforjani and D. Mba, Monitoring the Onset and Propagation of Natural Degradation Process in a Slow Speed Rolling Element Bearing With Acoustic Emission, Journal of Vibration and Acoustics, Vol. 130, Issue 4, 041013, August 2008.

- M. Elforjani and D. Mba, Detecting the Onset, Propagation and Location of Non-Artificial Defects in a Slow Rotating Thrust Bearing with Acoustic Emission, INSIGHT (Published by the British Institute of Non-Destructive Testing), Vol. 50, No 5, Pages 264-268, May 2008.

- M. Elforjani and D. Mba, Observations and location of Acoustic Emissions for a Naturally Degrading Rolling Element Thrust Bearing, Journal of Failure Analysis and Prevention, Vol. 8, Number 4, Pages 370-385, May 2008.

- M. Elforjani and D. Mba, Assessment of Natural Crack Initiation and its Propagation in Slow Speed Bearings, Journal of Non-Destructive Testing and Evaluation Vol. 24, Issue 3, Pages 261-275, September 2009.

- M. Elforjani and D. Mba, Natural Mechanical Degradation Measurements in Slow Speed Bearings, Journal of Engineering Failure Analysis, Volume 16, Issue 1, Pages 521-532, January 2009.

- M. Elforjani and D. Mba, Accelerated Natural Fault Diagnosis in Slow Speed Bearings with Acoustic Emission, Journal of Engineering Fracture Mechanics, Vol. 77, Issue 1, Pages 112-127, January 2010.

- M. Elforjani and D. Mba, Detecting of Natural Crack Initiation and Growth in Slow Speed Shafts with the Acoustic Emission Technology, Journal of Engineering Failure Analysis, Vol. 16, Issue 7, Pages 2121-2129, October 2009.

- M. Elforjani; D. Mba; B. Charnley, Observations of a Naturally Degrading Slow Speed Shaft, Journal of Non-Destructive Testing and Evaluation First Published (Online) on: 02 June 2010.

- M. Elforjani and D. Mba, Condition Monitoring of Slow Speed Shafts and Bearings with Acoustic Emission, Strain, (In Press).

1.5.2 Conference Publications

- M. Elforjani and D. Mba, Assessing AE Signals from Natural Degradation of Slow Speed Rolling Element Bearings, the 2nd World Congress on Engineering Asset Management (EAM) and the 4th International Conference on Condition Monitoring, UK, 2007.

- M. Elforjani and D. Mba, Role of Acoustic Emission in Condition Based Maintenance of Slow Speed Bearings, Cranfield Multi-Strand Conference, UK, 2008.

- Elforjani, M, and Mba, D., Acoustic Emission and natural degradation of a slow speed bearing, 22nd International Congress and Exhibition on Condition Monitoring and Diagnostic Engineering Management (COMADEM 2008), ISBN 978-80-254-2276-2, Pages 187-196, Prague, Czech Republic,11th – 13th June 2008.

- M. Elforjani and D. Mba, Acoustic Emissions Observed from a Naturally Degrading Slow Speed Bearing and Shaft, the 4th World Congress on Engin eering Asset Management (WCEAM 2009), Athens, Greece, 2009.

2 Literature Review

The literature study commences with an overview of the principal shaft and bearing faults and their causes. The role of available condition monitoring technologies, and their applicability in slow speed rotating machinery applications, is also briefly investigated. Next to this, a comprehensive and critical review of signal processing techniques and fault index extraction is discussed. In addition to that, an outline of the previous work on condition monitoring application for slow speed rotating machinery relevant to this study is presented.

2.1 Failure Modes and Their Causes in Rotating Machinery

In this section, each potential of failure modes and their causes in rotating machinery components is presented with a focus on shafts and bearings. Failure mode can be defined as the behaviour by which a failure is observed whereas the failure cause is the means or processes that are the basic reason for this failure [2]. *(It should be noted that all information on failure modes and their causes were taken from [3-7]).*

2.1.1 Shafts

A shaft is an essential part of any rotating machine. It is used to transmit power and motion and support rotating machine elements such as impellers, gears, pulleys etc. [7]. Shafts are critical components in rotating machines and are often expected to carry heavy loads and operate reliably. Undetected shaft failure can cause significant damage for machinery, influence production rates and even cause safety concerns. Generally, the shafts are designed to have an infinite life. This will be the case unless the shaft is overloaded or damaged.

Manufactured shafts have to pass the checks in the factory, checks for unbalance, as well as the check at test run. A poorly designed shaft can be detrimental for the system both at mount (high mounting forces, impacts) and at

run. Proper handling on site, however, will prevent the shaft from damage, corrosion, indents etc.

Fatigue is a major cause of a broken shaft. Stress concentration points such as a keyway or a sharp radius, or, in rare cases, from a material impurity can play the major role to start the crack. Further, scratches, indents, flaws in the surface of a shaft, or corrosion, may also favour the starting point of a fatigue crack. Bending loads from the hydraulic end or torsion loads from direct online starts are mainly the loads that drive a crack. In extreme load cases when debris is squeezed into a radial clearance, large deformations occur. As a consequence, this leads to plastic deformation on shafts.

Elastic deflection and slops are also critical phenomenon. Shafts can be estimated to have failed if the elastic deflections are greater than is acceptable for successful machine operation. Thus, the shafts must be designed properly to ensure that any deflections due to the applied loads are acceptable for the machine in question.

A loose connection can cause impacts that generate high loads and damage on the shaft. It is essential to tighten the bolts in a correct way and with correct torque and lubricate with appropriate lubricant. With conical joints, the lubrication is of great importance as the conical sleeve or conical part of the impeller climbs up on the shaft and creates the necessary pressure, enabling the holding force. Another failure cause is shaft misalignment. Misalignment can hardly be achieved but with incorrect mounting it may occur.

In some cases, where a thin shells shaft is designed, buckling can be considered as another issue. It is difficult to decide whether shafts will fail by buckling or not and therefore it is important at the early design stage to take into account that buckling could be an issue if the shaft design has thin shells or looks slender.

When machines operate at elevated temperature, typically in the range of 30-40 percent of material melting point, creep can also occur. Creep is the progressive

growth of plastic strain that can occur when a component is operated in a stressed state at elevated temperature over a period of time.

2.1.2 Bearings

A bearing is a vital component in rotating machinery. It is used to allow constrained relative motion between two or more parts, typically rotation or linear movement. Bearings may generally be classified according to the motions, principle of operation and the directions of applied loads they can handle. Sooner or later wear, fatigue or lubricant deterioration will ultimately destroy the bearings capability to function appropriately. In general, load is a factor in conditions leading to failure. Failure to use suitable tools for mounting may cause the mounting force to act on the rolling element which may cause indentations and destroy the bearing. Proper handling and storage on site and the use of correct grease or oil, however, will prevent the bearing from damage, corrosion, indents etc. Another failure cause is shock load. It may emerge from mounting of other parts, such as an impeller, or during transport and installation. The forms of bearings damage may be classified as primary damage and secondary damage. The former includes wear, indentations, smearing and corrosion whereas the later consists of flaking (spalling), fatigue and cracks.

Wear is a general term describing loss of material from the contacting surface of a bearing. Wear may occur as a result of rough particles that have entered the bearing. Abrasive contaminants in the oil can become trapped between the contacting surfaces of the bearing causing indentations which act as stress raiser. Contaminates can be eliminated by ensuring seals are in good condition and correctly fitted. Faults in the lubrication of bearings can also be another form of bearing wear. An inadequate lubricant or if the lubricant has lost its lubricating properties may also cause metal to metal contact between rolling elements and raceways. Thus, a regular check to ensure that the lubricant reaches the bearing is very important. Further, bearings can more frequently be re-lubricated.

A bearing is stabilized to a certain temperature and temperatures above may alter the internal structure of the material. If the allowed amount of grease is exceeded and the bearing is overfilled with grease, the temperature will increase. As consequence, the lifetime of the bearing will be reduced due to lower viscosity and faster degradation of the lubricant; nevertheless, the signs of the high temperature may not be so obvious. In cases where too much heat is generated, as a result of overloading the bearing, the cage may also be damaged if subjected to over-heating.

Faulty mounting or overloading may cause indentations in the raceways of both rings with spacing equal to the distance between the rolling elements. When the bearing is subjected to abnormal loading while not running or the mounting pressure is applied to the wrong ring, so that it passes through the rolling elements, raceways and rolling elements may become dented. Ingress of foreign particles into the bearing also causes indentations.

Smearing is another form of surface damage which may occur if two inadequately lubricated surfaces slide against each other under stress. High speed, light load, sudden acceleration/deceleration and entry of water are other causes of smearing. When smearing occurs, collection of small materials is transferred between bearing components. As a consequence, the material is heated to a certain temperature and re-hardening may take place; thereby this produces localized stress concentrations that may cause cracking or flaking.

If a fluid enters the bearing, corrosion may occur. Further, when the fluid is over rolled inside the bearing it will act as a jet and as a result it forces the grease out from the raceway. Particles are another issue. They generate high stresses or wear in the bearing components and thereby create premature fatigue failure that shortens the bearing life.

Fatigue is playing a major role in the bearing lifetime. The lifetime of a bearing can be defined as the time to the first sign of pitting or scaling, not a total failure. It is dependent on the number of revolutions, the load and the lubrication. Cyclic shear stresses that are highest just below the surface can form small cracks,

which are the signs of the initial fatigue damage. These small cracks will then propagate up to the surface and as the rolling elements pass over these cracks, small fragments will finally break off (scaling).

Fatigue pitting is a form of surface fatigue which may occur soon after operation begins. If a metal is repeatedly subjected to high surface or subsurface stresses, the surface may eventually develop fatigue cracks. When progressive pitting reaches a certain stage the metal between adjacent pits tends to be weakened and eventually breaks away forming very large, irregular shaped, shallow pits. This effect is known as flaking (spalling). If the process has proceeded to a certain stage, spalling can completely remove the raceways surfaces. Further, it may act as a fracture notch and lead to cracking of the bearing rings.

2.2 Condition Monitoring

Condition monitoring can be defined as the process of monitoring physical parameters, associated with machinery operation, for the purpose of determining machinery integrity. It can also be described as the measurement of various parameters related to the mechanical condition of the machinery (such as vibration, bearing temperature, oil pressure, oil debris, and performance), which makes it possible to determine whether the machinery is in good or bad mechanical condition [8]. Indeed, the costs of component downtime to industrial processes can be very significant therefore preventing equipment failures and minimizing stoppages due to servicing and maintenance are key priorities that can be reduced using condition monitoring. To keep machines functioning at optimal levels, condition monitoring of rotating machinery components is important because any wear, if is not caught in time, will often progress to more serious damage affecting the adjacent parts. This may lead to more costly repairs than replacing a part.

2.2.1 Condition Monitoring Technologies

In this section, a review of condition monitoring technologies, which are possibly viable for slow speed rotating machinery, has been made to include options, outlining both their capabilities and limitations for monitoring slow speed rotating machinery, and considering the value of using them. In this context, the following technologies are broadly used:-

- Vibration Analysis.
- Acoustic Emission.
- Strain Measurement.
- Thermography.
- Oil Analysis.
- Process Parameters/ Performance Monitoring
- Physical Condition of Materials

2.2.1.1 Vibration Analysis

Vibration is the most regularly measured condition parameter in rotating machinery, and it is continuously monitored in many important applications. The commonly monitored vibration signals are displacement, velocity, and acceleration. The most basic vibration monitoring technique is to measure the overall vibration level over a broad band of frequencies. The measured vibration level is trended against time as an indicator of deteriorating machine condition and/or compared against published vibration criteria for exceeding. The type of sensor is selected based on the frequency range, relevant for the monitoring applications [5,9,10] :-

- Accelerometers in the high frequency range.
- Velocity transducers in the middle frequency area.
- Displacement transducers for the low frequency range.

Signal analysis requires particular knowledge. A complete system, which includes signal analysis and diagnostics, has to be provided. Data analysis

techniques like time domain analysis, spectral analysis, synchronous signal averaging, cepstral analysis or adaptive noise cancellation can be used to analyse any obtained signals. Signals can also statistically be characterised by some parameters such as peak, RMS, crest factor or kurtosis.

Application of vibration analysis can be found in monitoring shafts, bearings, gearboxes, compressors, motors, turbines (gas and steam) and pumps. For monitoring slow speed rotating machinery components, vibration analysis is one of the viable technologies. However condition monitoring of slow speed rotating machinery using vibration analysis tends to be more difficult. With rotating machines working at less than 100 rpm it is difficult for vibration to diagnose damage or degradation because of the small amount of energy and vibration occurring over a long period [11].

2.2.1.2 Acoustic Emission Technology

Acoustic monitoring technology is effective technology in continuous monitoring of rotating machinery. It is classified under the non-destructive testing (NDT) technologies that do not affect the object's future usefulness [12,13]. In general, acoustic measurements are broadly divided into two major types namely, active type, where the excitation is externally implemented, and passive type, where the excitation is performed by the component itself. Typically the range of frequencies are in the order of 50 kHz to 1 MHz [12,13].

Commonly used sensors are resonance type piezoelectric transducers with the proper couplant [10]. In some applications where sensors cannot be fixed directly, waveguides are used. Sensors are carefully selected and calibrated for frequency response and sensitivity before any application. Extraction of the required information from the detected signal is the role of signal processing. Various signal processing techniques are used to analyze AE signals and extract features related to defects. Usually, a threshold level is defined. The AE threshold needs to be exceeded before further analysis. Signal waveforms can be analyzed in the time and frequency domains. Signals can also be

characterized by statistical averaged parameters such as Mean, Variance, Skewness, or Kurtosis.

The acoustic monitoring technologies, for instance AE, can successfully be applied for monitoring slow speed rotating machinery to give an advanced machine diagnostics and clear text messages regarding detected faults [12]. Acoustic Emission technology will be presented in more detail in the next chapter.

2.2.1.3 Strain Measurement

Strain gauges are frequently used in mechanical engineering research and development to measure the stresses generated by machinery. Slow speed rotating machinery components testing is one area of application, tiny strain-gauge strips are glued to structural members, linkages, and any other critical component to measure stress. Strain measurement by strain gauges is not often applied for condition monitoring. Strain gauges are not robust on a long term basis [10].

2.2.1.4 Thermography

It is a quick observation technique for determining the general health of engineering machines. The infrared radiation from the surface of the body is utilised to produce a thermal image which then can be used to identify hot spots on the body. Hot spots, due to deterioration of components or bad contact can be identified in a simple and fast manner, and therefore a thermographic camera is an invaluable tool in condition monitoring. Thermography is based on measuring the distribution of radiant thermal energy (heat) emitted from a target surface and converting this to a map of radiation intensity. Thermal energy is present with the operation of all machines (e.g., friction). Temperature can be a key parameter for monitoring the performance and condition of machines [9]. A simple check can be performed for the bearings. Misalignment condition will display a thermal pattern as the associated mechanical forces are converted to heat that can easily be detected. The technology is only applied for off-line

usage. At this moment the technology is not appropriate for on-line condition monitoring [10].

2.2.1.5 Oil Analysis

The use of oil analysis for machinery monitoring dates back more than fifty years. The railroad industry discovered that the metals found in a sample of used oil revealed the condition of the wearing parts in the diesel engine [14]. Oil analysis is one of the successful tools as it can help to provide advance warning of abnormal conditions that could contribute to machine and oil degradation. Developing proper oil analysis procedures and learning to properly interpret oil analysis data, is a long journey. Indicators of oil analysis can determine whether a machine's oil is fit for further use. That can be implemented by comparison analysis results with virgin oil. There are five main tests that are employed in this analysis process, depending on the application [14]:-

- Viscosity analysis.
- Oxidation analysis.
- Water content analysis.
- Particle counts analysis.
- Machines wear analysis.

This technique is commonly applied off-line. Oil analysis is mostly executed off-line, by taking samples. However for safeguarding the oil quality, the application of on-line sensors is increasing [10].

2.2.1.6 Process Parameters/ Performance Monitoring

Test of machine's parameters can be used for ongoing performance monitoring and to diagnose and troubleshoot the source of problems such as low horsepower, low torque, leaks or overheating. To monitor the reliability, durability and performance of engines, motors, turbines and other rotary machines, an intelligent system based on parameter analysis, is essential. For wind turbines, parameter readings, such as capacity factor of the plant, power,

wind velocity, rotor speed and blade angle, are compared to operator's manuals or manufacturer's performance specifications to determine whether the system is performing at optimum efficiency. When problems are detected, the initial reading can serve as a baseline when implementing modifications. Subsequent readings reflect the impact of the change and verify that the modification or repair was successful. At present, more intelligent usage of the signals based on parameter estimation and trending is not common practice in wind turbines [10].

2.2.1.7 Physical Condition of Materials

Data of Physical characteristics of rotary machines is necessary when planning for predictive maintenance. A material undergoes transition under the influence of temperature pressure and stress, are physical in nature, because their molecules remain unbroken. The use of physical condition monitoring of materials is mainly focussed on crack (nucleation and growth) detection. Methods are normally off-line and not suitable for on-line condition monitoring of wind turbines. Exception might be the usage of optical fuses in the blades and acoustic monitoring of structures [10].

2.2.2 Viabilities and Drawbacks of Technologies

Condition monitoring of rotating machinery, especially the critical components such as bearings and shafts can avoid catastrophic failures. It also increases industrial projects availability, revenues, and reduces operation and maintenance costs. Table (2-1) summarises the viability of condition monitoring technologies that are possibly viable for slow speed rotating machinery.

Table 2—1 Condition monitoring technologies available for slow speed rotating machinery.

Technology	Viability	Drawbacks
Vibration Analysis	Machine Components such as Bearing, Gear and Shaft, and Structural Components.	• Needs an existing defect within the components to excite frequency of vibration. • Applicable only for low frequency range (5Hz - 20 kHz). • Can detect failures of low speed machineries (speed<100 RPM) at late stage as energy generates over long period (perform poorly in low speed machinery).
Acoustic Emission Analysis	Machine Components such as Bearing, Gear and Shaft, and Structural Components.	• Sensitive to other ultrasonic sources such as turbulence, crushing, etc. • Requires highly specialised sensors and signal processing.
Strain Measurement	Structural Components.	• Applicable for component life span prediction only (no robustness for long term monitoring).
Thermography	Electronic Control Systems and Sensors.	• Executed mostly off-line. • Needs visible inspection. • Unable to detect the inside temperature if the medium is separated by glass/polythene material etc. • Costly instrumentations.
Oil Analysis	Machine Components such as Bearing, Gear and Shaft, and Hydraulics.	• Executed mostly off-line. • Applicable for limited number of components where lubricant is only used. • Taking samples to be analysed (needs accessibility and long process to perform).
Process Parameters/ Performance Monitoring	Machine Components such as Bearing, Gear and Shaft, Control Systems, Sensors, and Hydraulics	• Cannot establish defect positions within the machinery. • Cannot establish defect nature. • Needs baseline documents of machines (operator's manuals or manufacturer's performance specifications) to be compared with any measured parameters.

Continue Next Page

Technology	Viability	Drawbacks
Physical Condition of Materials	Structural Components.	• Executed mostly off-line. • Focuses only on crack detection, growth and materials properties.
Visual Inspection	Machine Components such as Bearing, Gear and Shaft	• Not applicable for remote areas as it needs frequent visible visits and high labour cost. • Needs accessibility to the machine components for visual inspections.

2.3 Signal Processing Techniques and Fault Index Extraction

To provide more ways for analyzing the signals and more ways for measuring deviations from the normal conditions, various fault index extraction and signal processing techniques were widely applied to the measured data. They include the information entropy (IE), signal shape factor (SHF), enveloping, and spectrum analysis (Fast Fourier Transform (FFT), Auto-regressive, Prony's Energy Method and Wavelet Transform).

Statistically tools such as the mean (μ), standard deviation (σ), root mean square (RMS), crest factor (CF), kurtosis (KU), shape factor (SHF) and impulse factor (IF) have been employed for bearing defect detection [15]. Although some of these factors such as CF and KU become very sensitive indicators as the presence of the defects is pronounced, their values may come down to the level of undamaged bearings when the damage is well advanced [15].

Acquired signals can be characterized using the mean (μ) or the standard deviation (σ). The mean is one of several indices of central tendency that is used to indicate the point on the scale of measures where the signal is centered. The mean is the average of the events in the signal. Numerically, it equals the sum of the events divided by the number of events [16,17]. The standard deviation is one of several indices of variability that is used to characterize the dispersion among the measures in a given signal. To calculate the standard deviation of a given signal it is first necessary to calculate that signal's variance. Numerically, the standard deviation is the square root of the variance [16,17]. For individual event (X_i) and sample size (N), μ and σ can be calculated respectively as:-

$$\mu = \frac{\sum_{i=1}^{N} X_i}{N} \qquad (2\text{-}1)$$

$$\sigma = \sqrt{\frac{\sum_{i=1}^{N} (X_i - \mu)^2}{N}} \qquad (2\text{-}2)$$

The Root Mean Square (RMS) is an electrical engineering power term defined as the rectified, time averaged signal, measured on a linear scale and reported in volts. It is also known as Quadratic Mean (QM) [18-20]. Until today this parameter is intensively used for signal analysis. For individual event (X) and sample size (N), RMS can be calculated as:-

$$RMS = \sqrt{\frac{X_1^2+X_2^2+.....+X_N^2}{N}} \quad (2\text{-}3)$$

One of the frequently used signal characteristics is energy [21]. The Signal Energy can be defined as the integral of the squared signal (α) over the test duration (T) and calculated using the equation [2.4].

$$SE = \int_0^T \alpha^2(t)dt \quad (2\text{-}4)$$

Whilst the Root Mean Square (RMS) is one of the widely used statistical parameters for condition monitoring measurements, it is typically recorded over a predefined time period. As such the RMS values are not necessarily sensitive to transient changes which typically are of a few micro-seconds. To overcome this inadequacy, a technique that is relatively more sensitive has been employed; the Energy Index (EI). EI can be defined as the square of the ratio of the root mean square of a defined segment ($RMS_{segment}$) in a given signal to the overall root mean square ($RMS_{overall}$) of the same signal [22]. The technique was successfully applied to simulated and experimental data of gears and bearings [22-24]. Al-Balushi [22] expressed mathematical correlation to undertake Energy Index analysis. In application, an Energy Index value of one is associated with non-transient type waveforms and greater than one where transient characteristics are present. For this particular investigation every AE waveform, recorded at each hour of operation, was split into one hundred segments. The square of the ratio of RMS value of each segment in a given AE signal was divided by the overall RMS of the same signal and EI was calculated using equation [2.5]

$$\text{Energy Index} = \left(\frac{RMS_{Segment}}{RMS_{overall}}\right)^2 \quad (2\text{-}5)$$

Data analysis can also be undertaken using the Kolmogorov-Smirnov test (KS-test). The KS-test was successfully applied to detect early fatigue cracks in gears and bearing [25-30]. The test is a time domain signal processing technique that compares two signals to indicate the likelihood that the two signals have the same probability density function. In essence, the test involves assuming a null hypotheses which means that the cumulative density function (CDF) of two signals $S(t)_1$ and $S(t)_2$ are statistically similar. Thus, a fault condition can be indicated by comparing the KS-test value for a signal with a number of signal templates of normal operating conditions. This method of analysis was applied to AE waveforms sampled at 2 MHz and acquired at various stages during the test programme. A measure of similarity between AE waveforms was determined by calculating the maximum absolute distance (D) between the CDF's of AE waveforms using the equation [2.6].

$$D = \max\left|S(t)_1 - S(t)_2\right|_{-\infty<t>\infty} \quad (2\text{-}6)$$

The statistical distance D can be converted into a similarity probability using the KS Probability Distribution Function (Q_{ks}) [28].

$$\text{Prop}\left(D_{S(t)_1 S(t)_2}\right) = Q_{ks}\left(\left[\sqrt{N_e} + 0.12 + \frac{0.11}{\sqrt{N_e}}\right] D_{S(t)_1 S(t)_2}\right) \quad (2\text{-}7)$$

$$N_e = \frac{\left(S(t)_1\right)\left(S(t)_2\right)}{\left(S(t)_1\right) + \left(S(t)_2\right)} \quad (2\text{-}8)$$

$$Q_{ks}(\lambda) = 2\sum_{j=1}^{\lambda}(-1)^{j-1} e^{-2j^2\lambda^2} \quad (2\text{-}9)$$

$$Q_{ks}(\lambda) = \begin{pmatrix} 1 & \text{as } \lambda \to 0 \\ 0 & \text{as } \lambda \to 1 \end{pmatrix} \quad (2\text{-}10)$$

The similarity probability will be one if the CDF's are similar and zero if the CDF's are different. Hence, if the two AE signatures are similar (i.e., have statistically similar CDFs), then the similarity probability tends to be one. On the other hand, if the signatures are different, then the similarity probability tends to be zero [28]. An algorithm to perform the KS-test can be devised and run using Matlab software.

The kurtosis (KU) is the normalised fourth statistical moment of a given signal. The amplitude distribution of a healthy machine is generally assumed to be Gaussian or "normal". It is known that KU is a measure of the peakness of a signal and on the basis that a signal will contain impulsive transient events during the onset of degradation [20], kurtosis values for a given signal can be estimated using the equation [2.11].

$$KU=\frac{1}{N}\sum_{i=1}^{N}\left(\frac{X_i-\mu}{\sigma}\right)^4 \qquad (2\text{-}11)$$

The Crest Factor (CF) is defined as the ratio of the peak value divided by the root mean square (RMS) value of the signal. It gives an indication of impulsiveness in the signal. Crest Factor (CF) is a traditional method of measuring the smoothness of a signal and a faulty bearing will generate a spiky AE signal profile [20]. As a consequence, CF increases as bearing problems become more severe. Crest Factor calculations can also be applied on the recorded signals. Equation [2.12] is employed to calculate the CF.

$$CF = \frac{\text{Peak Value}}{\text{RMS}} \qquad (2\text{-}12)$$

A faulty bearing will generate a chaotic system that is very sensitive to the initial conditions. In such a system, although the initial state is known, the ability to predict the future state diminishes due to the deviation from its normal conditions. To measure diminishing rate of information for future state estimation, information entropy (IE) is used. Information entropy is usually defined as a measure of uncertainty of a process [31,32]. As the working condition

of a machine system deteriorates due to the initiation and/or progression of structural defects, the number of frequency components contained in the AE signal will increase, resulting in a decrease in its regularity and an increase in its corresponding IE value. Shannon firstly proposed Information entropy to measure information's uncertainty and it holds the following properties [33,34]:-

- When the outcome of an event is certain, the entropy is zero.
- The increase of an events number results in an increase in entropy.
- The entropy is solely dependent on the probability distribution of the event occurrence.

The concept of entropy has been generalized in a number of different ways by different researchers [35] since the pioneering work of Shannon, ranging from communication, statistical mechanics, decision theory, and pattern recognition problems. In these disciplines, it is applied as a measure of disorder, unevenness of distribution, the degree of dependency, or complexity [36]. With a known number of events (N) and the probability distribution (P_i) of each event in a given signal, IE can be calculated for a set of events using equation [2.13].

$$IE = -\sum_{i=1}^{N} P_i * \log(P_i) \qquad (2\text{-}13)$$

Envelope Detection or Amplitude Demodulation can be defined as a technique of extracting the modulating signal from an amplitude-modulated signal. Envelope detection can also be defined as a method for intensifying the repetitive components of a dynamic signal to provide an early warning of deteriorating mechanical condition. Results of enveloped signals are the time history of the modulating signal [20,37-39]. This signal may be studied or interpreted as it is in the time domain or it may be subjected to a further frequency analysis. In the enveloping process, the acquired raw waveform is generally first high-pass or band-pass filtered, then enveloped, and processed through an FFT algorithm. Envelope analysis is often known as the FFT (Fast Fourier Transform) frequency spectrum or any spectrum analysis of the modulating signal [37]. Results of the envelope analysis can be used for diagnostics and

investigation of machinery where faults have an amplitude modulating effect on the characteristic frequencies of the machinery. Examples include faults in gearboxes, turbines and induction motors. Envelope analysis is also widely used as a tool for diagnostics of local faults like cracks and spallings in bearings as it can reduce the masking noise and enhance the significant spectral components relating to bearing performance [39].

The Fourier Transform (harmonic analysis) is a technique used to map time-domain functions (which can be a function of time or any time series abscissa) into frequency-domain representations. Time domain analysis is useful when the periodicity clearly exists in a signal to be analyzed. To describe exactly and analyze an arbitrary set of signals into periodic components, whether the signal might appear periodic or not Fourier Transform analysis can be one of the options. The FFT is an optimized tool of the Discrete Fourier Transform (DFT) to perform the same analysis, but in much less time [40,41]. It utilizes some clever algorithms that have either been built in some software such as Matlab or Labview or they can be written in any another computer programming languages by the analysts.

It was reported that FFT can provide an earlier prognosis of machine component failure and therefore it was widely used in the field of signal processing of vibration signals [42]. For instance, frequency-domain or spectral analysis of bearing signals is perhaps the most widely used approach for defect detection. FFT is classified as one of the linear methods of power spectral estimation, which is usually based on procedures employing linear methods that suffer from leakage, resolution etc. These methods, in effect, provide rectangular windowing in the time domain, which is equivalent to the convolution of the true spectrum of the data in the frequency domain. Naturally, this introduces a considerable amount of frequency leakage in the computed spectrum, which makes the detection of weak signals difficult [43]. The problem of leakage can be considerably reduced by the application of appropriate window functions, but at the expense of frequency resolution. In addition to this problem, minimum resolution is dependent only on the data length, irrespective

of a high signal-to-noise ratio. Though the linear methods give consistent estimates when the data length is large, the resolution that can be obtained becomes poorer as the data length decreases [43].

Another spectral estimation technique is the autoregressive technique (AR). An autoregressive model is defined as a model that used to predict the value of a given signal based on previous input values of the same signal. The main advantage of the AR method over traditional linear spectral estimation approaches such as FFT (Fast Fourier Transform) is that it can work with short data records and sampling rates. It also provides higher resolution capabilities, especially for short recorded data, over that achievable resolution with the conventional FFT [44]. The autoregressive technique was successfully applied to detect early fatigue cracks in rotating machinery [11,45-49]. Selection of a parametric model type, the use of the data samples to estimate the model parameters and the use of the model parameters to obtain the spectral estimation are the steps required to perform the spectral estimation using AR. It was reported that AR is an optimized tool that performs the same analysis, performed by conventional FFT, but in much less time by utilizing some clever algorithms [48].

Prony spectral estimation is another potential method for analyzing transient signals. Similar to the conventional Fourier transform, the Prony method first determines the linear prediction parameters that fit the sampled data. These parameters will then be used as coefficients to build a polynomial. The roots of this polynomial are finally employed to estimate frequency, amplitude, phase and damping components of a signal [43,50-52]. The Prony technique has been employed for monitoring of the machines health. Applications of the Prony method to determine the spectral estimation for transient vibration signals, generated from bearings, was computationally investigated. Unlike the conventional FFT, the Prony method was reported as an effective and efficient machine condition monitoring and diagnostic tool that can deal with short duration transient signals. Further, the Prony method was able to quantitatively determine the severity of faults [50].

The wavelet transform is a linear time-frequency representation method, similar to the spectrogram. The wavelet transform can overcome most of the FFT drawbacks [53]. It has particular advantages for characterizing signals at different localization levels in time. In the FFT, for instance the short time Fourier transforms, the length of window function will remain constant during the analysis of the signal. In the wavelet transform, this length can be changed by translation and expanding/contraction of a window function called the mother wavelet function [54]. Another important advantage of the wavelet transform is its ability to carry out local analysis. This property is of significant value in revealing any small change in the signal and distinguishes the wavelet transform from other signal analysis techniques. The variable time and frequency resolution of the wavelet transform is also one of its advantages; however, in the discrete wavelet transform, the frequency axis has a logarithmic scale (octave).

The octave scale of the frequency axis does not permit fine frequency resolution of the high frequencies. This characteristic of the frequency axis in the wavelet transform makes it a specialized method to be used for signals, which contain long-duration events at the low frequencies and short-duration events at the high frequencies. Wavelet analysis was widely studied to characterize vibration signals for machine health monitoring. The wavelet was reported as an effective tool that allows the machine operator to more easily detect the bearing faults which are impossible by the other frequency analysis methods. Further, it was recommended as a fault diagnostic tool for the practice in maintenance [37].

The spectrogram is a visual representation of a given signal. It can also be defined as the result of calculating the frequency spectrum of windowed frames of a given signal [55,56]. The results of conventional spectral estimation such as Fast Fourier transform, applied to an electronically recorded signal, describe the signal in terms of energy spread over its frequency components. A spectrogram does exactly the same but also takes the time into account. It displays the changes that occur over time, whilst spectra only provide stationary information about frequency and energy in a given interval in time. Analysis of a spectrogram can be displayed visually, with degrees of amplitude, represented

light-to-dark. At various frequencies, usually represented on the vertical axis by time on the horizontal axis, lighter spots mean lower energy densities whilst darker parts of the spectrogram represent higher energy densities [55,56].

2.4 Previous Work

2.4.1 Vibration Analysis

Condition monitoring of slow speed rotating machinery research dates to before the turn of the 21st century. For various applications, such as shafts, bearings, gearboxes, compressors, motors, turbines (gas and steam) and pumps, condition monitoring has remained a subject of intense study to the present day. An enormous amount of work has been performed on developing machine diagnostics and studying failure processes. Slow speed rotating machines are the mainstay of several industrial applications worldwide. They can be found in paper and steel mills, water industry, wind turbines etc. Operational experience of such machinery has not only revealed challenging design issues but has also presented opportunities for further significant improvements in the technology and economics of such machines. Failures associated with bearings represent the cause of extended outages and are typically caused by gradual deterioration and wear [42,57]. This section centres on the most relevant published work to the present study of monitoring technologies and schemes such as conventional vibration measurements and Acoustic Emission that have been used for monitoring slow speed rotating machinery components.

Universally accepted limit values, which classify machines as slow-speed or high-speed, have not been identified. However, 600 rpm is generally accepted as the minimum speed for intermediate-speed categorization [11]. As a consequence, any speed below this value can be classified as low-speed. Slow speed rotating machinery generates relatively reduced energy loss rates from damage related processes and therefore conventional condition monitoring technologies (e.g. vibration analysis) tend to be more difficult to apply [11,48]. Jamaludin et al [58,59] summarized the limitations in applying vibration to slow rotating machines.

These limitations make vibration monitoring of low-speed rotating machinery practically impossible. However, attempts have been made for monitoring both rolling element and plain journal bearings. Tandon et al [42] presented a detailed review of vibration and Acoustic Emission measurement methods to monitoring rolling element bearings. Kuboyama [60] suggested several techniques for monitoring low-speed (1 rpm) bearings. The Peak Level Differential Technique (PLDT) was applied to rolling element bearings. In this Kuboyama considered signatures generated from a number of bearings of the same type and size. Band pass filtering of the bearings natural frequencies was used to eliminate the Noise. Further, any acceleration peaks exceeding pre-set threshold levels were held by what was referred to as a "peak picker".

A comparison of two bearings is required to apply this technique. It was applied to pinch roller bearings which were operated at 1 rpm. When the peak level differential between both bearings and the number of occurrences exceeded a certain criteria the bearing was judged to have persistent damage. Kuboyama reported that flaking on the surface of the inner race on one of the bearings could successfully be detected. It should be noted that Kuboyama has neither described the measuring equipment nor characteristics of the sensor used. Moreover, Kuboyama concluded that technical difficulties prevented the techniques from being applied. The Self-Correlation method, Cycle Histogram method and Fe Content Detector are the other techniques employed by Kuboyama.

A Slow Speed Technology (SST) system was developed by Canada et al [61]. The system measured vibrations on low-speed machinery. The main function of the system was to discriminate the electronic noise of the sensor, with a specified level of statistical confidence, from the captured data. The adjusted data was further corrected for the distortion introduced by the analog integrator, i.e., introducing a gain to compensate for the roll-off characteristics of the integrator.

Another methodology for vibration monitoring of low speed machinery was proposed by Robinson et al [62]. The proposed technique is more or less similar

to the PLD method developed by Kuboyama. It divided the signal into segment time intervals, dependent on the sampling frequency, and obtained peak values for continuing time intervals until the desired number are captured for processing. Analogue or digital circuitry can be used to obtain the peak values. Further analysis of the peak values has involved spectral and waveform analysis. Comparisons of the peak value method with enveloping (demodulation) were also made. Enveloping involves high pass filtering, rectification (half or full wave), and low pass filtering to separate the assumed low-frequency modulating signal from the high-frequency carrier. The spectrum of the enveloped signal shows whether the vibration signal is random in terms of amplitude and phase, or whether there is a repetitive machine-speed related signature present. The proposed new method replaced the rectification process in demodulation with the peak value.

The mentioned method was applied on acquired signals and the results revealed that peak the value was shown to be independent of the speed of the machinery or analysing bandwidth whilst the enveloping was dependent on the speed of the machine, as well as analysing bandwidth. The sensitivity of the vibration technique decreases rapidly with decreasing machine speed and becomes unreliable for low-speed machines. Field measurements using low-frequency accelerometers on bearings rotating at 2 rpm showed that the peak value technique detected inner race defects one month prior to failure. It must be noted that Robinson has not defined the failure in this investigation.

Another attempt was made by Mechefske et al [63] to generate frequency spectra on low speed (<100 rpm) roller bearings with defects. In this investigation, parametric models (Auto-Regressive, AR) of amplitude demodulated vibration signals were used. It was reported that this technique has the advantage of using much shorter data lengths. To identify the bearing defects, differences in frequency spectra between good and faulty conditions were employed. Szrom [64] claimed successful detection of bearing defects at speeds as low as 48 rpm using a velocity-based vibration sensor.

It can be concluded that the conventional condition monitoring of slow-speed machinery using vibration analysis is fraught with difficulties. Further, where there have been claims of success, the period between detection and failure was very short. This will often progress to more serious damage affecting the operational performance of the machine. As consequence, the machine requires far more costly repairs than simply replacing a part. In addition to that, some of the authors failed to specify the equipment used for experiments. However, this is not the case for the Acoustic Emission (AE) technology which is well suited to detecting very small energy release rates. As a result AE is able to detect subtle defect related activity from machinery [65-68]. To date most published work on the application of AE to monitoring bearing mechanical integrity have been on artificially or 'seeded' damage which are generally induced with an electrical discharge system, engraving machine or by introducing debris into the lubricant [66].

2.4.2 Acoustic Emission Technology

A tremendous amount of work has been undertaken over the last 20-years in developing the application of Acoustic Emission technology for bearing health monitoring. Mba et al [69-71] undertook a laboratory test for condition monitoring of low speed rotating machinery using stress waves (SW's). A test rig was built to simulate mechanical defects such as frame looseness, a result of loss of tightening torque, rubbing of a broken support rod and media disc movement, as a result of creep. This investigation was divided into two parts. The first part presented an investigation of high-frequency stress wave analysis as a means of detecting the early stages of the loss of mechanical integrity in low-speed machinery. Investigations were centered on the rotating biological contactor (RBC) which rotates between 0.6 and 1 rpm.

In the second part, the authors were involved with the development of a monitoring system for RBC's and they also used the opportunity to assess the viability of the application of SW's to monitoring low-speed bearings having bore diameters ranging from 80 to 125 mm. SW signatures were obtained for each

fault condition on the testing rig. These signatures were recorded while the rig was operating with a mass loading equivalent to a thickness of 5 mm biomass growth. A commercially available piezoelectric type sensor, with an operating frequency range between 100 and 1000 kHz at temperatures ranging from -65 to 177 °C, was used. The pre-amplifier used on all experimental and 'on-site' tests was a PAC (Physical Acoustics Corporation) type 1220 A, specifically designed for AE measurements, having a bandwidth of between 20 and 1.2 MHz, at 20 V peak to peak. The pre-amplifier had a noise specification of less than 2 mV plus a switchable gain of (40–60 dB). A dual-channel 8-bit analogue-to-digital converter (ADC), Rapid Systems R2000 was used for data acquisition. The system provided sampling rates of between 1 Hz and 20 MHz, 128 Kb memory capabilities per channel, 100 percent pre-trigger and post-trigger capability and a selectable gain range of between 0.256 and 1280 V. The electronic noise level on the ADC system, with 60 dB amplification, had a peak voltage of 30 mV. AR (Autoregressive) coefficients were calculated instead of traditional AE pattern recognition techniques such as RMS., energy, counts and amplitude. It was concluded that the application of high-frequency SW analysis to monitoring low-speed rotating machinery has proved successful. It offers the diagnostician an opportunity to use this technique for monitoring all types of low-speed machinery, and not just rotating machinery.

Jamaludin et al [59] conducted an investigation into the applicability of stress wave analysis for detecting early stages of bearing damage at a rotational speed of 1.12 rpm (0.0187 Hz). Attempts had been made to generate a natural defect on the bearing components by fatiguing. However, after allowing the test bearing to operate for a period of 800 hrs under conditions of grease starvation, no defect and/or wear was visually detectable on any of the bearing components.

Stress Wave Analysis Technology Company (SWANTECH) [72] recently announced a new condition monitoring technology based on stress wave technology. It has been said that the patented SWANTECH stress wave analysis and monitoring system is ideal for applications where the equipment

being monitored is subject to rapidly changing operating conditions and external forces. The condition monitoring system, which used for wind turbine applications, is called SWAN*wind*. A further report stated that the SWAN*wind* system uses sound, rather than motion, to identify and directly measure friction and mechanical deterioration. Stress wave indications provide a direct measurement of the friction and wear, even early in the turbines life cycle.

In a further study, Morhain et al [73] examined the application of standard AE characteristic parameters on a radially loaded bearing. The use of typical AE parameters such as RMS and count values was validated as a robust technique for detecting bearing damage and was shown to correlate with increasing speed, load and defect size. Al-Ghamdi and Mba [74] conducted a comparative experimental study on the use of acoustic emission and vibration analysis for bearing defect identification and estimation of defect size. It was concluded that AE offered earlier fault detection and improved identification capabilities than vibration analysis. Furthermore, the AE technology also provided an indication of the defect size, allowing the user to monitor the rate of degradation on the bearing; unachievable with vibration analysis.

In another study, Holroyd [65] introduced Acoustic Emission as a relevant technology for condition monitoring of very slowly rotating machinery. It was stated that AE technologies can be successfully applied to monitoring the condition of very slowly rotating machinery. Holroyd has reported that a wide range of signal processing methods can be employed to detect the presence and amount of damage although cost and complexity limit their application. New signal processing algorithms (software algorithms for Extent®), which were developed by Holroyd Instruments based on their patented Acoustic Emission/ stress wave sensing technology [75], were introduced.

The software algorithm for Extent® was incorporated within portable instruments that include the MHC-Memo, MHC-Classic and MHC-Solo data loggers. Holroyd instruments also developed a system for online analysis. It should be noted that all Holoryd data loggers require the use of a special Holoryd sensor. They interpret the results in terms of two parameters i.e.

Distress® and decibel (dB) level. The natural frequency content of Holroyd AE transducers is around 100 kHz. To amplify and filter the signal into narrow band around this resonance, Holroyd AE transducers were incorporated with in-built electronics. A measured AE signal is processed through a series of components and the subsequent output is an overall voltage level in decibels that represents the mean RMS of the signal detected by the transducer with minimal error [76].

The Distress® parameter can be determined by passing the analogue dB level of a measured signal through analogue envelopers. These analogue envelopers will separately extract the means of the slowly changing (DC), and rapidly fluctuating (AC), parts of the signal and convert them into logarithmic form. The mean AC component of the signal is a function of the number and amplitude of short duration excursions in the RMS envelop. Thus, it represents the number and magnitude of impulsive Acoustic Emission events occurring in the machine. Distress® is then calculated by subtracting one mean form from the other. As these are in logarithmic format, this is equivalent to dividing the AC mean by the DC mean and therefore it compensates for any changes due to operating conditions or electrical nose. It was reported that Distress® is very sensitive to lubrication problems and can be used for scheduling the optimal times to re-lubricate. Furthermore, it can be used to give an early indication of bearing and gears faults.

Miettinen and Pataniitty [77] described the use of Acoustic Emission in the monitoring of faults in an extremely slow rotating rolling bearing (5 rpm). Prior to testing the test bearing had been naturally damaged on its outer race. It was concluded that the acoustic emission measurement was a very sensitive method for fault detection in an extremely slowly rotating bearing.

Choudhury and Tandon [78] applied the spark erosion method for seeding defects in bearings. AE measurements from bearings without defects and with defects of different sizes were undertaken. It was shown that the use of AE parameters such as ring-down counts and peak amplitudes could identify bearing defects. Price et al. [79] employed a four-ball lubricant test machine to simulate pitting fatigue and scuffing wear commonly experienced by gear and bearing

components. The principal monitoring technique utilized in this investigation was Acoustic Emission (AE). The study concluded that scuffing wear and pitting was detectable with AE.

To date the only investigation on identification of the onset of natural degradation in bearings involves the work presented by Yoshioka [80]. This focused on detection of a rolling contact subsurface fatigue crack using AE technology. An acoustic emission source locating system was developed and it was reported that the system was able to locate the AE source based on analysis of the time delay associated with AE events acquired simultaneously from different sensors. Yoshioka stated that cracks were identified parallel to the surface (maximum length of approximately 200 µm in the rolling direction of the balls, and were distributed between 50 µm and 200 µm below the surface). It must be noted that the tests undertaken by Yoshioka were on a bearing with only three rolling elements which is not representative of a typical operational bearing. Furthermore, tests were terminated once AE activity increased therefore the propagation of identified sub-surface defects to surface defects was not monitored.

Rotating shafts are fatigue loaded, have to resist a large number of cycles, are difficult to access for maintenance and inspection and are vulnerable to crack nucleation and growth. Although a tremendous amount of work has been undertaken over the last decades in developing the application of the condition monitoring technologies for machine health monitoring, to date there are no off the-shelf techniques developed for monitoring low speed rotating shafts.

3 Acoustic Emission Technology

In the preceding chapter, available condition monitoring technologies, both their applicability and drawbacks in slow speed rotating machinery applications were briefly discussed. In this chapter, Acoustic Emission technology is discussed in more detail.

3.1 Introduction

The condition monitoring and diagnosis of slow speed rotating machinery requires a variety of measurement technologies. Condition monitoring technologies, that are available for use such as vibration diagnostic, Acoustic Emission, thermography, and oil analysis, are frequently applied. The selection of a condition monitoring system is not a simple task. Many factors must be considered when selecting the condition monitoring system for a particular application and slow speed rotating machines are not any exception. These factors include, for instance, the fault detection sensitivity, applicability of technology and accessibility of monitoring, instrumentations costs, number of components, and size of machine requiring inspection.

Slow speed rotating machines are the mainstay of several industrial applications worldwide. Slow speed rotating machinery generates relatively reduced energy loss rates from damage related processes and therefore conventional condition monitoring technologies (e.g. vibration analysis) tend to be more difficult to apply. Jamaludin et al [58] summarized the main problems associated with applying the conventional vibration monitoring techniques to such slow rotating machines. However, Acoustic Emission (AE) technology is well suited to detecting very small energy release rates. The high sensitivity of AE in detecting the loss of mechanical integrity as compared to the well established vibration monitoring technique has become its principle advantage for machine health monitoring. As a result AE is able to detect subtle defect related activity from machinery, even when it is rotating very slowly [59,66].

Acoustic Emission has received a great deal of interest during the last few decades. A recent review has detailed the application of AE technology to monitoring a range of rotating machines [66]. Further, Acoustic Emission systems are reported to be the most robust and powerful diagnostic tools for condition monitoring, as they apply excellent and appropriate analytical tools to the problem. When the fault detection sensitivity is the primary consideration for choosing a condition monitoring technology, Acoustic Emission sensors show their effectiveness and superiority of producing a detectable indication from a small defect. In other words, AE can provide an early warning of incipient problems, so that proactive maintenance can be conveniently planed and performed while actual damage is still minor. Acoustic Emission is also more reliable and cost effective than conventional systems for global scanning of rotating machinery. It also provides flexible portable instrumentation.

3.2 Definition of Acoustic Emission (AE)

Acoustic Emission (AE) is defined as the class of phenomena whereby transient elastic waves are generated by the rapid release of energy from localized sources within a material [81]; typical frequency content of AE is between 100 kHz to 1 MHz. The source of these emissions in metals is closely associated with the dislocation movement accompanying plastic deformation and the initiation and extension of cracks in a structure under stress. It can be also defined as: The monitoring technique which analyses elastic wave frequencies naturally generated above the human hearing threshold, in the order of 25 kHz to 1 MHz. It is associated with a range of phenomena which generate broadband activity from the transient release of stored energy from localized sources. This high frequency elastic wave activity is typically structure borne but certain source processes additionally generate airborne activity [82]. Sources of AE in rotating machinery include impacting, cyclic fatigue, friction, turbulence, material loss, cavitations, leakage, etc. For instance, the interaction of surface asperities and impingement of the bearing rollers over a defect on an outer race will result in the generation of acoustic emission. Other sources of AE emissions include [83]:-

- Plastic deformations, dislocation motion, rupture of the inclusion, phase transformation, twin/slip deformation.
- Different stages of crack propagation (static, fatigue, stress corrosion). AE is sensitive enough to detect newly formed crack surfaces down to a few hundred square micrometers and less.
- The weld defects: lack of penetration and fusion, cracks, inclusions and porosity.
- Corrosion: localised corrosion / pitting corrosion. Detecting and monitoring of active corrosion, corrosion fatigue, and intergranular stress corrosion cracking.
- Friction.
- Mechanical impact.
- Leaks (liquid or gas).
- External noise (mechanical, electrical, and environmental).

These emissions propagate on the surface of the material as Rayleigh waves and are measured with an AE sensor. Other wave types associated with the propagation of AE include Lamb, Longitudinal and Shear waves. Basically, there are two types of AE signals, burst (transient) and continuous signals. The beginning and end of the signal deviate clearly from the background noise with AE burst (transient) signals. In the continuous AE signals variations of amplitude and frequency can be clearly seen but the signal never ends.

Detection and conversion processes of these high frequencies elastic waves into electrical signals, which AE technology is based on, can be implemented by coupling sensitive AE sensors on the surface of structure under test and applying an external stimulus. Outputs of AE sensors are amplified through a low-noise preamplifier, filtered out to remove any unwanted noise and further processed by suitable electronics systems. The most important aspect of AE, compared to other non destructive techniques, is that the material itself generates the signals [12]. Some factors affect the relative amplitude of the acoustic emission response. These factors are presented in table (3-1) [77].

Table 3—1 Factors that affect the relative amplitude of AE response.

Factors Increase AE Response Amplitude	Factors Decrease AE Response Amplitude
High Strength	Low Strength
High Strain Rate	Low Strain Rate
Low Temperature	High Temperature
Non-homogeneity	Homogeneity
Thick Sections	Thin Sections
Brittle Failure (Cleavage)	Ductile Failure (Shear)
Materials Containing Discontinuities	Materials Without Discontinuities
Material Phase Transformations	Plastic Deformations
Crack Propagation	Wrought Materials
Cast Materials	Small Grain Size
Mechanically Induced Twinning	Thermally Induced Twinning

The so-called Kaiser Effect is a particular phenomena that affects the activity of the Acoustic Emission. The Kaiser Effect can be described as the absence of detectable acoustic emission until the previous maximum applied stress level has been exceeded, see figure (3-1). The Kaiser effect means that when a defined stress has been applied on the material and it has caused Acoustic Emission, additional emission will not be induced in to the material until the defined level of stress has been exceeded, even if the load is completely removed and then reapplied [77].

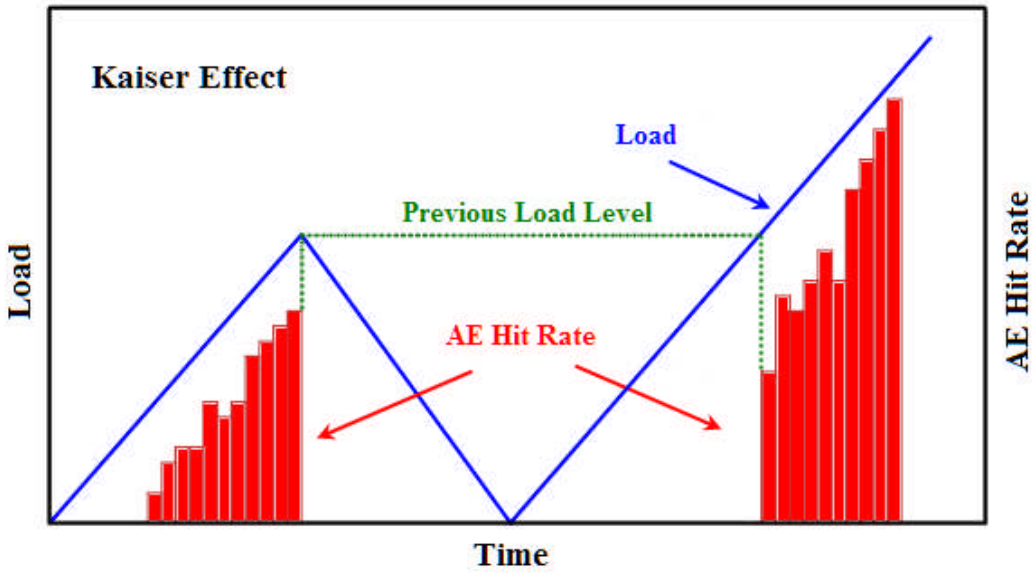

Figure 3—1 Example of Kaiser Effect

3.3 Applications of Acoustic Emission Technology

Different kinds of materials can non-destructively be monitored using Acoustic Emission technology. This includes:-

- Metals: steels, stainless steel, carbon steel, alloy, ferritic steel, aluminium, aluminium alloys, magnesium alloys, and others (e.g., copper and its alloys, uranium alloys, titanium, and zirconium alloys).
- Composite materials and polymers: sandwich composite, glass-reinforced plastic (GRP) and carbon fibre.
- Concrete, reinforced concrete.
- Rocks.
- Woods.

As a consequence, AE technology is now experiencing an important renaissance as a valuable predictive maintenance and condition-based monitoring (CBM) tool. With the increased focus on cost-effective ways of optimizing machine and equipment and availability reliability, the applications of Acoustic Emission are very extensive. Applications of Acoustic Emission technology can be found in [84,85]:-

- Pressure equipment: Fundamental research and development efforts in the control of the damage in materials by acoustic emission have grown in the last twenty years. This technique has become a reliable and standard method of non-destructive testing for pressure vessels. AE is used to monitor flaws, corrosion, and leakage in pressure vessels, LPG, tanks, piping systems, steam generators.
- Aircraft and aerospace: aerospace structures, wings, bulkhead, fuel tanks, rocket engine, real time monitoring.
- Petrochemical and chemical: storage tanks, reactor vessels, offshore and onshore platforms, drill pipe, pipeline.
- Marine: corrosion, composite shell, engine and power plant;
- Civil engineering: bridges, dams, suspension cable bridges, concrete structure reinforced by composite.
- Research and development: acoustic emission is a good technique to monitor and study the damage in materials and their mechanical properties (new materials, smart materials, Shape memory alloys (SMA)).

- Wind turbine: blades damage.

3.4 Acoustic Emission Sensors

The right selection of sensors is the fundamental of any successful monitoring process. A wide variety of sensors have been utilized to monitor machine health. Most of the attempts were centered on component condition monitoring such as component wear, component breakage and component life. Acoustic Emission sensors are attached to an object's surface to detect dynamic motion resulting from Acoustic Emission events and then convert this detected motion into voltage-time signals that are used for all subsequent steps in the Acoustic Emission measurements. The type and the characteristics of the sensor strongly influence the characteristics of the obtained electrical signal. As a consequence the success and repeatability of Acoustic Emission testing depends so strongly on the resulting electrical signal, and its characteristics.

To detect Acoustic Emission events, a wide range of basic transduction mechanisms, capacitive transducers, displacement sensors or even laser interferometers, can be used. Most commonly Acoustic Emission tests are performed with sensors that use piezoelectric elements for transduction. A special ceramic such as lead zirconate titanate (PZT), see figure (3-2) [86], is usually used as the transduction element [87,88]. The surface of the sensor is acoustically coupled to the surface of the structure under test so that the dynamic surface motion propagates into the piezoelectric element. Finally, the dynamic strain in the element produces voltage-time signals, which are further processed, as the output of the sensor.

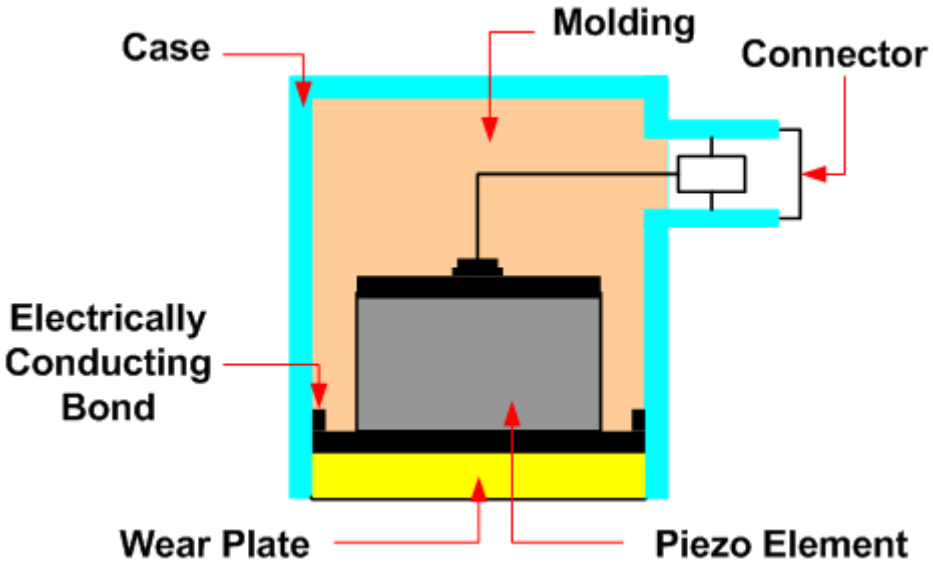

Figure 3—2 Basic setup of an AE sensor

3.5 Calibration and Attenuation Test

There are two common groups of calibration techniques typically distinguished as equipment testing and sensor calibration. AE equipments are commonly designed to extract a set of parameters from the recorded AE signals and are later stored. Thus, the characterizations of these signals are mainly based on the type of equipments commercially available and therefore verifying the AE signal parameters recorded by these equipments is very essential. This can be implemented by a comprehensive check on all devices (equipments) used in any AE measurements. However, prior to the real full scale AE tests, the verification performance test of AE equipments must be done and results are compared against published performance criteria provided by the manufacturers.

Techniques used on AE sensor calibration for different AE applications; both for laboratory or field scale were presented and sufficiently discussed in several documents [89]. In general, manufacturers provide calibration certificates which come with all AE sensors. These certificates display the characteristics and the used method for calibration, see figure (3-3) [90]. It should be noted that ASTM-E976, is the Standard Guide for Determining the Reproducibility of Acoustic

Emission Sensors Response whereas ASTM-E1106, is the Standard Method for Primary Calibration of Acoustic Emission Sensors [91].

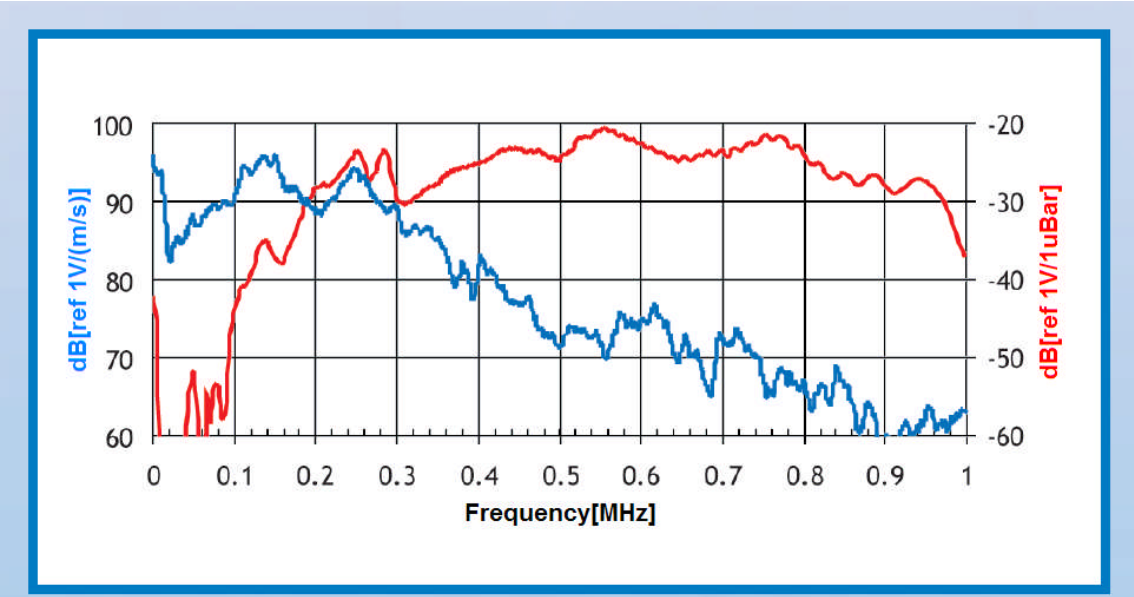

Figure 3—3 Example of AE sensor calibration certificate

AE sensor calibration can regularly (quality guarantee) be performed using the attenuation test. In practice, AE waves, which propagate through the structure under test, may be deviated and strongly attenuated. Attenuation can be described as any reduction (or loss) in the AE signal strength (in form of amplitude or intensity). Attenuation occurs as a natural consequence of long distance travelled by a signal (analogue or digital) through the medium and it is expressed in decibels (dB's). Attenuation is the term used to describe the reduction in the amplitude of a wave as a result of a range of natural processes. As an AE wave spreads from its point of origin the most significant initial reduction in amplitude is due to geometrical expansion of the wave-front [82]. In acoustic emission applications, attenuation is very important property because it determines the signal strength as a function of distance; therefore, it plays a significant role to validate the locations of AE sensors. Thickness and type of medium can directly affect the attenuation value [82]. There is an attenuation coefficient (β) for each type of medium used to determine how much AE signal

amplitude decays based on its frequency. Attenuation can be expressed therefore as a function of medium coefficient (β), transmission distance (r) and the signal frequency (f).

$$At = \beta * r * f \tag{3-1}$$

The amplitude of a given signal is a maximum (positive or negative) AE signal departure during an AE hit and it can be calculated as function of the maximum amplitude of a given signal.

$$SA = 20\ Log_{10}\left(\frac{V_{max}}{10^{-6}}\right) \tag{3-2}$$

The attenuation between two different locations i.e. a signal source and a signal destination can be calculated by knowing the signal power and/or the signal voltage at each location. If (P_s) and (V_s) are the signal power and the signal voltage at the signal source location respectively and (P_d) and (V_d) are the signal power and the signal voltage at the signal destination location respectively, the attenuation between the two locations can be calculated as:

$$SE = \int_0^{T(sec)} \alpha^2(t)dt \tag{3-3}$$

$$SP = \frac{SE}{T(sec)} = \frac{1}{T(sec)} \int_0^{T(sec)} \alpha^2(t)dt \tag{3-4}$$

$$At_P = 10\ Log_{10}\left(\frac{P_s}{P_d}\right) \tag{3-5}$$

Or by signal voltage:

$$At_V = 20\ Log_{10}\left(\frac{V_s}{V_d}\right) \tag{3-6}$$

A sensor attenuation test is carried out before performing any AE test. The first assignment is to simulate the AE source and the most common technique uses the Hsu–Nielsen source, shown in figure (3-4). This technique is based on pencil lead breaks [92]. The test is performed by breaking the lead pencil with

specific dimensions against the surface of the structure being monitored. A device (named after developer of the technique) is an aid to simulate an acoustic emission event using the fracture of a brittle graphite lead in a suitable fitting. This test consists of breaking a 0.5 mm (alternatively 0.3 mm) diameter pencil lead approximately 3 mm (+/- 0.5 mm) from its tip by pressing it against the surface of the piece. This generates an intense acoustic signal, quite similar to a natural AE source that the sensors detect as a strong burst [93]. Hsu–Nielsen sources provide a sufficient verification of good excursion of AE events from the source to the AE sensors. Further they also verify the accuracy of a good acoustic contact between AE sensors and the surface of the structure under test.

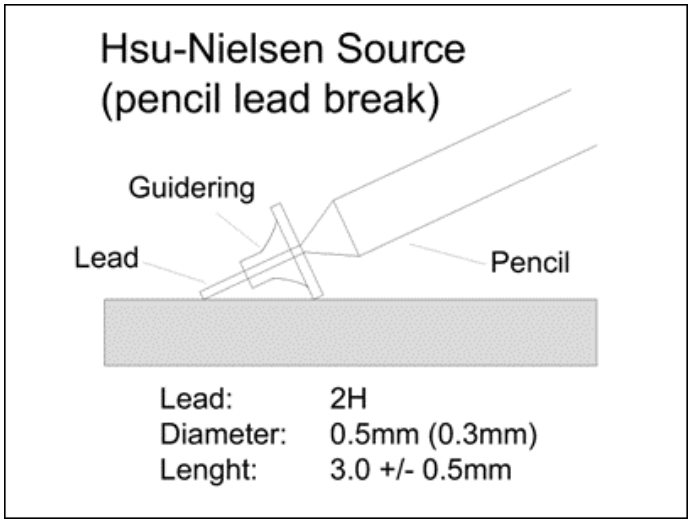

Figure 3—4 Hsu-Nielsen source

3.6 Acoustic Emission Measurements

AE signals are typically recorded and analyzed with success in different applications using different techniques. Two approaches were used in this research program. The first approach is called the classical AE technique (Hit Driven Data Measurements) whereas the second approach is a signal based AE technique (Time Driven Data Measurements). Extraction of the required information from the detected signal is the role of signal processing.

3.6.1 Hit Driven Data Measurements

In this method, AE events are recorded using AE sensors and a set of conventional parameters such as counts, amplitude, rise time, peak levels and the area under the rectified signal envelope (energy) is extracted from the signal and later stored (traditional AE method). The signal itself is not stored. A correlation between these AE features and the failures and defect formation can further be developed. In these investigations, AE characteristics represent only the recorded signals (i.e. signals crossing the threshold) without accounting for wave propagation and source of the signals. Other parameters such as pressure, load, deformation, and temperature can also be measured as inputs. Figure (3-5) shows the relationship of the most commonly used features [86].

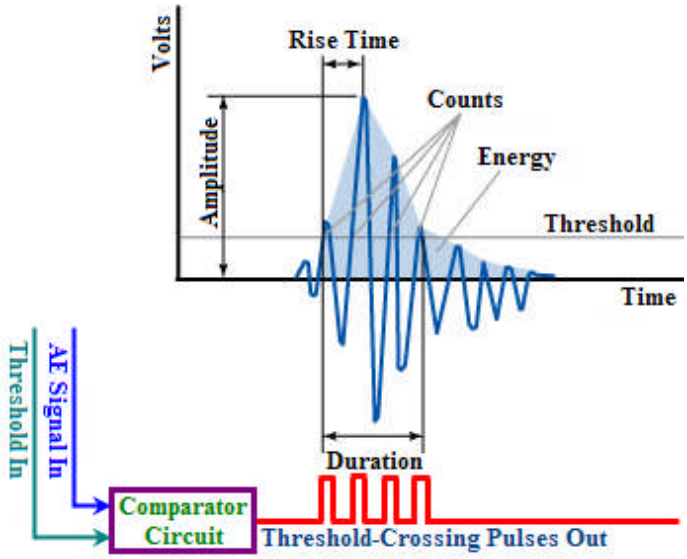

Figure 3—5 Common measured parameters of AE signals

- Ring down count: the number of times the signal amplitude exceeds the present reference threshold.
- AE event: a micro-structural displacement that produces elastic waves in a material under load or stress.
- Rise time: the time taken to reach peak amplitude from the first present threshold voltage crossing of the signal.
- Peak amplitude: this can be related to the intensity of the source in the material producing an AE signal.

- RMS voltage: a measure of signal intensity.
- Arrival time (time of first threshold crossing, needed for location calculation).
- Signal duration (time between first and last threshold crossing).
- Energy (integral of the squared (or absolute) amplitude over time of signal duration).

3.6.2 Time Driven Data Measurements

In this method, the global AE waveform of any AE test can continuously be recorded. AE waves are converted from analogue-to-digital and stored. Using this approach will lead to more comprehensive (time-consuming) analysis of the data. The capability of wide-band, high-sensitivity sensors developed recently and the rapid improvement of computer technology made quick data acquisition and analysis of AE waveforms viable. Since the new AE systems can continuously acquire AE waveforms at different sampling rates and therefore characterization of the nature of AE sources from the waveform captured by AE systems is now possible. Figure (3-6) shows three examples of the typical trend of the AE waveforms. The software (AE signal processing package) incorporated within the PC's also allows to monitoring and recording of AE parameters such as counts, RMS, amplitude and energy at defined time constants and sampling rates.

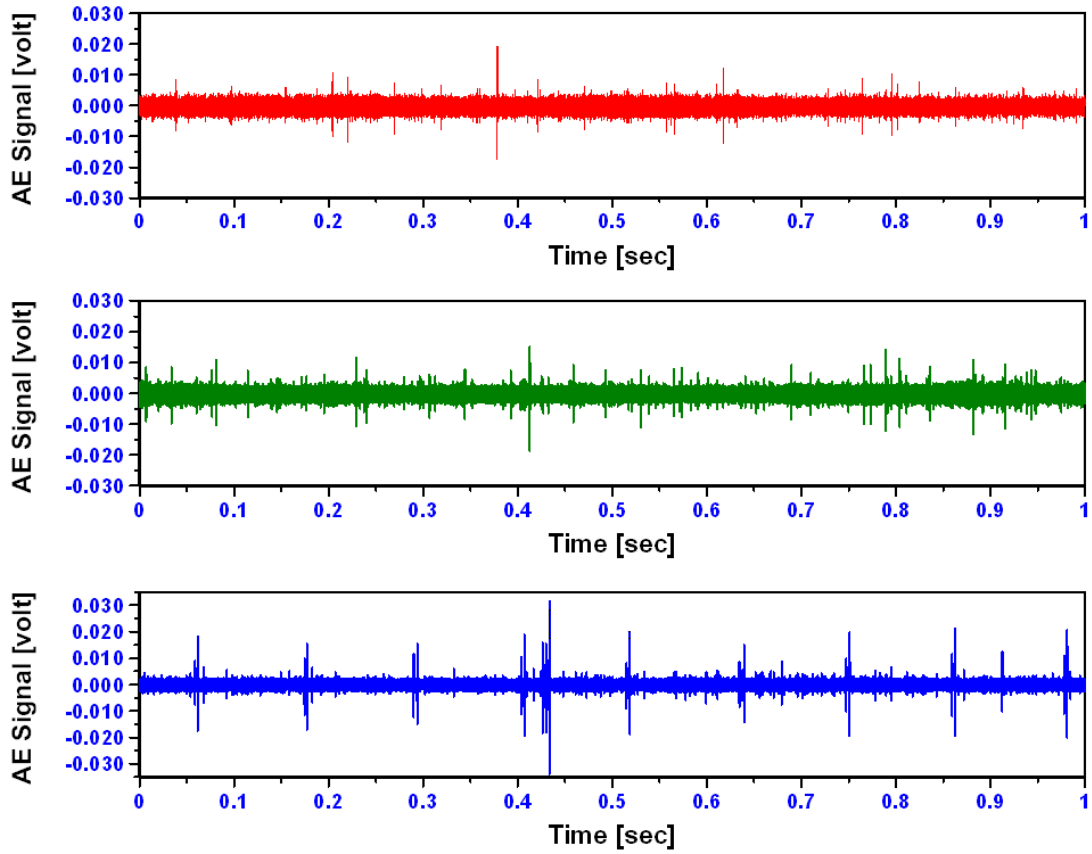

Figure 3—6 Example of Acoustic Emission waveforms

Various signal processing techniques are used to analyse AE signals and extract features related to defects. Usually, a threshold level is defined. The AE threshold needs to be exceeded before further analysis. Signal waveforms can be analysed using the time and frequency domains. There are several time and frequency domain techniques used to analysis AE signals. The main methods include calculation of enveloping curves, time series analysis, Fast Fourier transform (FFT), Gabor transform (or window (local) Fourier transforms), Wigner–Ville distribution, and wavelet transform [94]. Signals can also be characterised by statistical averaged parameters such as Mean, Standard Deviation, Skewness, Kolmogorov-Smirnov Test (k-s test), Energy Index (EI) or Kurtosis. The most commonly used techniques were discussed in the preceding chapter.

3.6.3 Acoustic Emission Source Location

One of the major advantages of the AE technique as an on-line monitoring tool over other non-destructive test methods is its capability to detect signals in real-time that are emanating from the structure under test [95]. Further, it can locate active defects in larger structural components without having to physically scan them. Determination of the AE source location is an extremely powerful tool in AE analysis and can be used to monitor a relatively large structure with a minimum number of sensors. For instance, this is a tremendous advantage in the case of vessels, especially when they are insulated, as very few access holes are needed for placement of AE sensors to determine structural integrity of the vessel. All other NDT techniques require all the insulation to be removed for full inspection, making them much more expensive than AE examination techniques.

AE signals travel from the source through the structure under test and can be detected by an AE sensor placed on the structure. Thus the Acoustic Emission source can be located if more than one sensor are located some distance from the source. Although AE sensors are subject to attenuation dispersion due to in-homogeneity and geometry of the material they still detect the signals [86].

AE source location is mainly based on the wave propagation principles within the materials. It is achieved by measuring the signal's arrival time at different sensors and processing triangulation calculations. By known arrival time difference and sound velocity, the distance difference between a source (defect) and different sensors can be determined. Figure (3-7) shows an example of the principle of AE localization and the arrival time differences between AE channels. The arrival time at the sensor 1, which was hit first in this example is marked as the zero value of the time axis of channel 1. The arrival time differences between channel 1 and the channels 2, 3, and 4 can be read at the time axes of the waveform diagrams, see figure (3-7) [86].

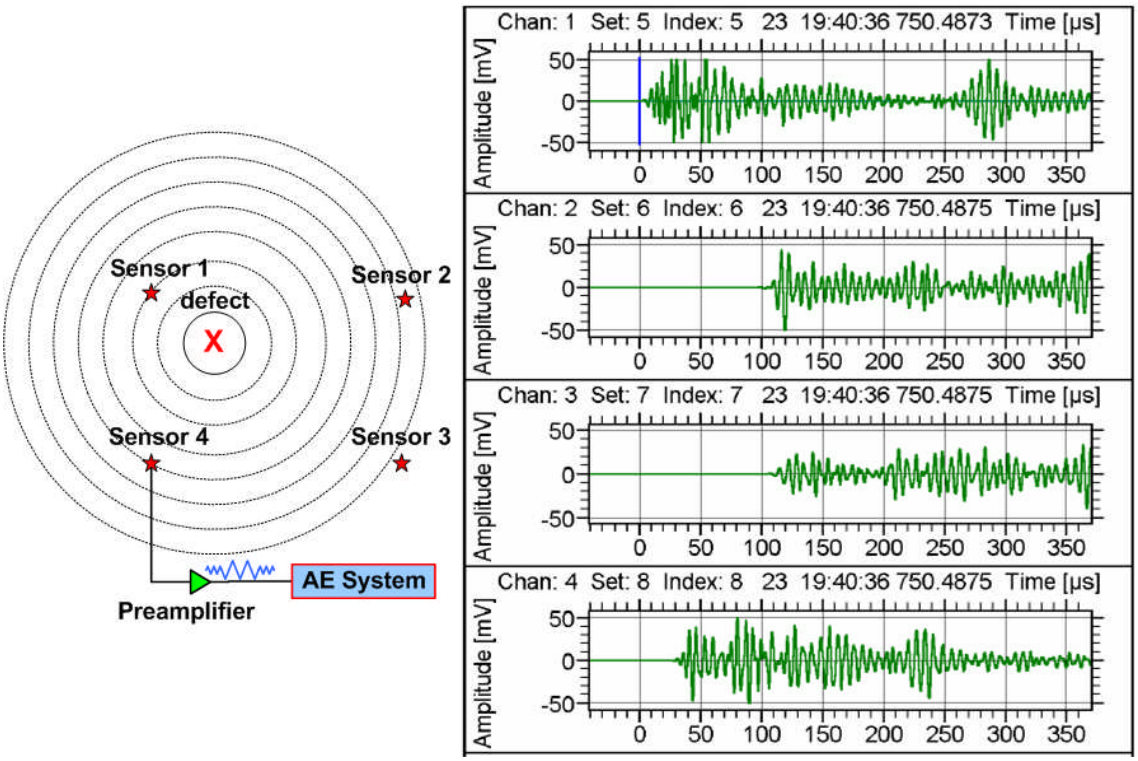

Figure 3—7 Principle of AE localization and the arrival time differences

Different methods that are commonly used for source location include one dimension, two dimension and three dimension approaches [86,96]. In the one dimension approach (a line), two sensor arrivals are required to determine the source location. To identify the location in two dimensions (over a surface or plane) three sensor arrivals are used whilst a minimum of four sensor arrivals are required in the three dimension approach.

Another location analysis, the so-called zone location technique, is used. It is based on the principle that the sensor with the highest AE output will be located closest to the source. The aim of this is to trace the waves to a specific zone or region around a sensor. The dimensions of the selected zones can be areas, lengths or volumes depending on the dimensions of the array. More accurate results, using time differences and attenuation characteristics of the wave, can be achieved if additional sensors are added [97].

The cluster technique can also be applied to analyze the severity of an AE source by monitoring multiple AE events in the same area. Clustering can be defined as a mathematical method used to find the point density within a certain

area [86,96]. Figure (3-8) depicts an example of clustering analysis applied on a spherical storage tank for natural gas where big circles represent concentrations of location [86]. The cluster circle indicates the number of located events within the cluster. These clustered areas encompass a high number of events that show places of repetitive AE-sources. These sources indicate a potential for defects or disturbers and can occasionally be quickly identified as rubbing materials, annexes etc.

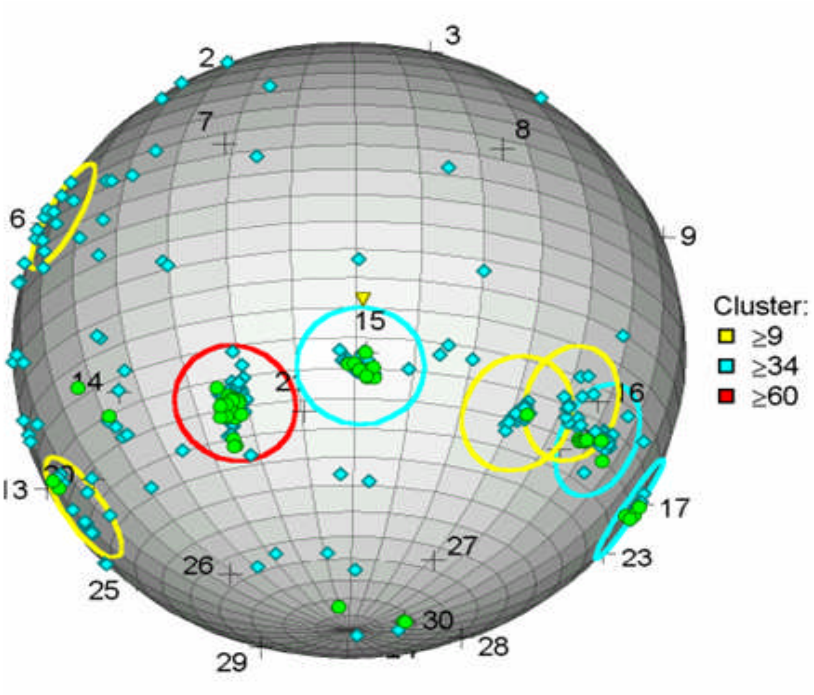

Figure 3—8 Cluster analysis for spherical storage tank for natural gas

3.7 Advantages and Disadvantages of AE Technology

Acoustic Emission technology offers distinct and essential advantages compared to conventional non-destructive inspection techniques. Compared with the alternative methods of condition monitoring, AE has its own advantages and disadvantages. Advantages and disadvantages of AE technology are listed below [77].

Table 3—2 Advantages and disadvantages of AE technology.

Advantages	Disadvantages
Unaffected by typical environmental noise.	Requires highly specialised sensors and signal processing.
Applicable to all machines irrespective of operational speed.	Sensitive to sources e.g. turbulence, crushing, etc.
More sensitive to activity from faults than from normal running.	Signals are weaker than vibration signals.
Can provide sensitive yet simple indications of fault presence.	Attenuation
Provides good trending parameters.	
Localisation of measurements to the machine being monitored.	

4 Bearing Condition Monitoring

In this chapter, details of bearing test rig design, laboratory experiments, results and observation are discussed. Figure (4-1) summarises in sufficient detail the steps followed from the basic design till the results interpretation.

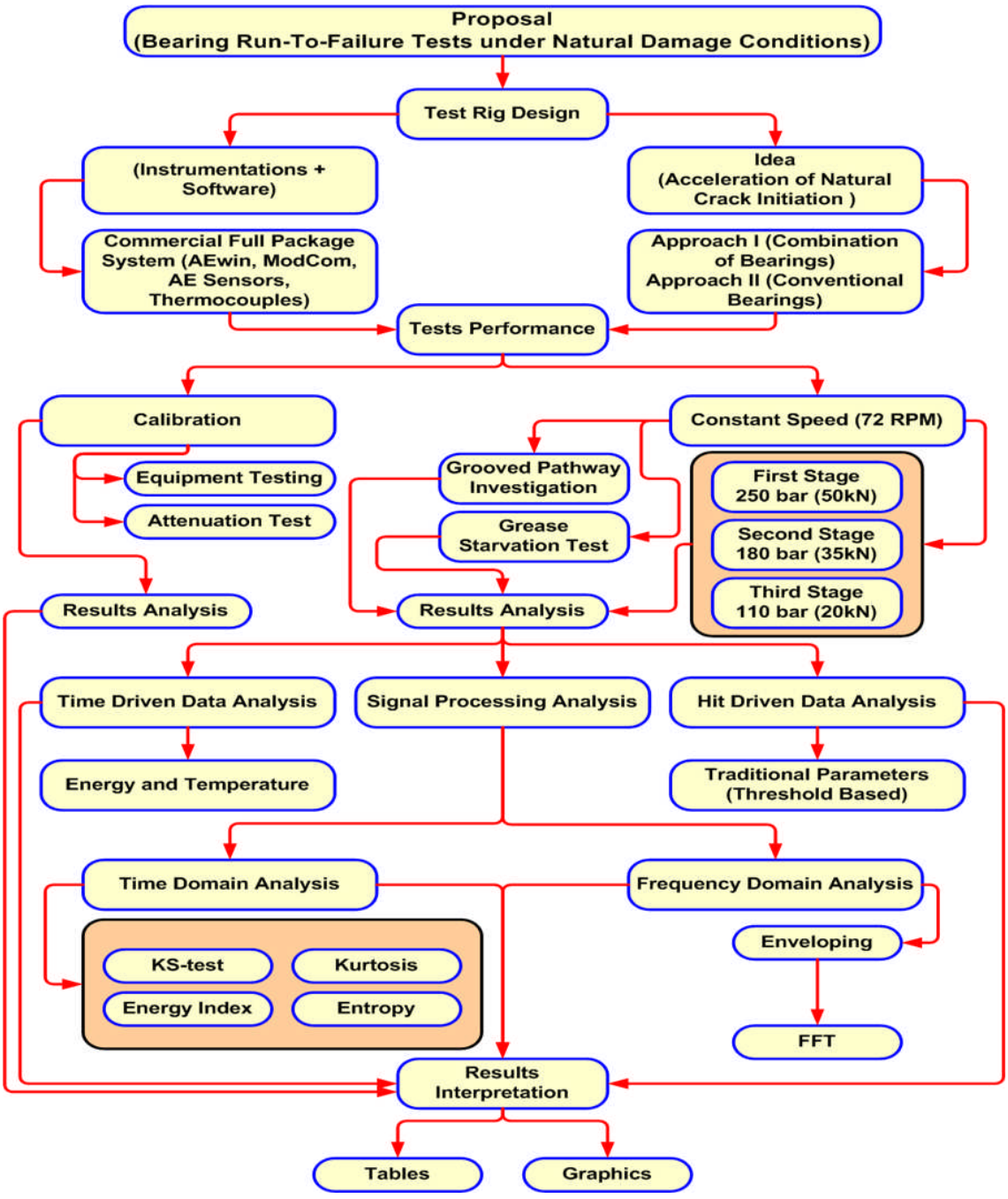

Figure 4—1 Steps of bearing test from basic design to the results interpretation

4.1 Test-Rig Design and Layout

In order to investigate the feasibility of the use of AE technology for incipient bearings deterioration, an experimental test rig was required. One of the challenges was to accelerate the natural crack signatures at the early stage of defect development. To implement this, a combination of a thrust ball bearing and a thrust roller bearing was selected for the first approach at loads ranging from 20, 35 and 50 kN. One race of thrust ball bearing (SKF 51210) was replaced with a flat race taken from thrust roller bearing (SKF 81210 TN) of the same size, as shown in figure (4-2). As a consequence, this arrangement caused higher contact pressure on a flat track relative to the grooved track due to the reduced contact area between the ball elements and the flat race. In the second approach, attempts had been made to generate a natural defect on the bearing components by allowing the conventional thrust roller bearing (SKF 51210) to operate under conditions of grease starvation, see figure (4-3).

For this study, bearing run to failure tests were performed under natural damage conditions. A specifically designed test-rig, as shown in figure (4-4), was employed for this investigation. It consisted of a hydraulic loading device, an electrical geared motor (MOTOVARIO-Type HA52 B3-B6-B7 j20, 46-Lubricated: AGIP), a coupling and a supporting structure. The test bearing was placed between the fixed thrust loading shaft and the rotating disk, which housed the grooved race. The flat race was fitted onto the loading shaft in a specifically designed housing. This housing was constructed to allow for placement of AE sensors and thermocouples directly onto the race, see figure (4-2). The thrust shaft was driven by a hydraulic cylinder (Hi-Force HYDRAULICS-MODEL No: HP110-HAND PUMP-SINGLE SPEED-WORKING PRESSURE: 700 BAR) which moved forwards to load the bearing and backwards to allow periodical inspections of the test bearing face. The rotating disk was driven by a shaft attached to a geared motor with an output speed of 72 rpm. A thrust bearing (SKF 81214 TN) was placed between the coupling and the test bearing to react to the axial load. A flexible coupling was employed between the shaft and the geared motor.

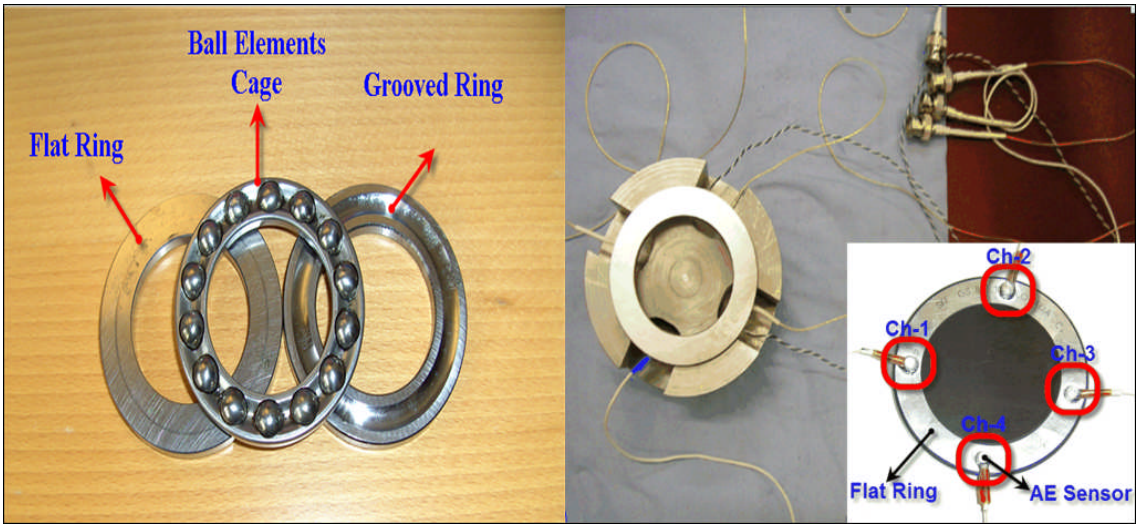

Figure 4—2 Test bearing arrangement for accelerated failure on the flat race

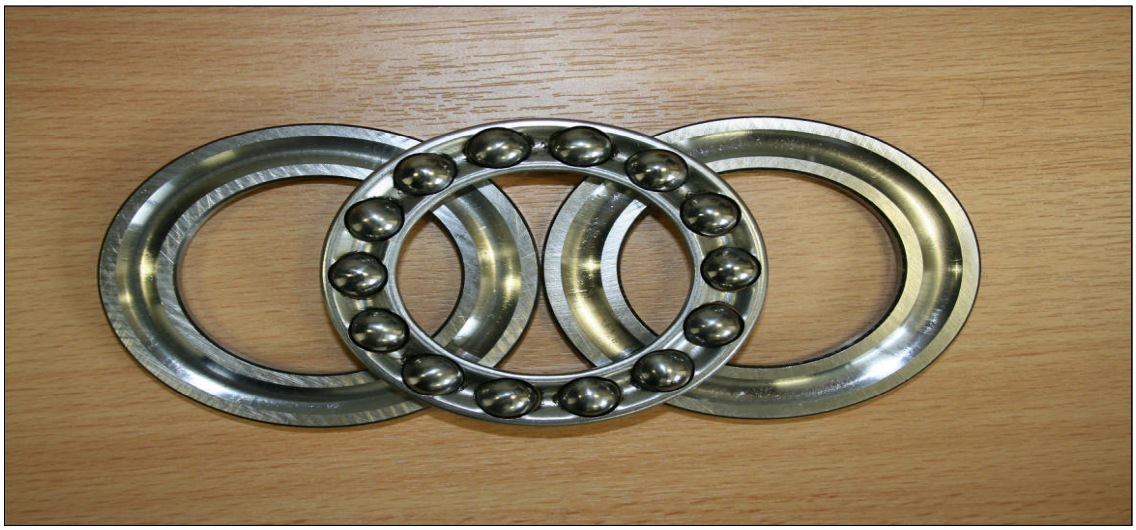

Figure 4—3 Test bearing run under starvation of grease

Under normal conditions of load, rotational speed and good alignment, surface damage begins with small cracks, located between the surface of the flat track and the rolling elements, which gradually propagate to the surface generating detectable AE signals. To determine the sub-surface stresses on the test bearing and thereby estimate the time, or number of cycles, to surface fatigue on the race the following theories were employed: the Hertzian theory for determining surface stresses and deformations [98], Thomas and Hoersh theory for sub-surface stress [98] and, the Lundberg and Palmgren theory for fatigue evaluation [99]. For the grooved race the standard procedure, as described by BS

5512; 1991 [100], was employed for determining the dynamic load rating. Further, the SKF interactive engineering catalogue was used for the test bearing selection [101].

Finally, the anticipated life for defined stresses were computed for both the grooved and flat races and results of the first approach clearly illustrated that surface fatigue, such as flaking, could be initiated on the flat race within a few days depending on the load condition thereby authenticating the test-rig design. It should be noted that the theoretical estimation of rolling contact fatigue is known to be subject to variability or scatter when compared to experimental results and this has been attributed to the probability of inclusions in the steel material located in the highest load zones of the race. It is also worth noting that the actual test period leading to visual damage on the flat race was much faster than predicted by the theoretical calculations. This variation was random but always earlier than predicted; see table (4-1) and appendix A. This is attributed to issues such as misalignment, unbalance, etc, which are not incorporated in theoretical estimates; however, best efforts were undertaken to minimise this.

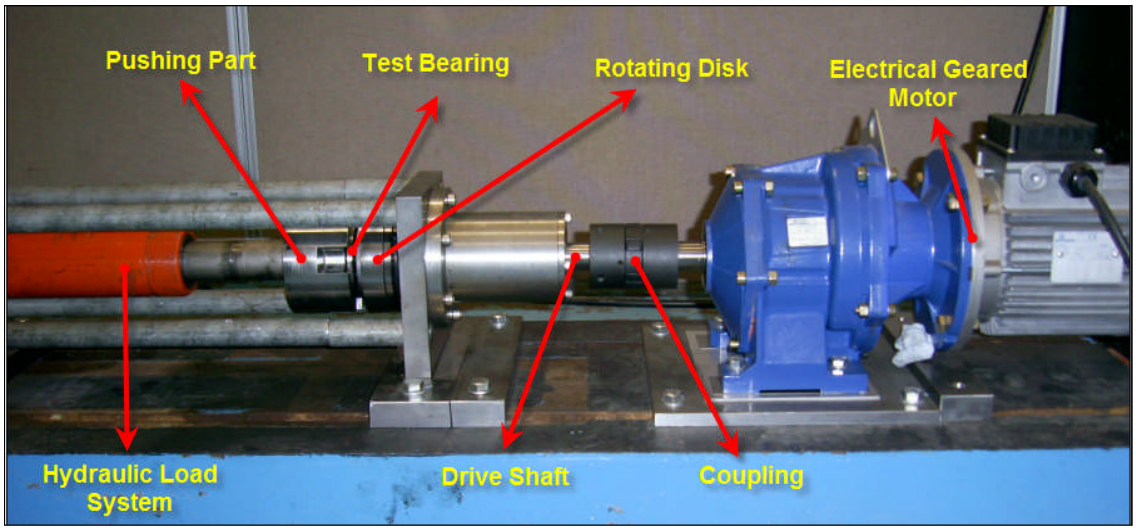

Figure 4—4 Test-Rig layout

Table 4—1 Predicted and experimental life of test bearing races (Approach I).

Case	Load (kN)	Predicted Life (hr)		Experimental Life (hr)	
		Flat Race	Grooved Race	Flat Race	Grooved Race*
I	50	24	432	16	-
II	35	72	1272	20	-
III	20	384	6864	50	-

*Tested were terminated once the crack has occurred on the flat races.

4.2 Instrumentation and Acquisition System Calibration

A schematic of the data acquisition process is detailed in figure (4-5). The AE acquisition system employed commercially available piezoelectric sensors (Physical Acoustic Corporation type "PICO") with an operating range of 200-750 kHz at temperatures ranging from -65 to 177 ^{o}C. Four AE sensors, together with two thermocouples (RoHS-Type: J x 1M 455-4371) were attached to the back of the flat raceway, see figure (4-2). The acoustic sensors were connected to a data acquisition system through a preamplifier, set at 40dB gain, see figures (4-5). The system was continuously set to acquire AE absolute energy (Joules) over a time constant of 10 ms (millisecond) at a sampling rate of 100 Hz. The absolute energy is a measure of the true energy and is derived from the integral of the squared voltage signal divided by the reference resistance (10 k-ohms) over the duration of the AE signal. In addition to continuous recording of AE absolute energy (Atto-Joules = 10^{-18} Joules), traditional AE parameters such as counts, amplitude and ASL were also measured. The ASL is a measure of the continuously varying and averaged value of the amplitude of the AE signal in decibels (dB's). The ASL is calculated from the root mean square (RMS in Milli-volt) and is given as [97]:-

$$ASL=20\ Log_{10}\left(1.4 * RMS/100\right) \qquad (4\text{-}1)$$

The traditional parameters were calculated over an AE event duration of 1500 µsec and a threshold of 52 dB. The threshold value was set at approximately 3 dB above the operational background noise of the bearing. In addition AE

waveforms were periodically acquired at a sampling rate of 2 MHz. In all cases, AE measurements were taken simultaneously from all four AE sensors.

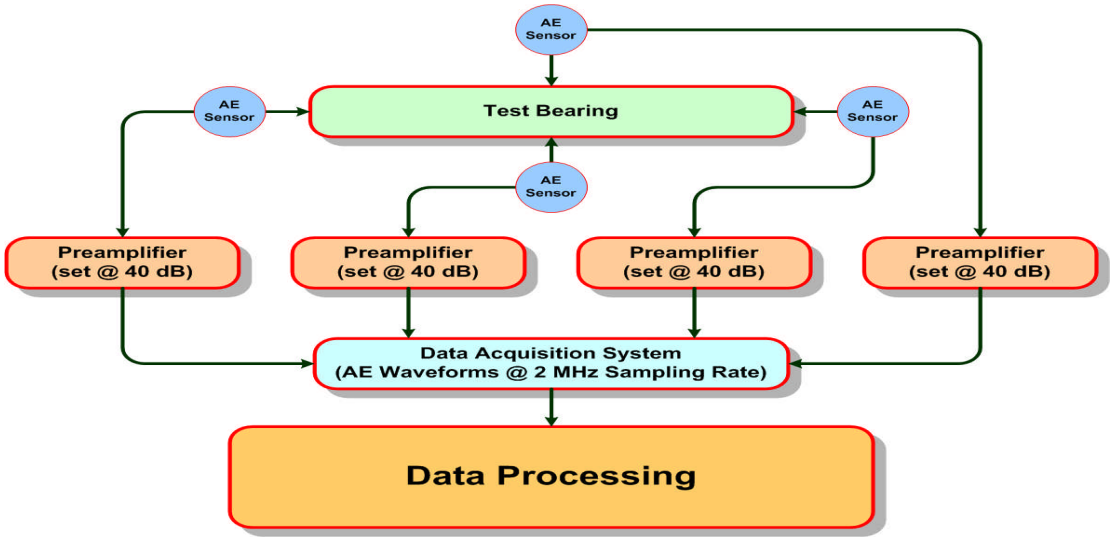

Figure 4—5 Schematic of the data acquisition systems

Prior to testing calibration tests were undertaken to understand the attenuation properties of the test bearing. Attenuation can be described as any reduction (or loss) in the AE signal strength (in the form of amplitude or intensity) and it is expressed in decibels (dB's) [82]. In acoustic emission applications, attenuation is a very important property because it determines the signal strength as a function of distance; therefore, it plays a significant role in specifying locations of AE sensors for the purposes of identifying sources of AE events.

A bearing attenuation test was carried out prior to laboratory tests. Hsu–Nielsen sources were used for attenuation tests. This test consists of breaking a 0.5 mm diameter pencil lead approximately 3 mm (+/- 0.5 mm) from its tip by pressing it against the surface of the piece. Two different programs of attenuation test were undertaken. The first involved breaking a 0.5 mm diameter lead pencil of hardness 2 H onto the flat raceway directly adjacent to the AE sensors labelled channel-1, channel-2, channel-3 and channel-4, see figure (4-6). A detection threshold was set at 52 dB for the acquisition of AE's generated from the lead breaks and an average value of maximum signal amplitude of ten pencil breaks from each position was calculated. Signal amplitude and relative attenuation were calculated using equations [3-2] and [3-6] respectively. Analysis revealed

that the AE signals on the flat ring are attenuated with increasing the distance from the emanating AE source as expected. For instance, lead breaks at channel-1 showed greatest attenuation at channel-3 (3 dB) which is the maximum distance from the source (channel-1). A summary of results is presented in figure (4-7) and table (4-2).

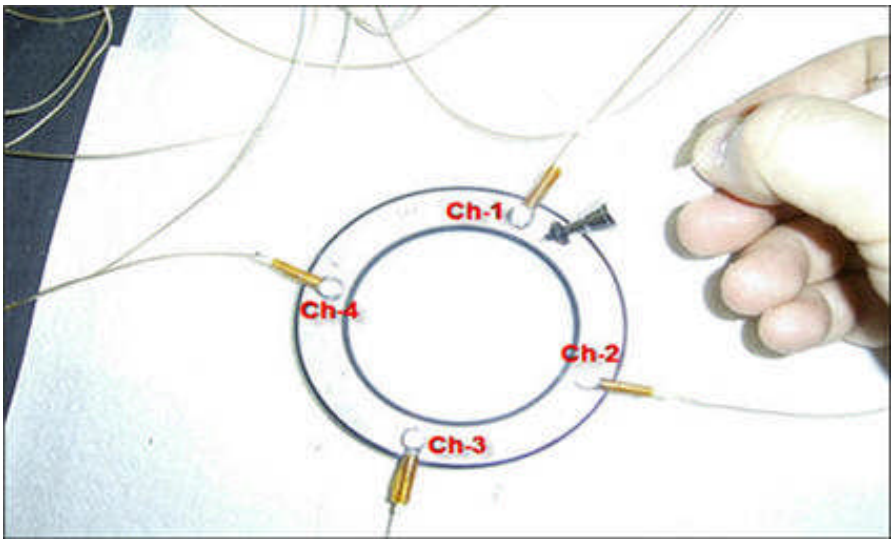

Figure 4—6 Breaking lead pencil at four different positions (Program I)

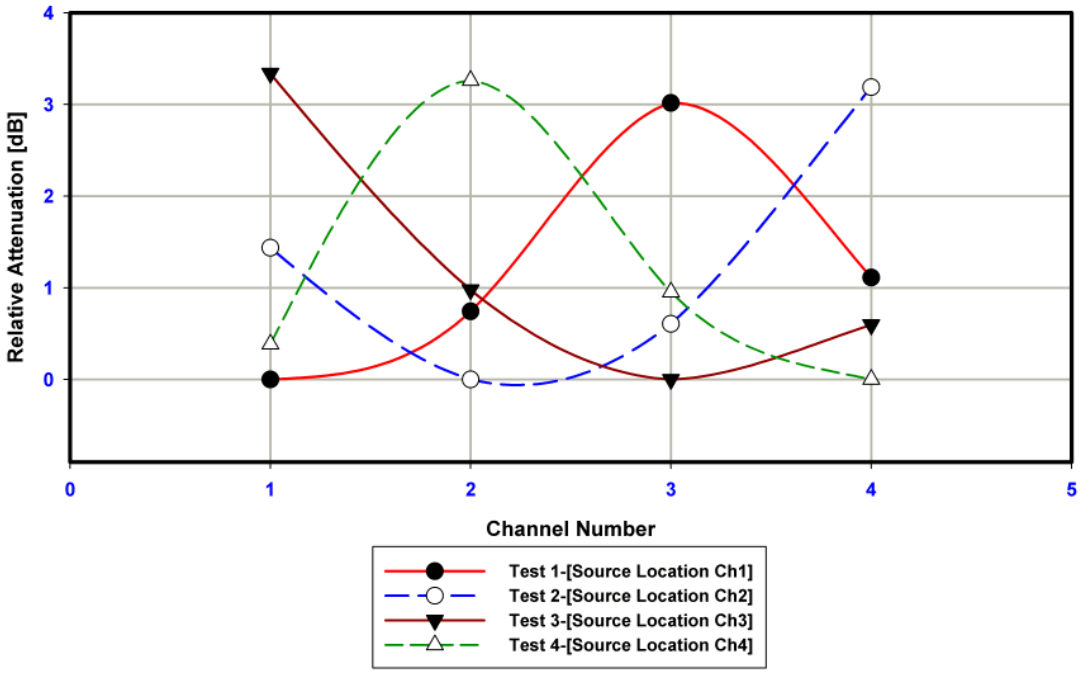

Figure 4—7 Relative attenuation at four different positions (Program I)

Table 4—2 Results for the attenuation test (Program I).

Test 1			
Channel	**Signal Amplitude (v)**	**Amplitude (dB)**	**Attenuation (dB)**
1*	0.17214	104.71	0
2	0.15805	103.97	0.7417
3	0.12165	101.70	3.0153
4	0.15145	103.60	1.1122
Test 2			
Channel	**Signal Amplitude (v)**	**Amplitude (dB)**	**Attenuation (dB)**
1	0.20211	106.11	1.4361
2*	0.23845	107.54	0
3	0.22238	106.94	0.6060
4	0.16521	104.36	3.1872
Test 3			
Channel	**Signal Amplitude (v)**	**Amplitude (dB)**	**Attenuation (dB)**
1	0.13466	102.58	3.3379
2	0.17672	104.94	0.9770
3*	0.19776	105.92	0
4	0.18465	105.32	0.5957
Test 4			
Channel	**Signal Amplitude (v)**	**Amplitude (dB)**	**Attenuation (dB)**
1	0.20647	106.29	0.3834
2	0.14825	103.41	3.2607
3	0.19337	105.72	0.9528
4*	0.21579	106.68	0

*Channels used as signal source locations (reference points) during the attenuation test.

The second program to understand the attenuation of the bearing ring involved breaking lead at another two positions labelled as the mid-points between channel-2 and channel-3, and channel-3 and channel-4, shown in figure (4-8). In-plane wave tests were also undertaken at the mid-point between channel-2 and channel-3. The experimental settings were kept the same as the previous attenuation test. For these tests, ten lead breaks at each position were again performed and the average maximum signal amplitudes and attenuation rate, as described in the first part, are presented in figure (4-9) and table (4-3). During the test, where the source location was at the midpoint between

channel-2 and channel-3, channel-2 recorded the maximum signal strength of 0.209 volts whilst the highest attenuations of 3.13 dB and 3.44 dB were observed at channel-1 and channel-4 respectively, see figure (4-9). It should be noted that the position (3) on figure (4-9) is not channel-3 but the mid-point between channel-2 and channel-3, see the figure legend.

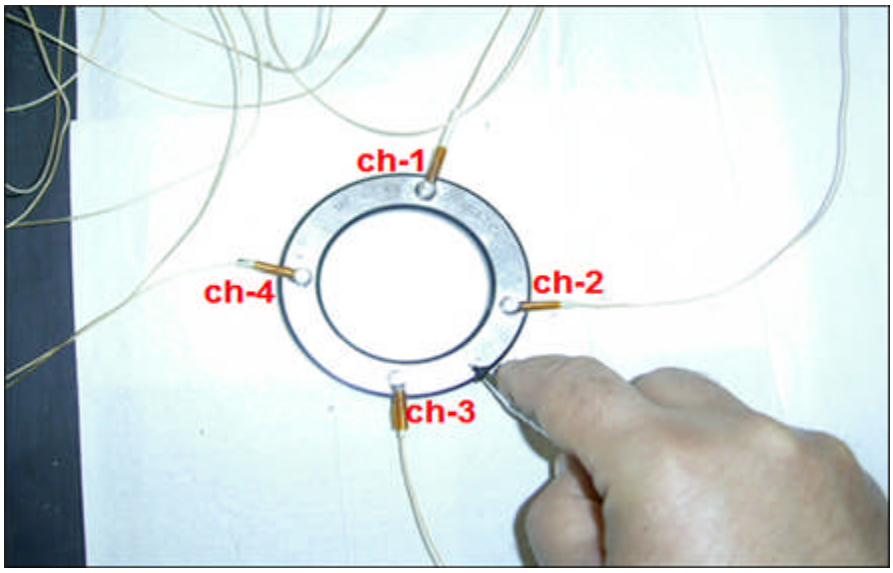

Figure 4—8 Breaking lead pencil at three different positions (Program II)

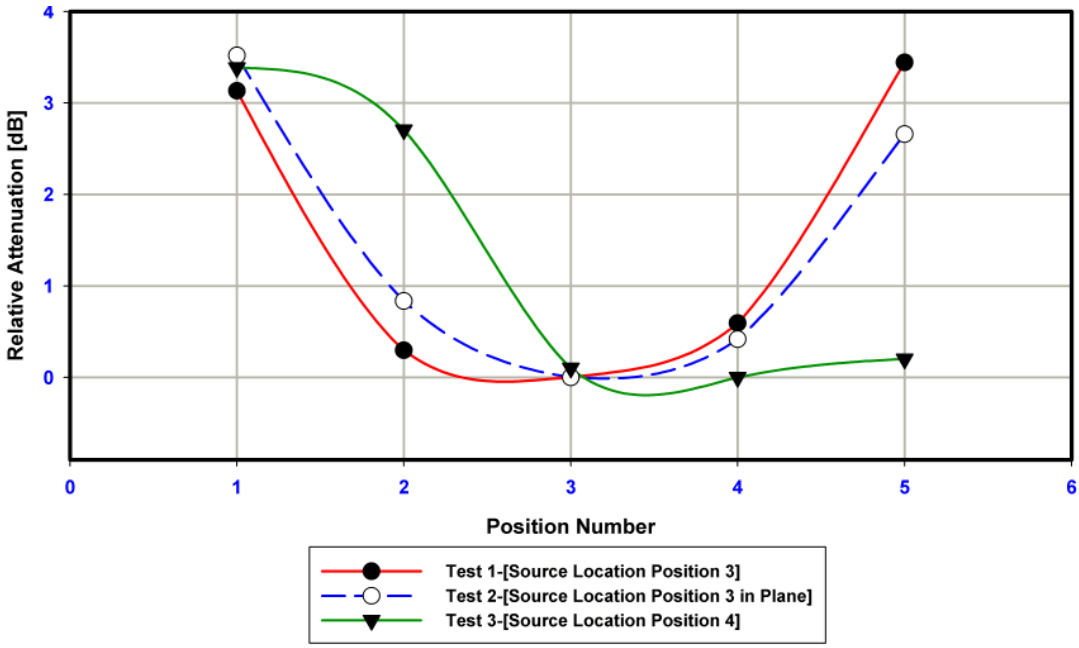

Figure 4—9 Relative attenuation at four different positions (Program II)

Table 4—3 Results for the attenuation test (Program II).

Test 1			
Channel	**Signal Amplitude (v)**	**Amplitude (dB)**	**Attenuation (dB)**
1	0.15148	103.60	3.1323
2	0.20997	106.44	0.2962
Ref. Point [1]	0.21726	106.73	0
3	0.20293	106.14	0.5924
4	0.14617	103.29	3.4420
Test 2			
Channel	**Signal Amplitude (v)**	**Amplitude (dB)**	**Attenuation (dB)**
1	0.17619	104.91	3.5187
2	0.24002	107.60	0.8335
Ref. Point [2]	0.26419	108.43	0
3	0.25181	108.02	0.4167
4	0.19451	105.77	2.6593
Test 3			
Channel	**Signal Amplitude (v)**	**Amplitude (dB)**	**Attenuation (dB)**
1	0.18482	105.33	3.3841
2	0.19986	106.01	2.7045
3	0.26975	108.61	0.1000
Ref. point [3]	0.27288	108.71	0
4	0.26666	108.51	0.2001

1. Reference point was taken between **channel 2** and **channel 3**.
2. Reference point was taken between **channel 2** and **channel 3** **in plane**.
3. Reference point was taken between **channel 3** and **channel 4**.

4.3 Bearing Tests

For this particular thesis four experimental cases are presented that reflect the general observations associated with over a dozen experimental tests. Two different approaches to ascertaining the applicability of the AE technology for monitoring cracks on slow speed bearings were undertaken. The first approach consists of three cases that employed a combination of a thrust ball bearing and a thrust roller bearing to accelerate the natural crack initiation on a bearing flat race at loads ranging from 20, 35 and 50 kN, whilst the second involved the results for one test load of 50 kN applied on a real-sized test bearing, which was run under grease starvation. Figure (4-10) shows the general trend of AE

energy throughout the bearing tests. It should be noted that each plot presents two different cases at the same applied load. It is worth mentioning that in the first approach cases, the test bearing was lubricated during the testing with Castrol, Moly Grease (650-EL). To ensure a consistent lubricant viscosity throughout the bearing test period, the measurement of temperature was also continuously undertaken. The significance of this is to ensure that friction properties between the bearing elements were relatively constant.

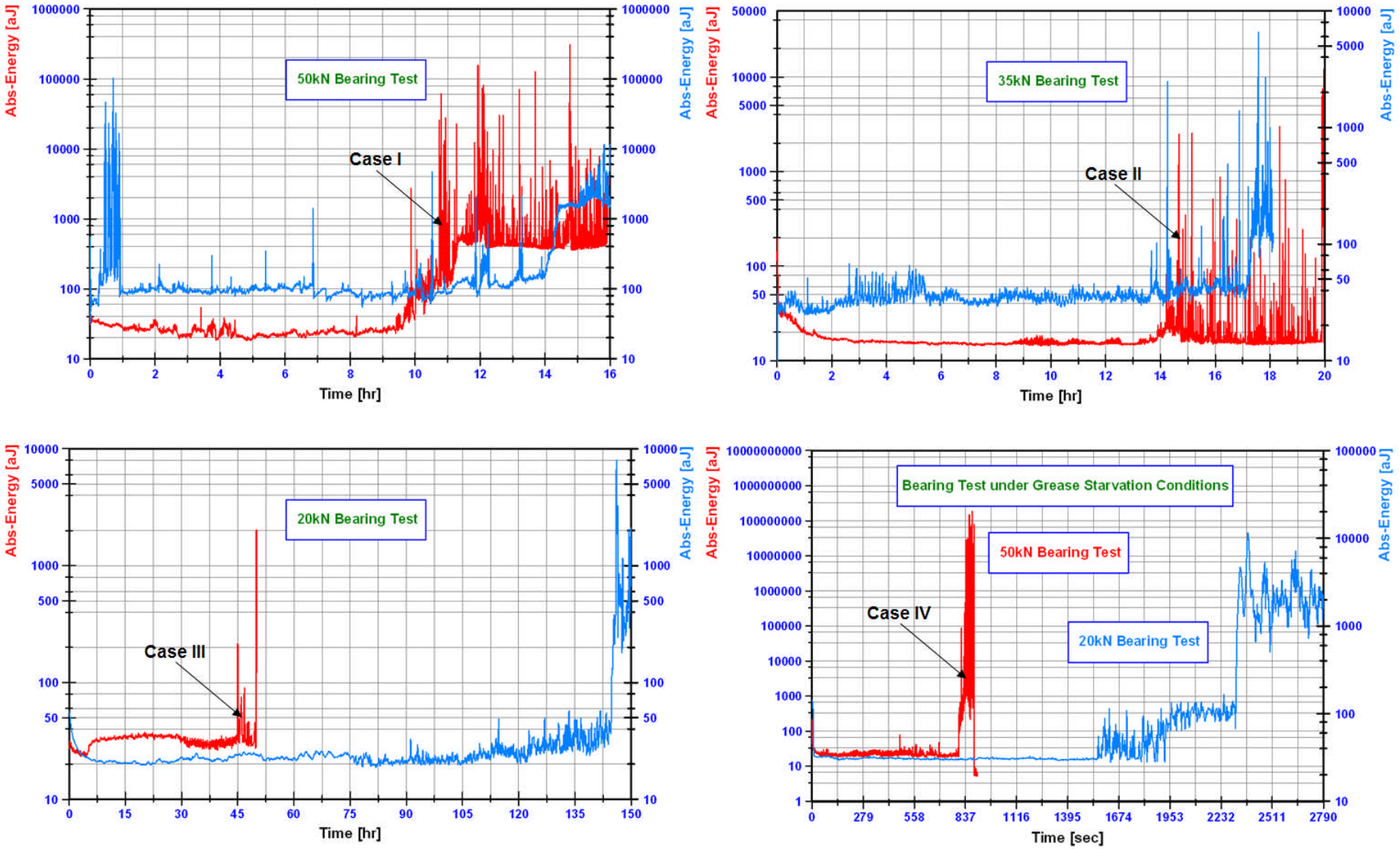

Figure 4—10 General trend of AE energy throughout the bearing tests (Approach I & Approach II)

4.3.1 Case I

Observations of continuous monitoring of the AE levels, in addition to traditional AE parameters, for 16-hrs of bearing operation are presented in figures (4-11) and (4-12). At the end of the test (16-hrs) there was visible surface damage. It was observed that at approximately 9-hrs into operation AE emission levels began to increase steadily. The increase in AE energy levels from early in the test run (between 2- to 6-hrs) to the condition of surface damage was in the order of 10,000%, as depicted in figure (4-11). Figure (4-12) shows trends of traditional AE parameters all of which show significant increase in AE activity from 9-hrs of operation. It is worth mentioning that a significant increase in the temperature measurements was noted between 0- to 2-hrs of operation. This was attributed to the experimental error, which accrued in the thermocouple channel attached to the bearing flat race.

Interestingly observations of the AE waveform, sampled at 2 MHz showed changing characteristics as a function of time. This is presented in figure (4-13) where a typical AE waveform associated with spurious AE transient events is presented after 4-hrs of operation. It is particularly interesting to note that the frequency of the transient event reduced from 18 Hz to 9 Hz (from 10-hrs operation to the end of the test at 16-hrs). As surface defects, such as spalls, are continually developing, it is postulated that a newly formed spall will contribute relatively higher AE events as the edges of this newly formed defect will be rougher in comparison to an already existing spall which becomes smoother with the passage of time. As such at 16-hrs operation one of the spalls developed was relatively ‘less mature’ than others and resulted in high AE levels at the defect frequency. Hence the strong evidence of 9 Hz indicating one defect on the race. This also explains the sharp bursts of AE activity noted during observations of continuously monitored AE energy levels, see figure (4-11).

Even though the overall energy levels are increasing from 9-hrs operation, relatively large transient rises were noted during the period from 10-hrs to 16-

hrs. It is postulated that these large transient bursts are attributed to regions that have newly developed surface damage; this is an evolutionary process giving rise to peaks and troughs in AE levels. On termination of the test (16-hrs) a visual inspection revealed surface damage at three locations on the race, see figure (4-14).

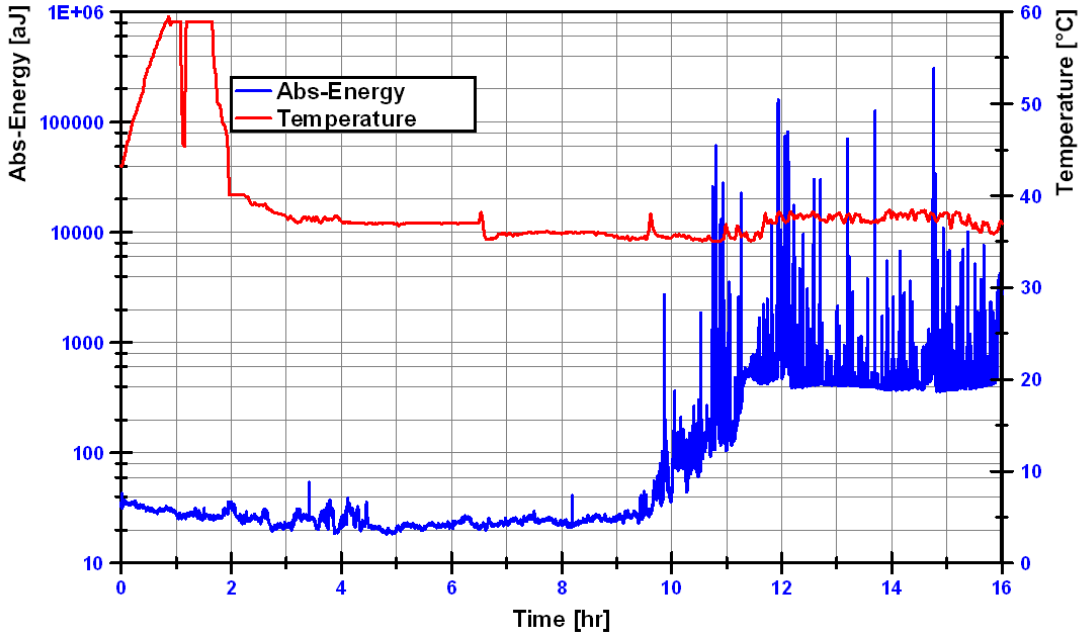

Figure 4—11 Test conditions run until visually observable surface damage

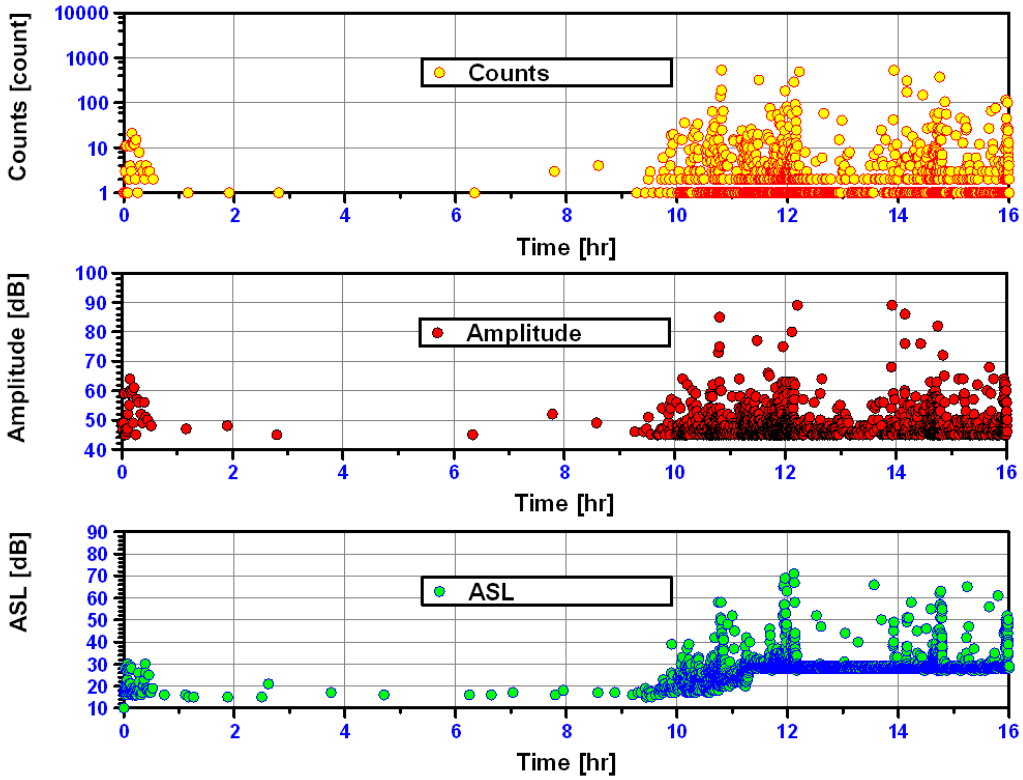

Figure 4—12 Classical AE parameters

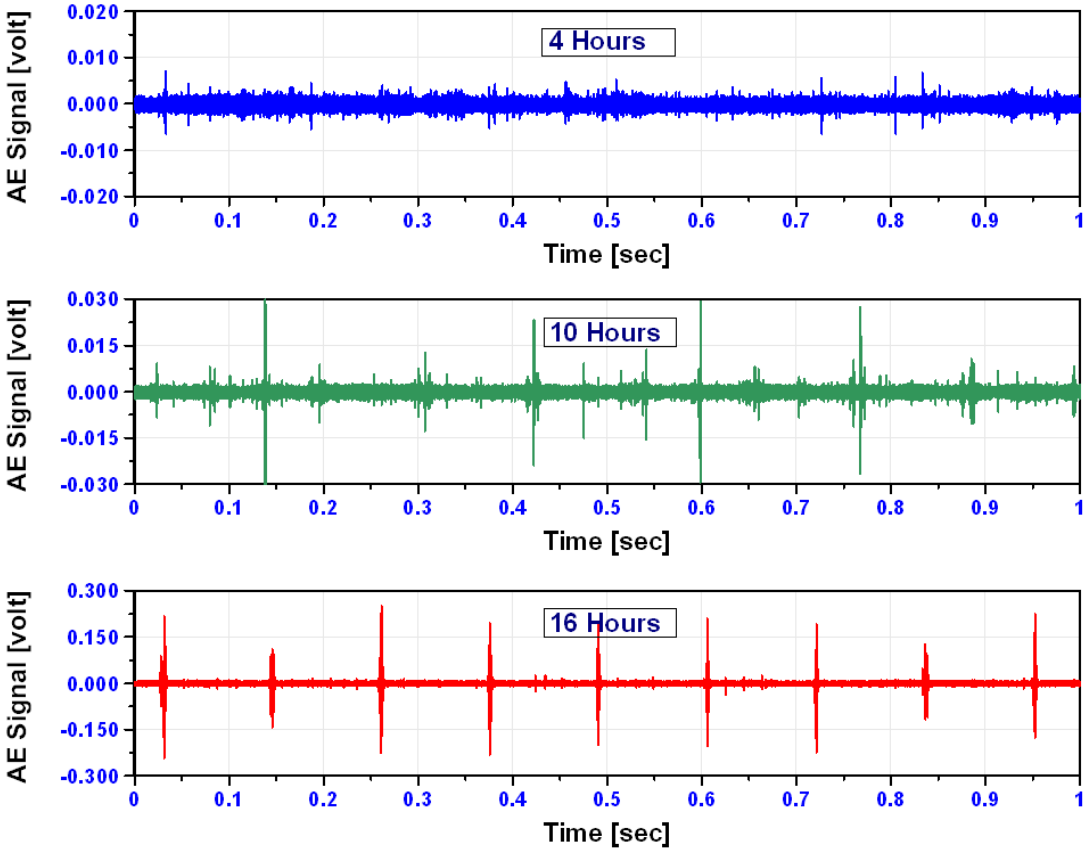

Figure 4—13 Typical AE waveforms associated with case-I

Figure 4—14 Crack zones on flat ring

Time domain analysis techniques also provided another simple and rapid means to detect the crack initiation and propagation on the bearing race. From figure (4-15), an increase in EI level from earlier in the test run between 10- to 14-hrs was noted; an EI value of 10.5 after 10-hrs operation was observed. It was also noted that after about 9-hrs a relative rise in EI value was recorded. After running for 12-hrs, EI raised to a maximum value of 42.48, after which the level reduced with increasing bearing damage, see figure (4-15).

Results showed that as early as 4-hrs into the operation of the bearing test, a KS value of 0.015 was noted. It is also worth mentioning that KS values began to increase steadily as the test passed 9-hrs of operation, reinforcing the previous observations of continuous monitoring of AE activity, as shown in figure (4-11). On the termination of the test (16-hrs), a maximum KS value of 0.41 was recorded, see figure (4-15).

After 4-hrs into the test a KU value of 4.1 was recorded. Due to the high transient nature of AE, a steady increase of KU after 9-hrs operation was noted. As the damage increased KU values reduced to the undamaged levels, see figure (4-15).

It was shown that the IE increased as early as 9-hrs operation; as the test passed with time, an IE value of 0.011 was observed (after running 9-hrs). It is

also worth noting that at the end of the test (16-hrs), the IE reached its maximum value of 0.79, see figure (4-15).

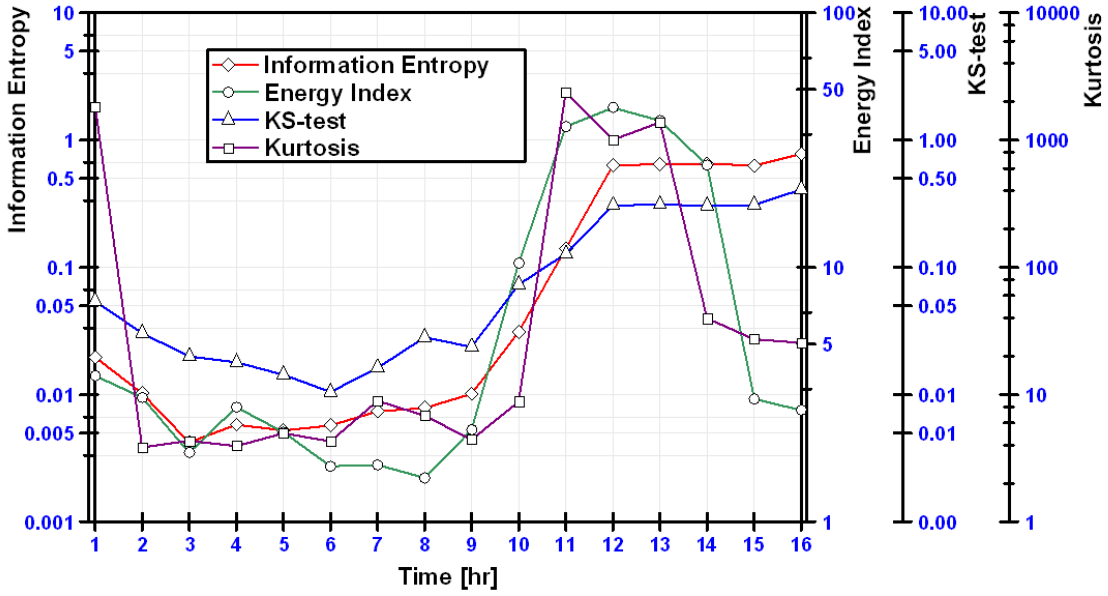

Figure 4—15 IE, KU, EI and KS-test results

Lastly, undertaking data analysis using multiple processing methods also provided alternative means of assessing deviations from normal conditions. In addition to time domain analysis, enveloping (demodulation) of AE waveforms were also undertaken to investigate the periodicity of the transient nature of the AE's from the test bearing. As a consequence, higher frequency components could be removed, whilst the periodicity of AE bursts associated with a defect can be emphasised. It should be noted that the Hilbert transform [102,103] was applied for envelope analysis.

A frequency spectrum of the AE waveforms recorded throughout this test period is also presented. The use of the FFT is particularly appropriate as it gives information about the measured AE signals in the frequency domain. Some AE waveforms taken at various periods during the test were enveloped and frequency analyzed. AE waveforms recorded at 4-, 10- and 16-hrs were enveloped; results of which are presented in figures (4-16) to (4-18). Just prior to the termination of the test (16-hrs), the measured AE waveforms developed a

periodicity of AE transient bursts of 9 Hz, which is associated with the defect frequency of the bearing that was observed, see figure (4-18).

It was noted that the frequency spectrum of the enveloped AE response at 4-hours did not highlight any specific frequency component, see figure (4-16). About 9- to 10-hrs into the test, Fourier analysis of the enveloped signal started to show the periodicity of AE transient bursts, presented in figures (4-17). Figure (4-18) shows a clear periodicity of AE activity at 9 Hz, as high periodic transient AE events were observed at the end of the test (16-hrs). The relevance of this will be evident later in the chapter of source location analysis.

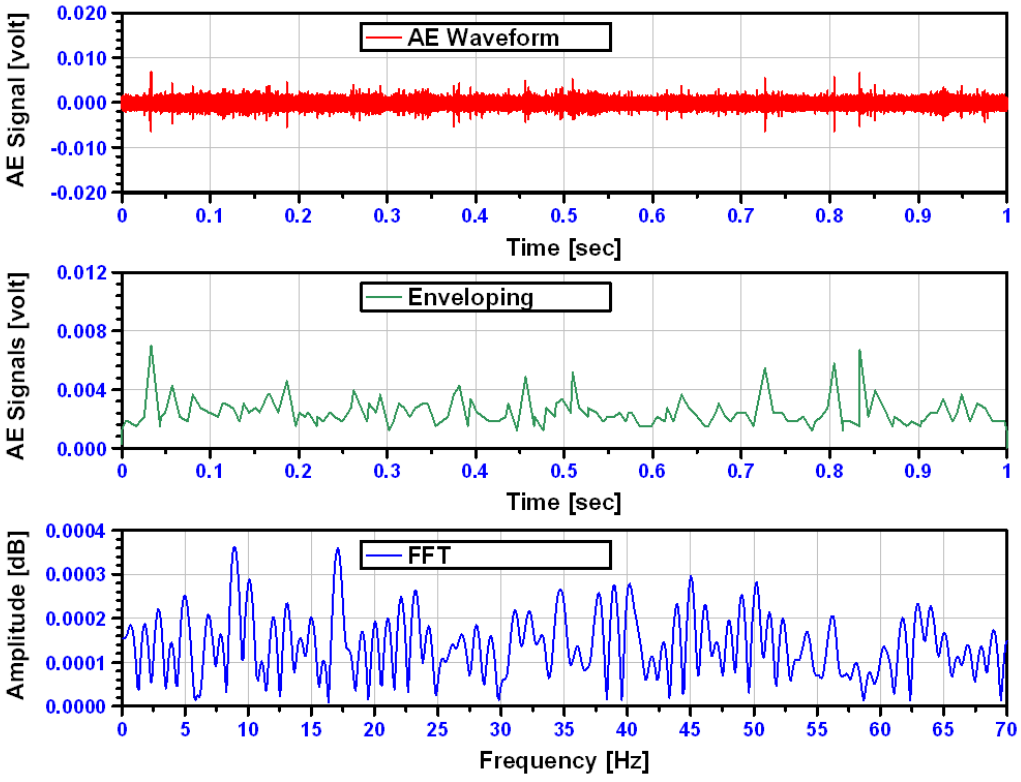

Figure 4—16 AE waveform, enveloping and FFT after 4-hrs

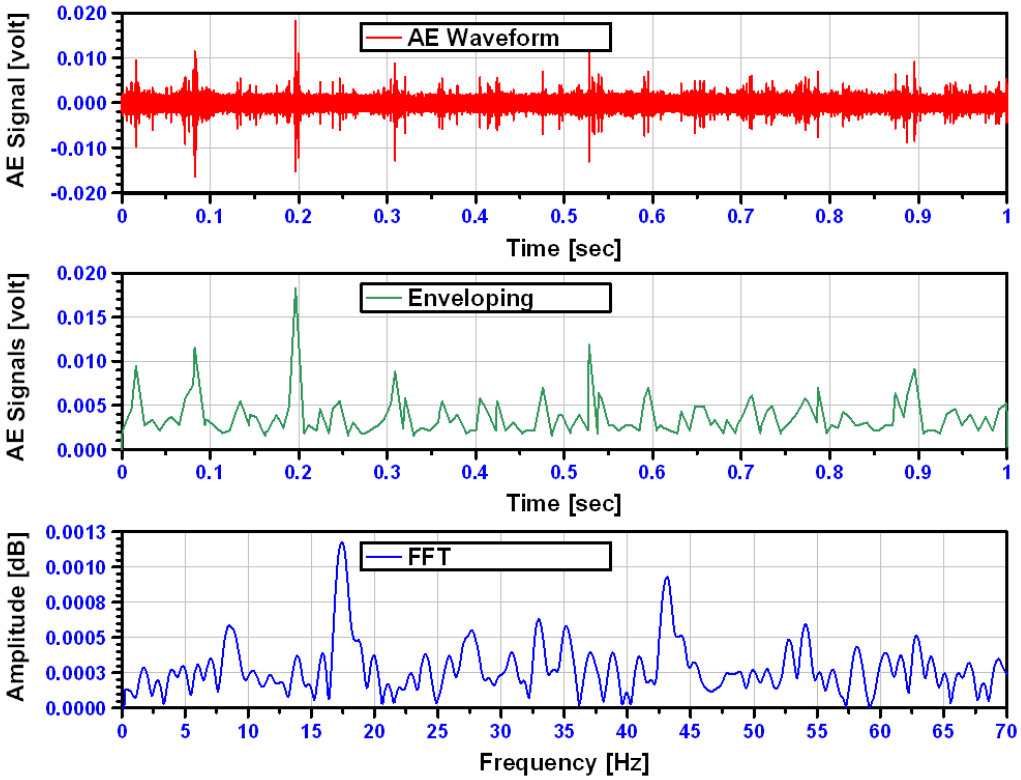

Figure 4—17 AE waveform, enveloping and FFT after 10-hrs

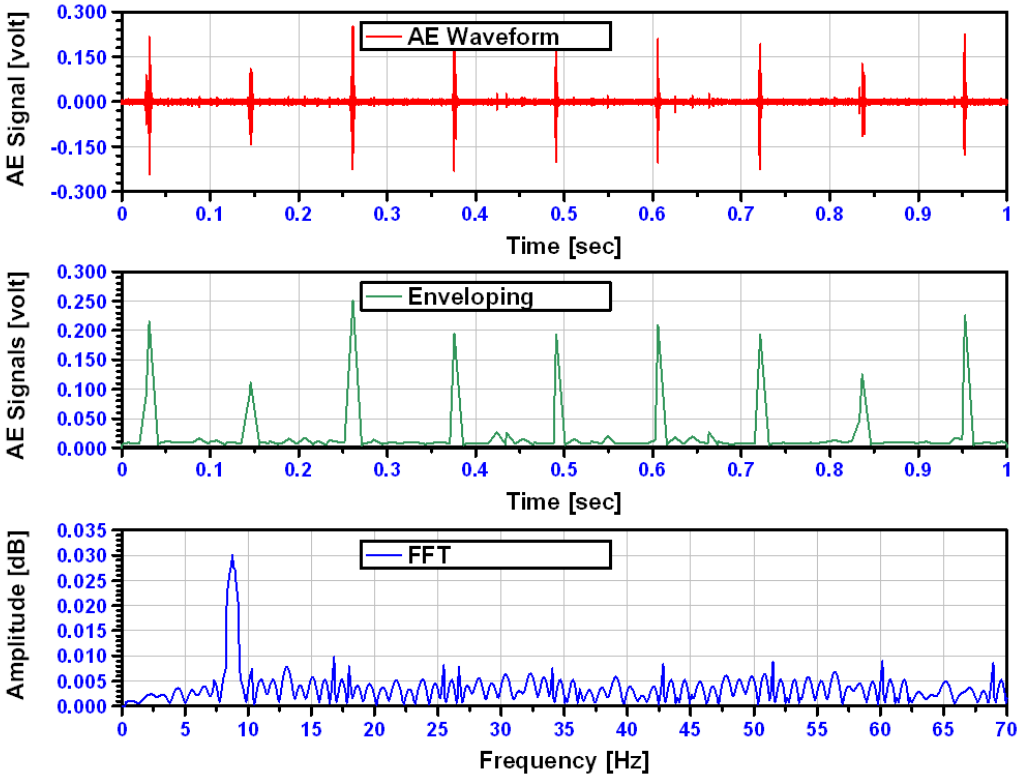

Figure 4—18 AE waveform, enveloping and FFT after 16-hrs

4.3.2 Case II

The applied load on this test bearing was 35 kN. Observations of continuous monitoring of the AE levels for 20-hrs of bearing operation are presented in figure (4-16). It was noted that relatively high levels of AE activity were observed during the first hour of operation; this was attributed to run-in as after this period (1-hr) all measured AE parameters and temperature stabilized. After 14-hrs of operation significant high levels of AE activity was noted, particularly the activity associated with AE energy. The bearing temperature recorded a value of 37 ^{o}C and it remained constant throughout the test, see figure (4-19). On the termination of the test, high levels of AE activity were noted, particular the activity associated with AE counts see figure (4-20). Also noted on the AE waveform at 14-hrs operation was the high transient nature of the waveform. It is also particularly interesting to note that the waveform observed after 20-hrs of operations showed a periodicity of AE transient bursts at 9 Hz; this periodicity is associated with the defect frequency (9 Hz) of the bearing and is a clear indication of a damaged bearing, see figure (4-21). On termination of the test (20-hrs) a visual inspection revealed surface damage at two locations on the race, see figure (4-22).

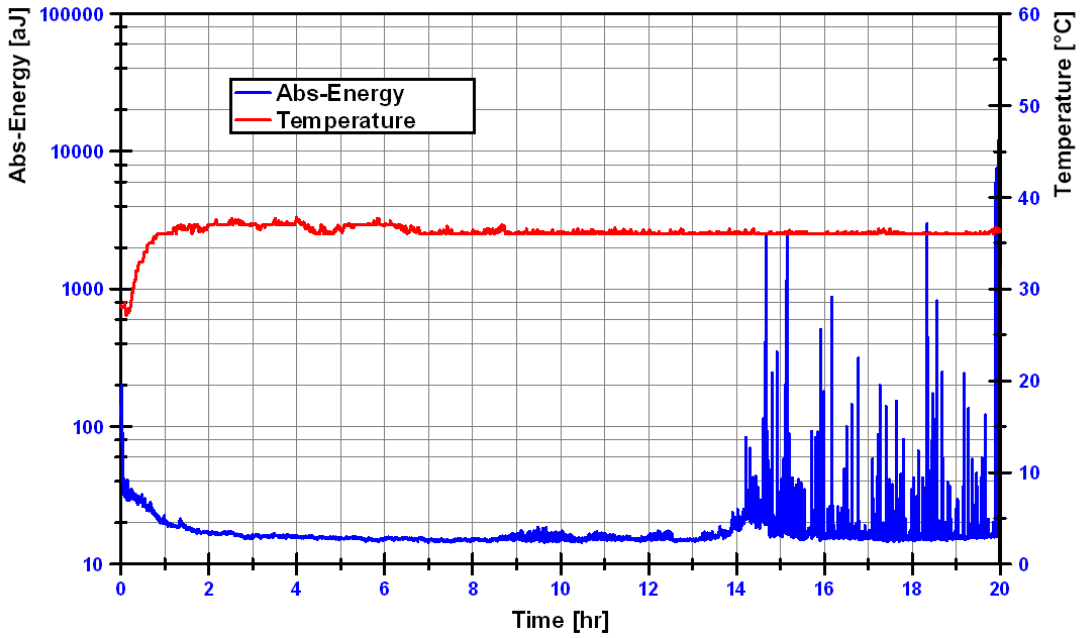

Figure 4—19 Test conditions run until visually observable surface damage

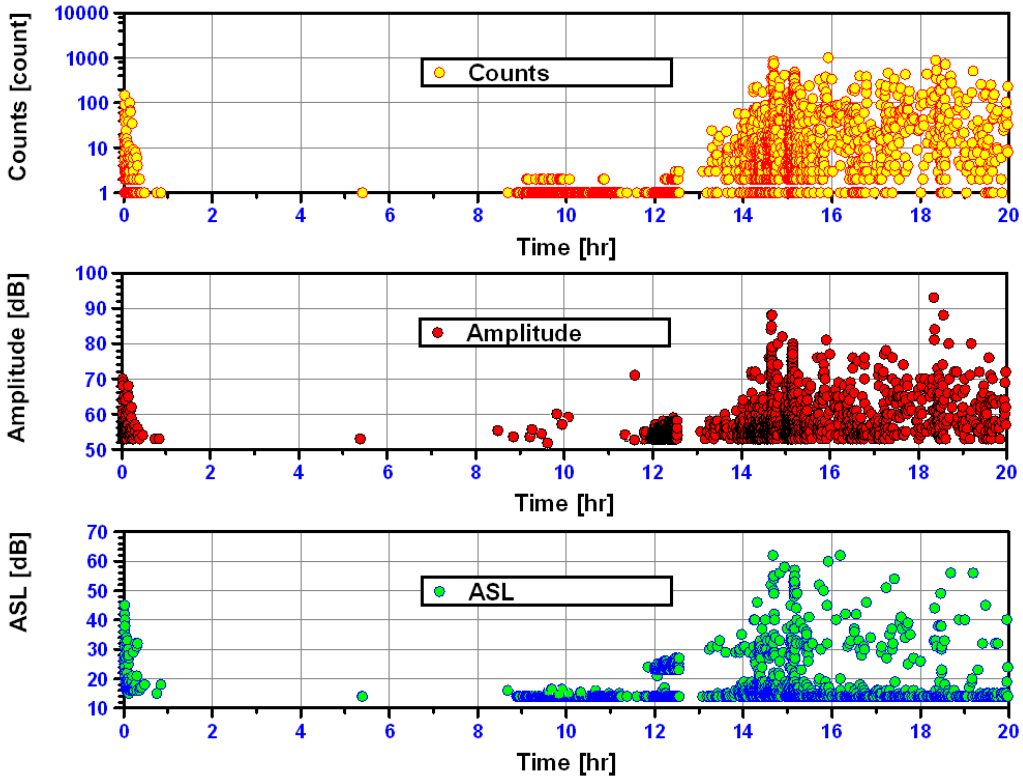

Figure 4—20 Classical AE parameters

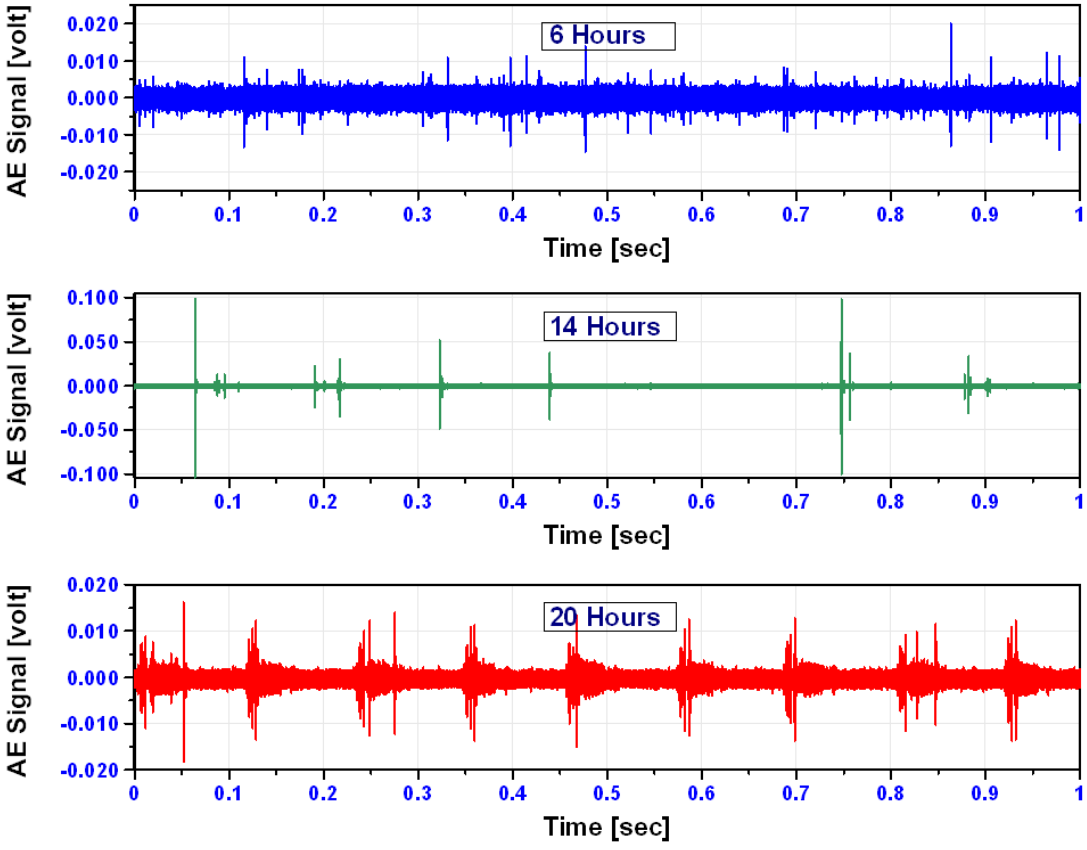

Figure 4—21 Typical AE waveforms associated with case-II

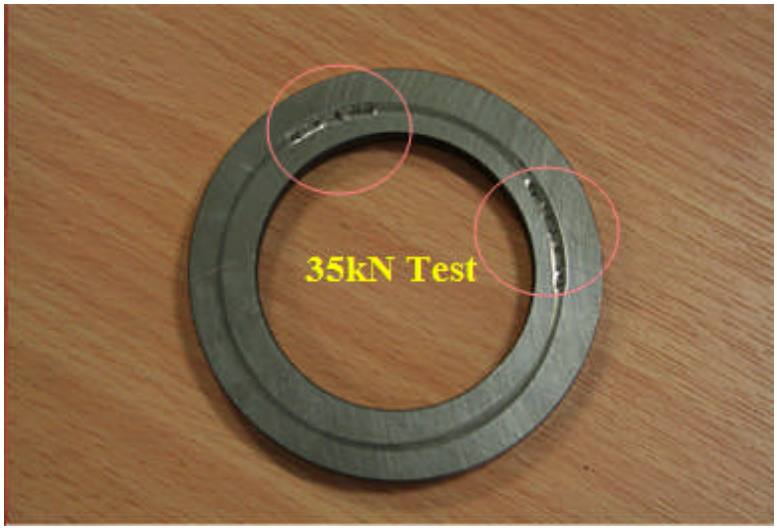

Figure 4—22 Crack zones on flat ring

At 2-hrs operation results indicated that all indicators IE, KU, EI and KS-test have relatively high values of about 0.047, 192.2, 4.78 and 0.024 respectively. It is worth stating that after 5- to 8-hrs all calculated IE and KS-test values remained almost constant whilst KU and EI values showed an unsteady trend. As the test progressed with time (13- to 15-hrs), all indicators values were very sensitive to the variation in bearing signals, see figure (4-23); at 15-hrs operation, maximum values of 6066.32 and 13.20 for KU and EI were recorded respectively. After running 15- to 20-hrs IE and KS-test values started to increase steadily while the sensitivity of KU and EI values decreased with the size and the number of localized defects; on the termination of the test (20-hrs) IE and KS-test values recorded a maximum value of 2.70 and 0.75 respectively whereas KU and EI values reduced towards the end of the test, shown in figure (4-23).

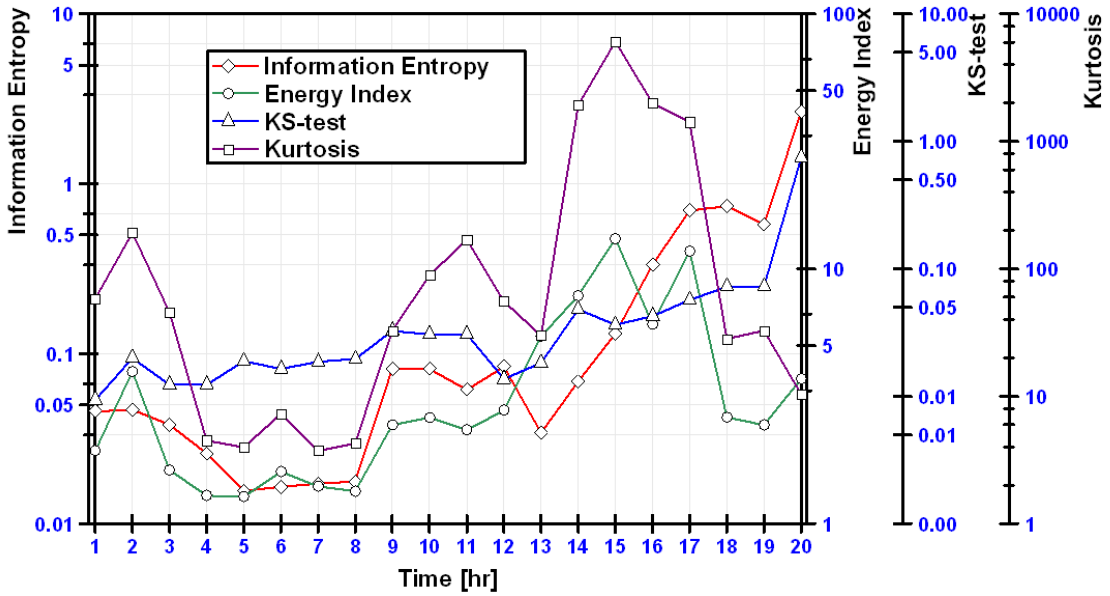

Figure 4—23 IE, KU, EI and KS-test results

The power spectrum results of AE signals are highlighted in figures (4-24) to (4-26). It is clear that early into the test (6- to -8 hrs) the results showed a broadband frequency and there was no defect frequency observed, see figure (4-24). Approximately 14-hrs into the test, observations of the spectrum analysis revealed that FFT method was relatively noisy, shown in figure (4-25). It is also particularly interesting to note that on the termination of the test (20-hrs) the spectrum showed a strong frequency component of 9 Hz, see figure (4-26), the relevant evidence of this will be presented in the next chapter.

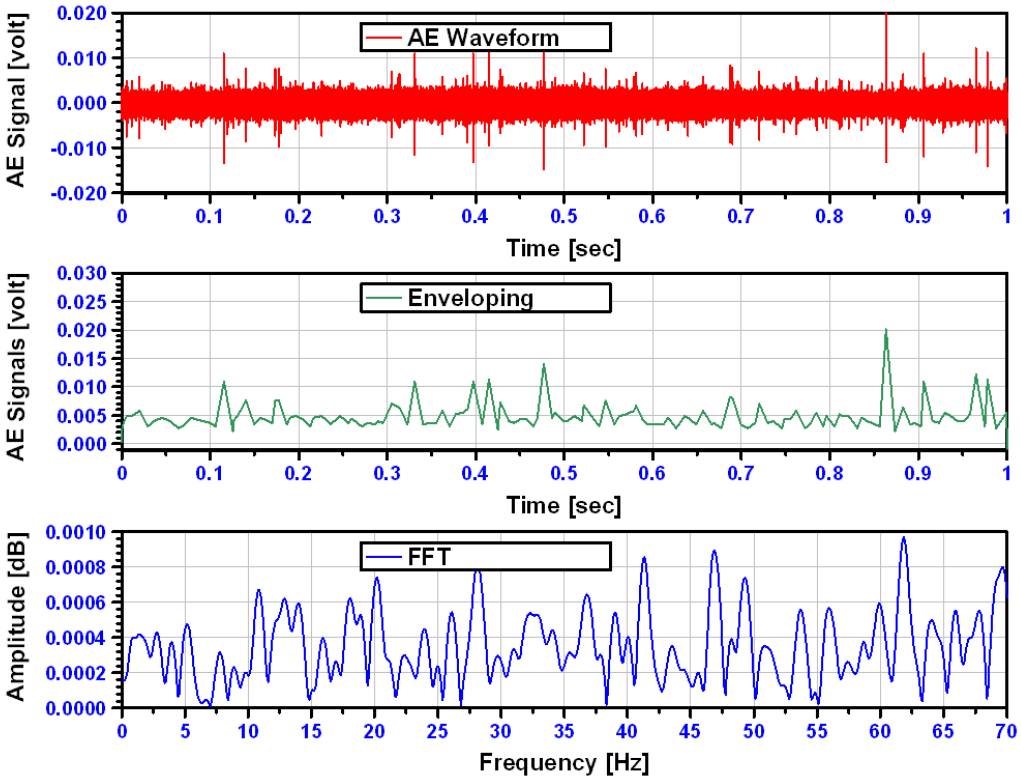

Figure 4—24 AE waveform, enveloping and FFT after 6-hrs

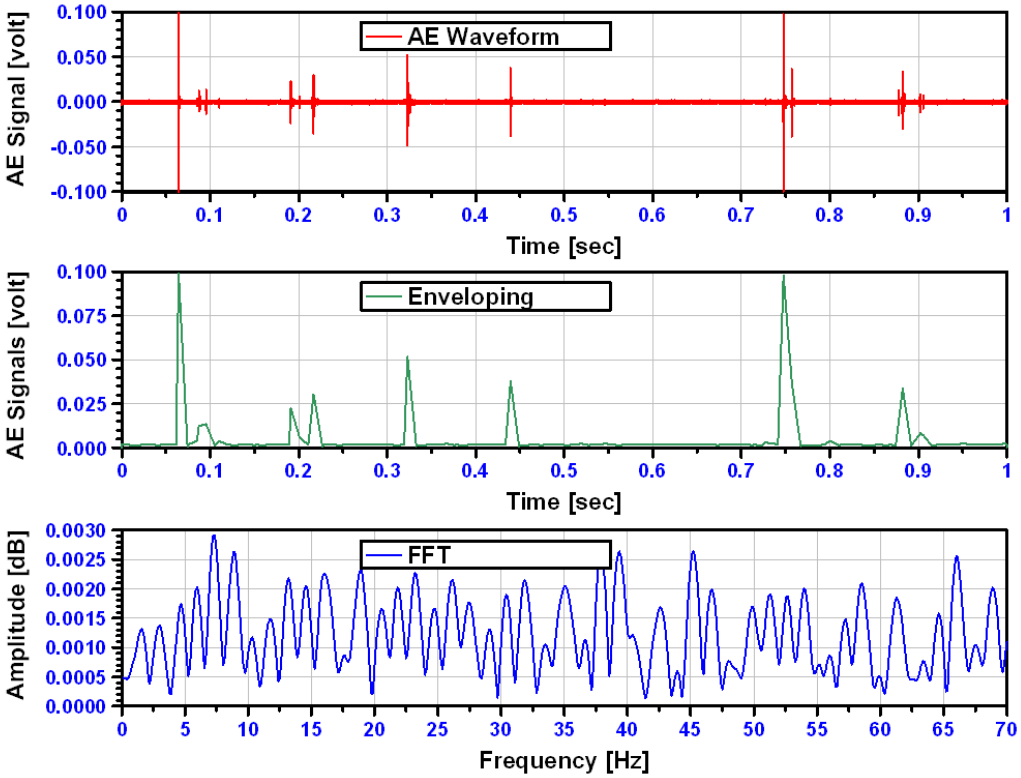

Figure 4—25 AE waveform, enveloping and FFT after 14-hrs

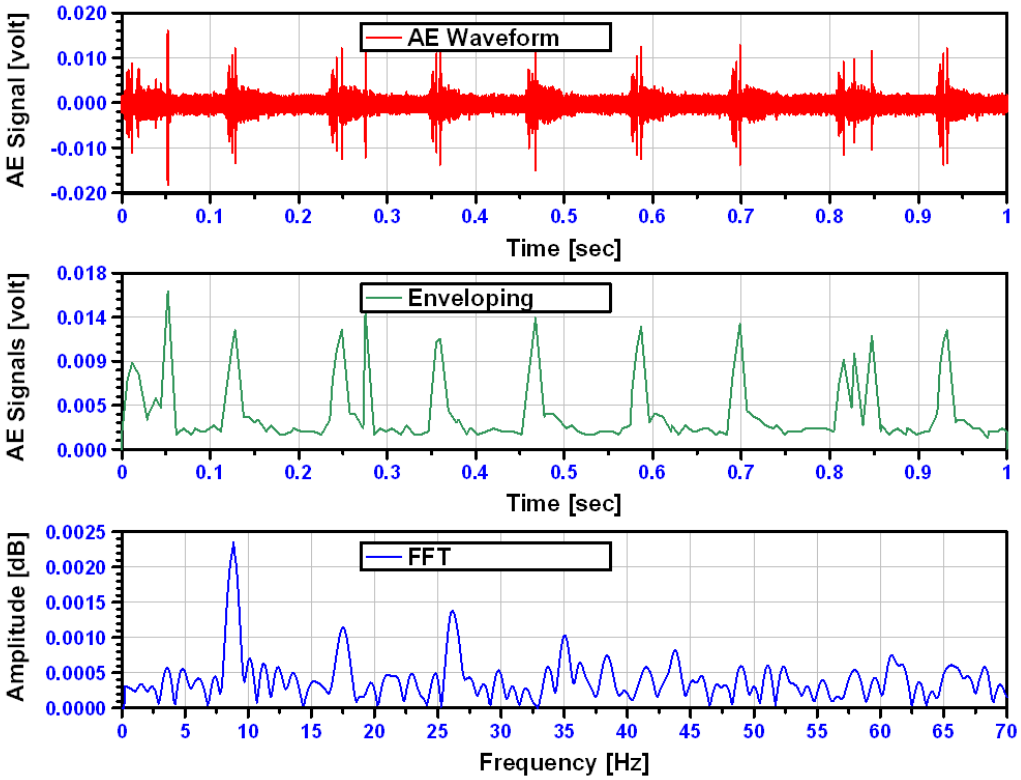

Figure 4—26 AE waveform, enveloping and FFT after 20-hrs

4.3.3 Case III

During the start of the test, the relatively high levels of AE and temperature noted in the previous cases were not noted; observations of continuous monitoring of the AE levels, in addition to bearing temperature, for 50-hrs of bearing operation did not show any considerable rise at (0- to 1-hr) of testing. This was attributed to a lower axial load of 20 kN applied on this test bearing, see figure (4-27). A significant increase in AE levels was noted from 45-hrs of operation until the test was terminated, as shown in figure (4-27). On the termination of the test, bearing temperature recorded its maximum value of 39 ^{o}C. The results of measurement of traditional AE parameters such as counts are detailed in figure (4-28) where it was noted that high levels of AE activity were observed from 45-hrs of operation. This highlighted the fact that traditional AE events are just as sensitive to changes in bearing mechanical state as the continuous measurement of AE parameters such as AE energy. AE waveforms recorded after 20-, 45- and 50-hrs of testing are presented in figure (4-29). It

clearly shows AE transient events, observed after 45-hrs which eventually developed into periodic transient events as the test progressed; the eventual periodicity was 9 Hz which corresponded to the defect frequency of the bearing. Visual inspection after 50-hrs operation indicated surface damage had occurred in the region, which was located approximately 20 mm from channel-2 AE sensor, see figure (4-30).

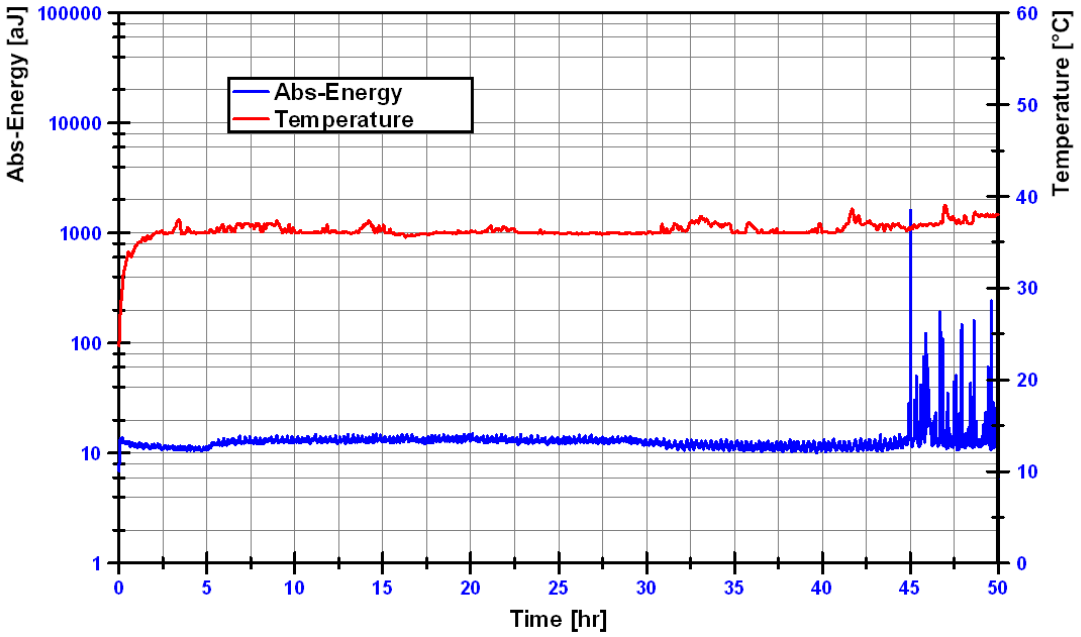

Figure 4—27 Test conditions run until visually observable surface damage

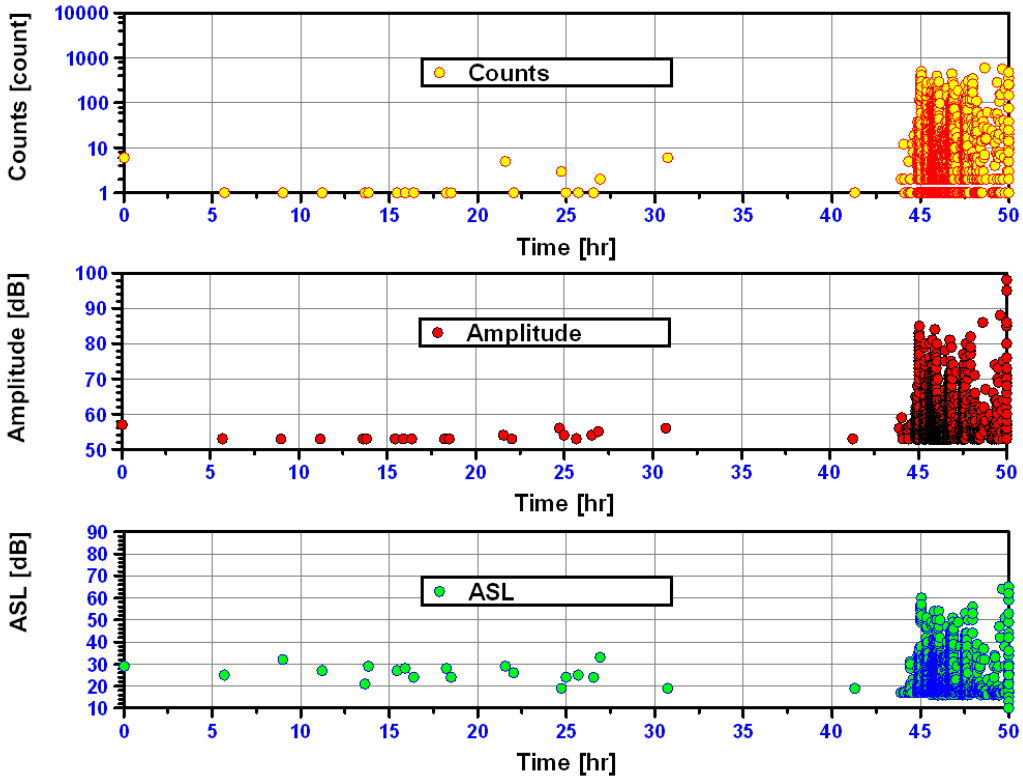

Figure 4—28 Classical AE parameters

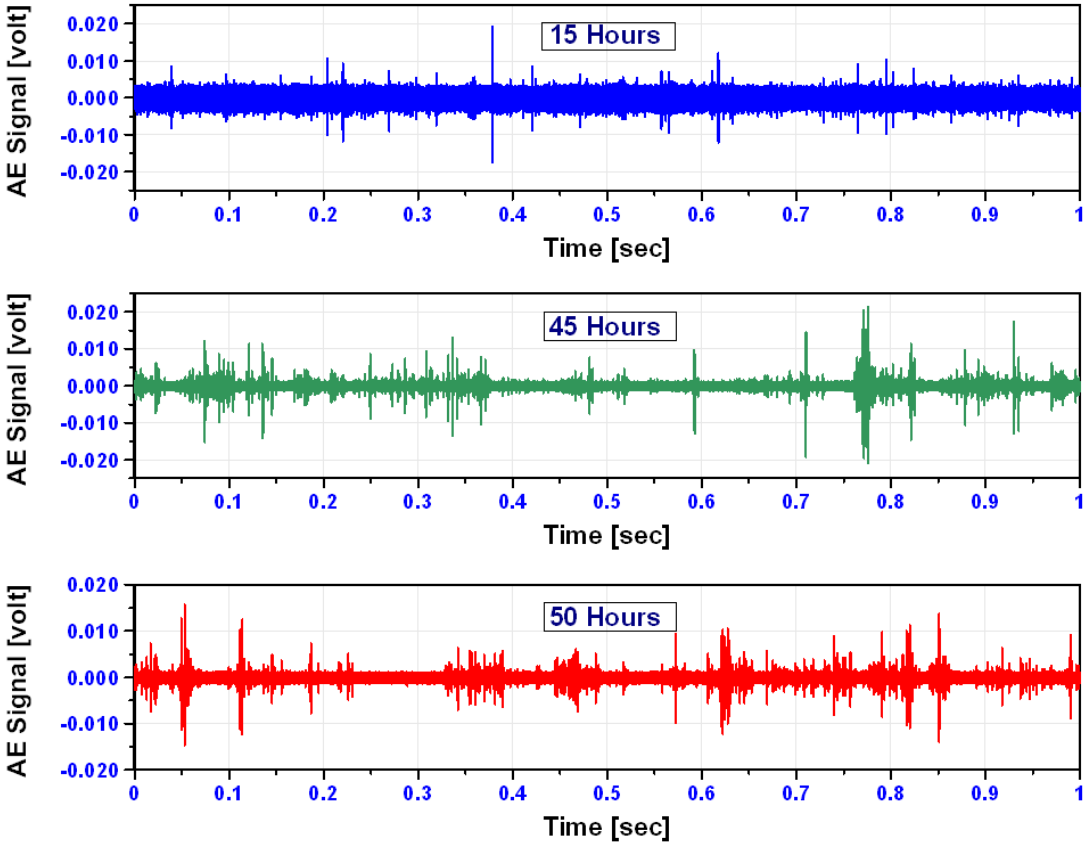

Figure 4—29 Typical AE waveforms associated with case-III

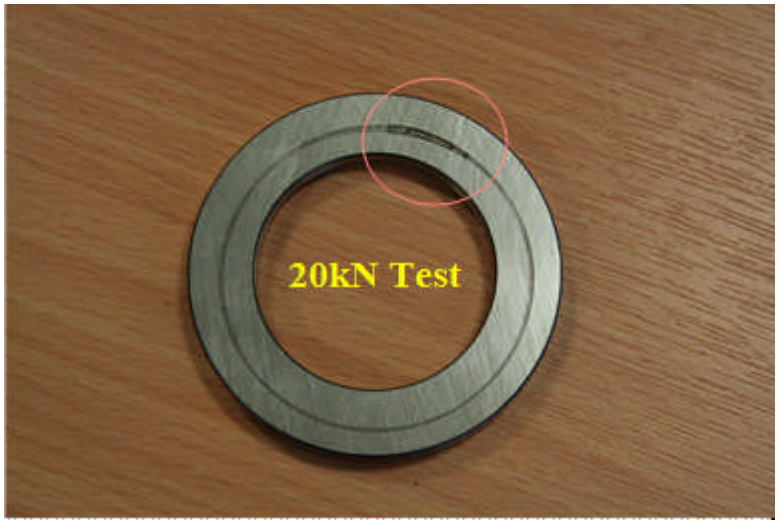

Figure 4—30 Crack zone on flat ring

In this case, time domain indicators present different characteristics to that noted in the earlier cases. Results indicated that during the start of the test, all indicators maintained a constant value. A significant increase in KU and EI at 40-hrs of operation was noted; the KU and EI registered their maximum values of 98.50 and 12.89 respectively. The observations from the results presented in figure (4-31) showed that the IE and KS-test are more sensitive and representative of periods of high transient AE activity, typical for natural degrading bearings, than KU and EI; IE and KS-test responded to the significantly increasing damage in the bearing whilst a sharp drop in KU and EI values were observed as the damage was well advanced.

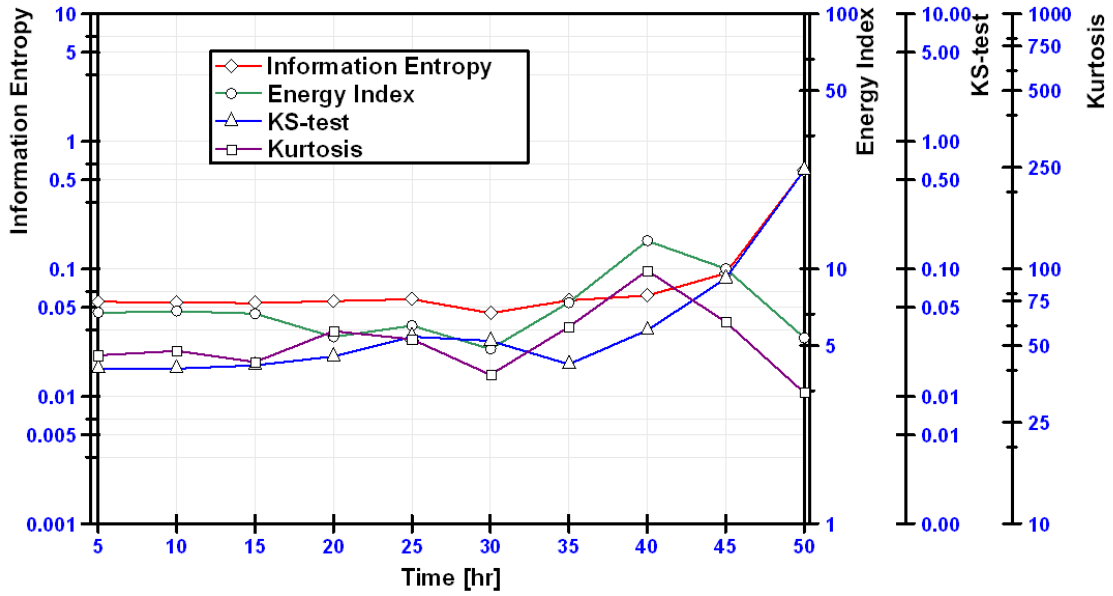

Figure 4—31 IE, KU, EI and KS-test results

The frequency spectrum of AE waveforms recorded at 15-, 45- and 50-hrs into operation are shown in figures (4-32) to (4-34). Noted is how gradually the amplitude map generated by FFT presents a visual picture of the faulty bearing. As the crack initiated at 45-hrs into the test, FFT could not show any evidence of periodicity, see figure (4-33). Some minor evidence of periodicity were noted at the end of the test (50-hrs), presented in figure (4-34). A continuous increase in evidence of periodicity, originated from a bearing defect, will be presented in the next chapter.

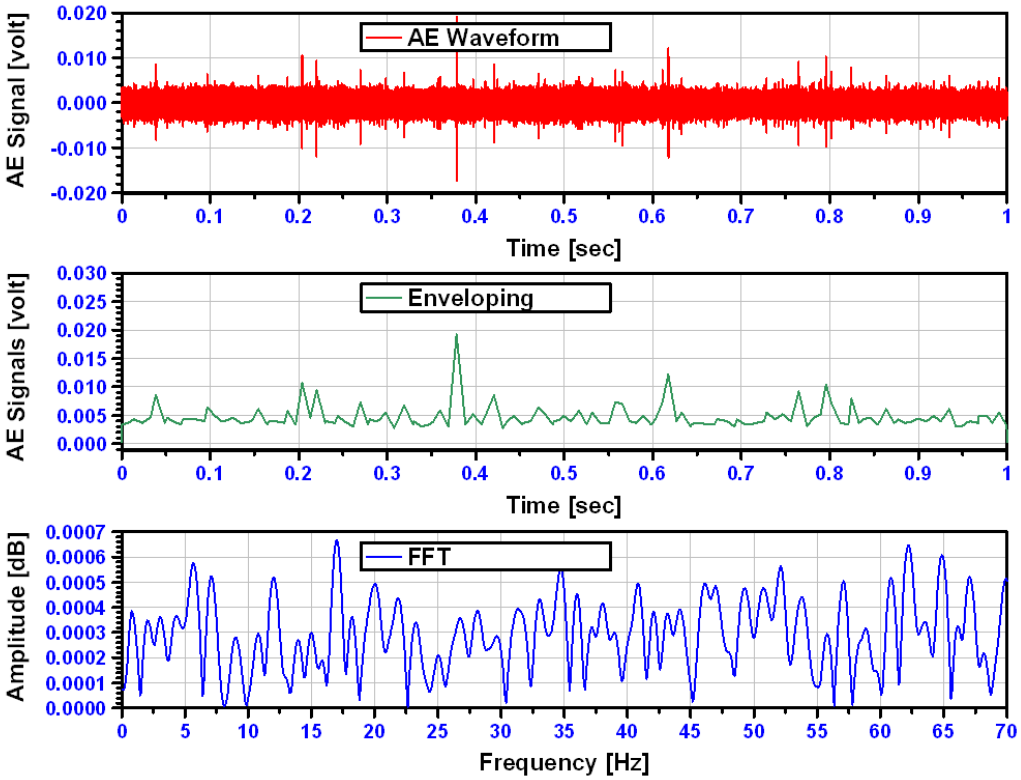

Figure 4—32 AE waveform, enveloping and FFT after 15-hrs

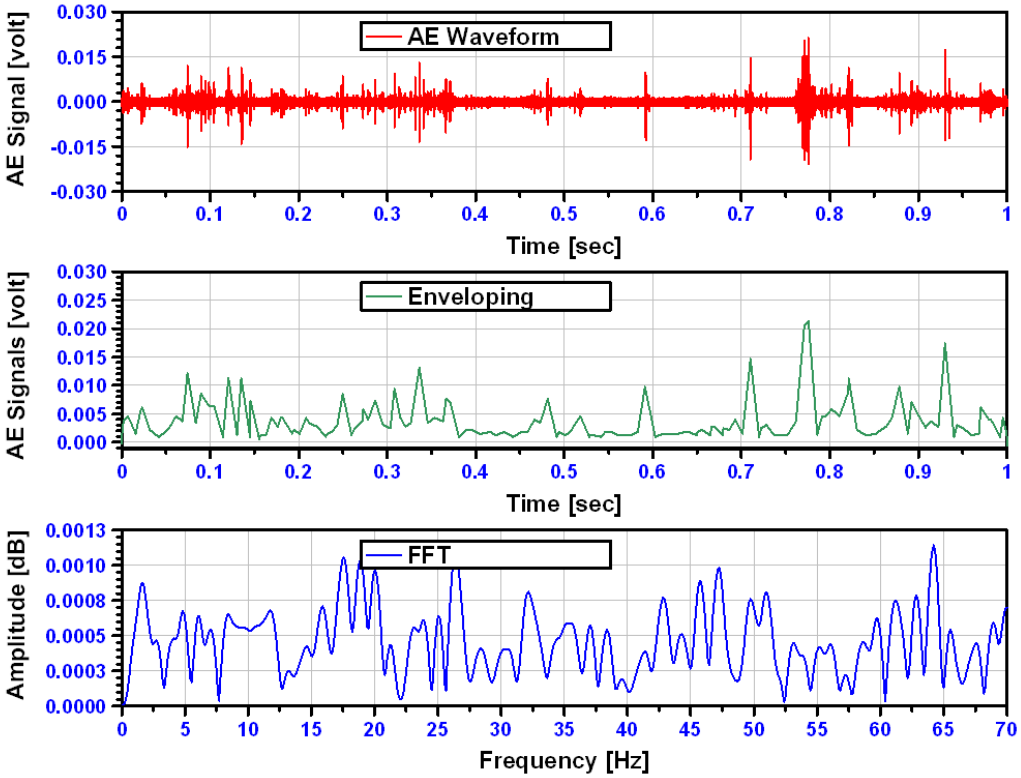

Figure 4—33 AE waveform, enveloping and FFT after 45-hrs

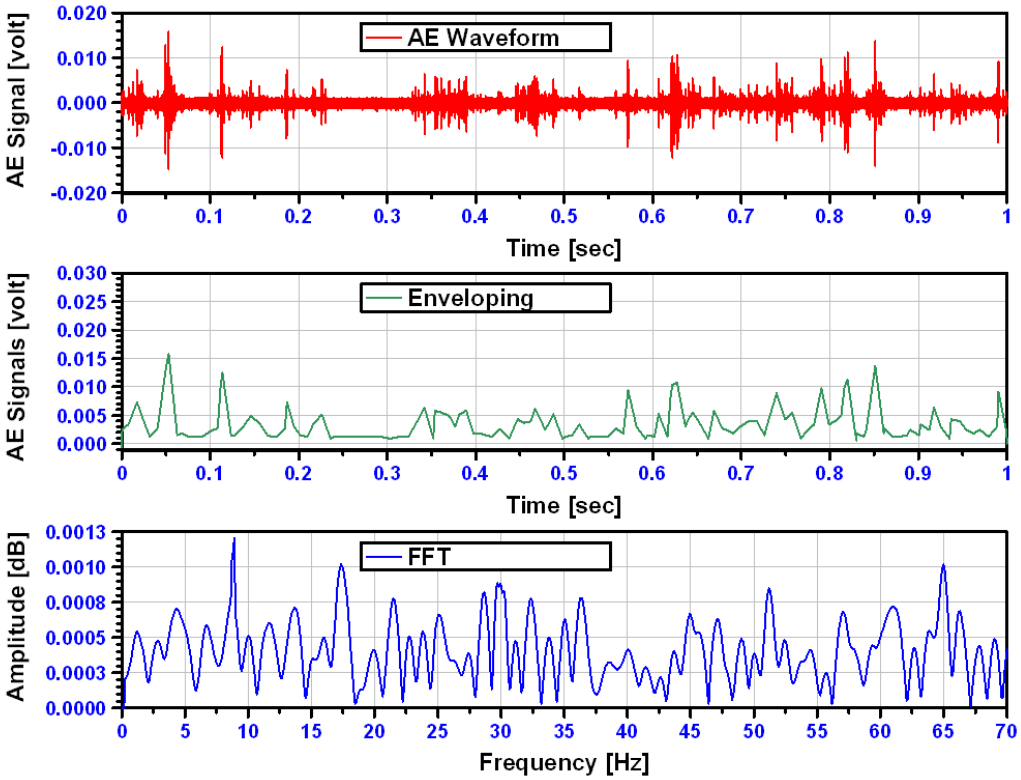

Figure 4—34 AE waveform, enveloping and FFT after 50-hrs

4.3.4 Formation of Grooved Pathway on the flat Bearing Race

In some experiments undertaken in the first approach, a phenomenon of a relative increase in AE energy levels was noted between 2- and 7-hrs of operation. Approximately at 6-hrs operation, AE levels reduced to that prior to the increased AE activity (before 3-hrs), presented in figure (4-35). Further investigation for the exact reason for this phenomenon was experimentally carried out. For this purpose, several bearing tests were run for just between 6- to 7-hrs. Tests were terminated once the level of AE reduced to that prior to the increased AE activity (3- to 6-hrs).

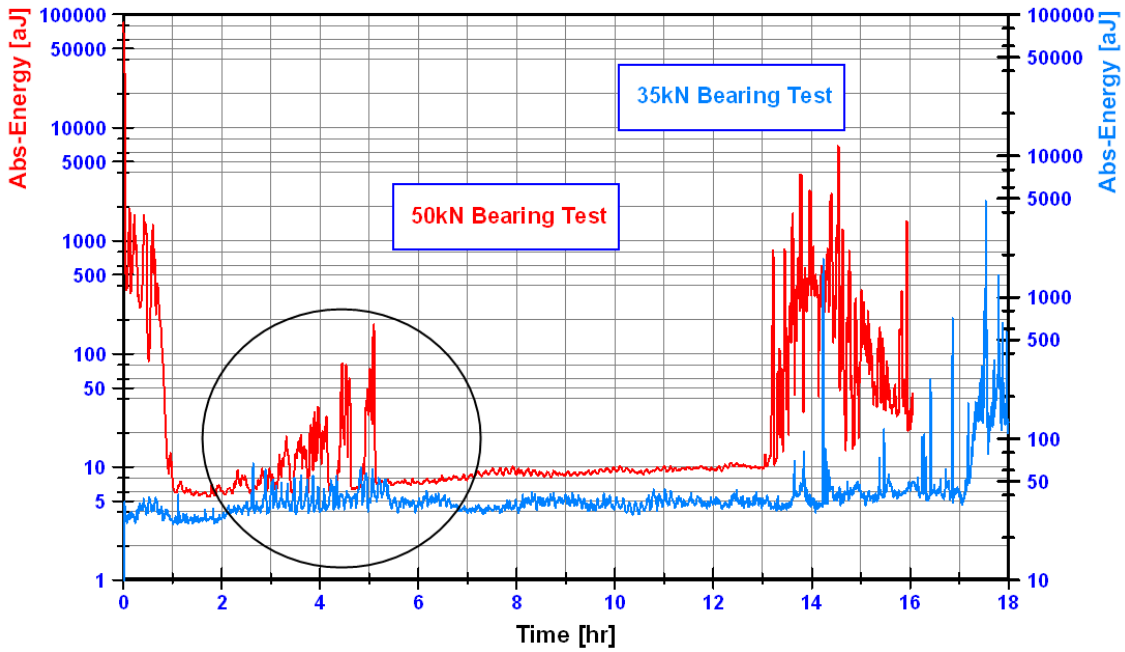

Figure 4—35 Phenomenon of an increase in AE levels between 2- and 7 hrs of operation

Results, shown in figure (4-36) highlight the investigation of continuous monitoring of AE parameters for one case, which is representative of the other cases. With almost all tests, it was noted that during the first hour AE activity was present and this was attributed to a running-in period as after this period all measured AE and temperature levels remained constant. Observations of continuous monitoring of the AE levels, noted at approximately between 2- to 4-hrs during operation, showed a significant increase in the AE activity amplitude, see figure (4-36). Also noted from the AE waveforms was high transient nature of the AE waveform at 3-hrs which reduced in amplitude at 5-hrs operation, shown in figure (4-37). On termination of the test (7-hrs) a visual inspection revealed that a grooved pathway (plastic deformation) on the flat race was formed, see figure (4-38). The initiation of the grooved pathway explains the reason of the sharp bursts of AE activity (2- to 4-hrs) noted during observations of continuously monitored AE levels. Once this plastic deformation region is fully developed; its surface becomes smoother, the contact area between the rolling ball elements and flat track increased, causing lower contact pressure on the flat race relative to the contact pressure of the test period prior to the increased

AE activity period (from 2- to 4-hrs). As a consequence, the drop in AE activity amplitude was observed at 4- to 7-hrs operation.

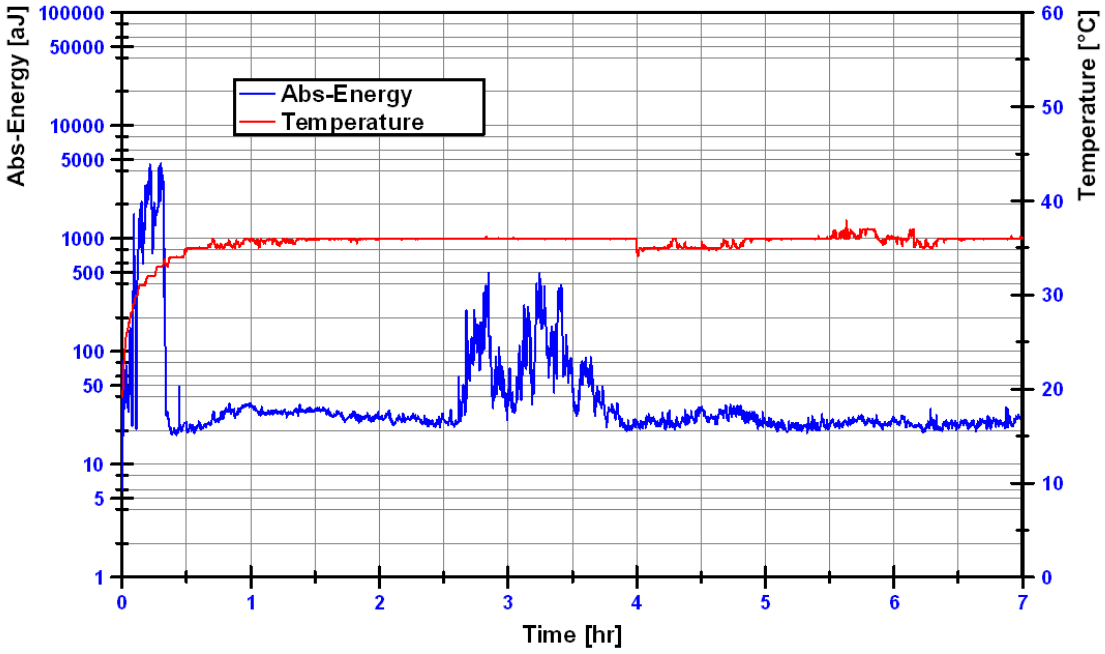

Figure 4—36 Bearing test operated to 7-hrs only

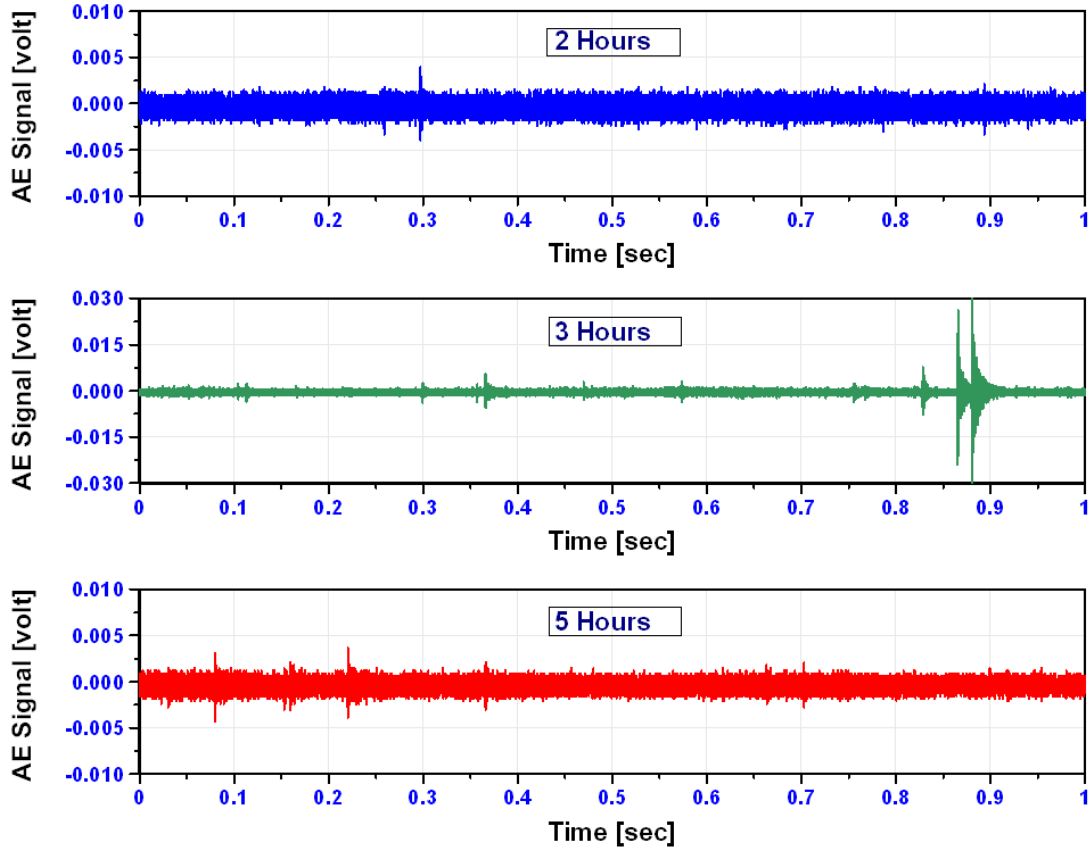

Figure 4—37 AE waveforms at 2-, 3- and 5-hrs

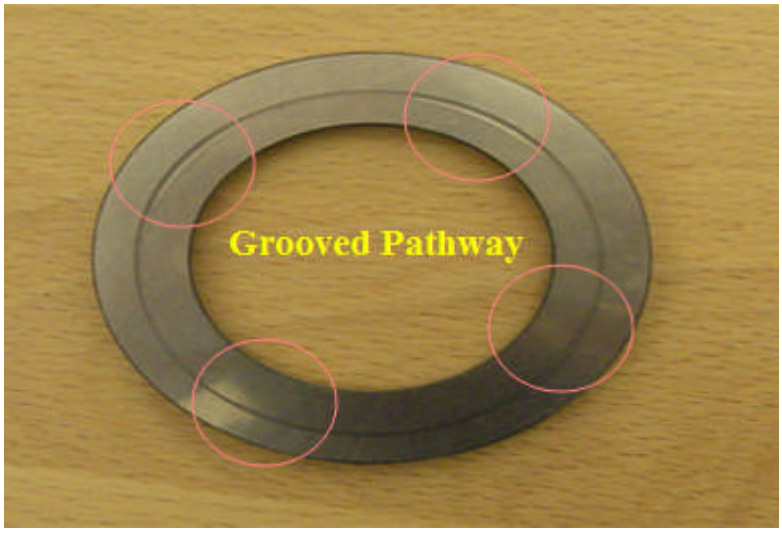

Figure 4—38 Grooved pathway on the flat bearing race after 7-hrs

4.3.5 Defect Size

Several attempts have been made to identify the defect size on bearings using AE technology. Most published work has focused on determining the size of artificial defects 'seeded damages' which are generally induced on bearings beforehand [104-106]. For this particular investigation, the Acoustic Emission technique was employed to identify the presence and size of a natural defect on bearings that were tested throughout the study. This was accomplished by identifying the duration of the AE bursts that are associated with the bearing defect. With knowledge of the duration of AE bursts and the angular velocity (S), the defect size (L) on the bearing can be calculated using equations [4-2] and [4-3] respectively.

$$S = 2\pi * \frac{\varnothing}{2} * \omega \qquad (4\text{-}2)$$

$$L = S * \zeta \qquad (4\text{-}3)$$

For this particular calculation, the case presented here is associated with the case presented in figure (4-27). The time duration of the roller elements passing over the defect was measured from the AE waveform recorded at 20-hrs into the test. The measured time duration in this study is referred to the big size defect on the bearing flat ring. With known the rotational speed of the rig (ω

= 1.2 rps), bearing diameter (Ø = 65 mm) and the duration of the roller elements passing over the load zone (ζ = 0.05 sec), the defect size was found to be 12.25 mm, see figure (4-39). Defect size results of the above three cases are presented in table (4-4).

Table 4—4 Results for the defect size measurements.

Case	Load (kN)	Speed (mm/sec)	Duration (sec)	Defect Size (mm)
I	50	245	0.054	13.10
II	35	245	0.050	12.25
III	20	245	0.041	10.01

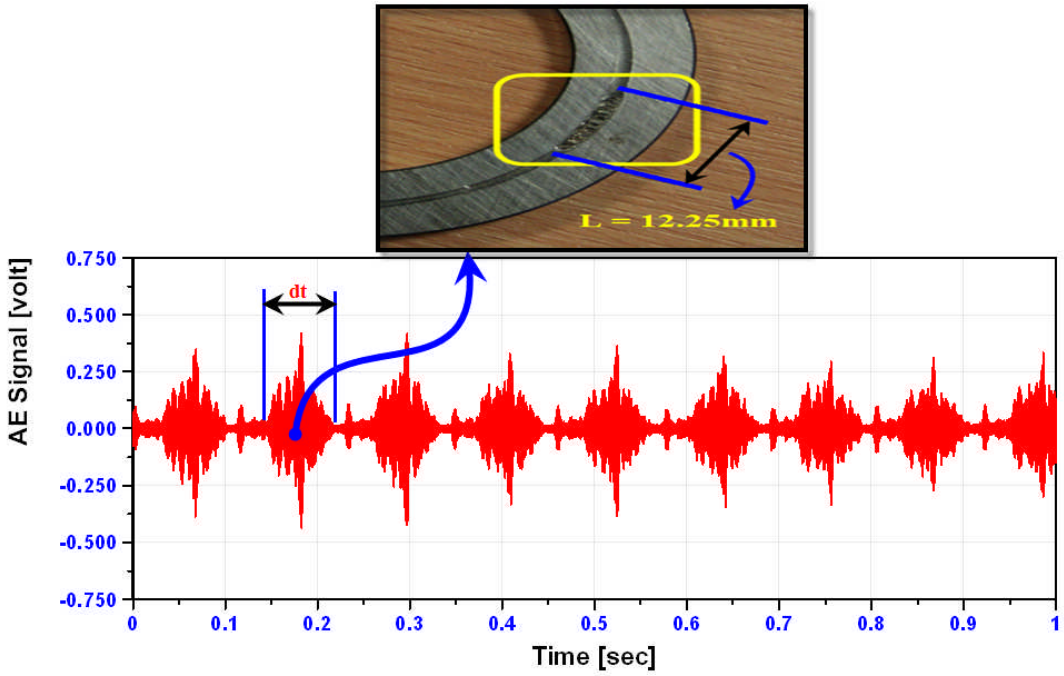

Figure 4—39 Defect size measurement

4.3.6 Case IV

The second approach (Grease Starvation Test) presents different trends to that noted in the previous cases. During the start of the test, steady AE activity was noted; observations of continuous monitoring of the AE levels of bearing operation did not show any considerable rise at the start of testing. A significant rise in AE energy levels was observed at approximately 792-sec and the AE activity gradually increased with time until the test was terminated (900-

seconds), presented in figure (4-40). The increase in AE energy levels from the start of the test to the termination was in the order of 36,937%. Traditional AE parameters such as counts showed high levels of AE activity at the end of the test, see figure (4-41). This significant rise in AE energy levels also suggested that damage, visually observable, had occurred on the bearing.

Waveforms of AE recorded throughout the test duration, presented in figure (4-42), provided another simple and rapid means to verify damage on the test bearing. They clearly show AE transient events, which grow in amplitude as the test progressed with time, eventually developing a high transient nature of AE events at the end of the test. These high transient events correspond to the bearing defect. The nature of the AE waveform for the grease starvation test case differs from the other tests as the mechanism for the generation of AE is quite different. For the grease starvation test, the main source of emission is the sliding and rolling action of the asperities between the roller and race. In addition the fragments of debris from the fractured cage will also generate AE. Such source mechanisms will result in a high amplitude continuous AE signal superimposed by even higher amplitude transient AE bursts. The damage observed for this test conditions is presented in figure (4-43).

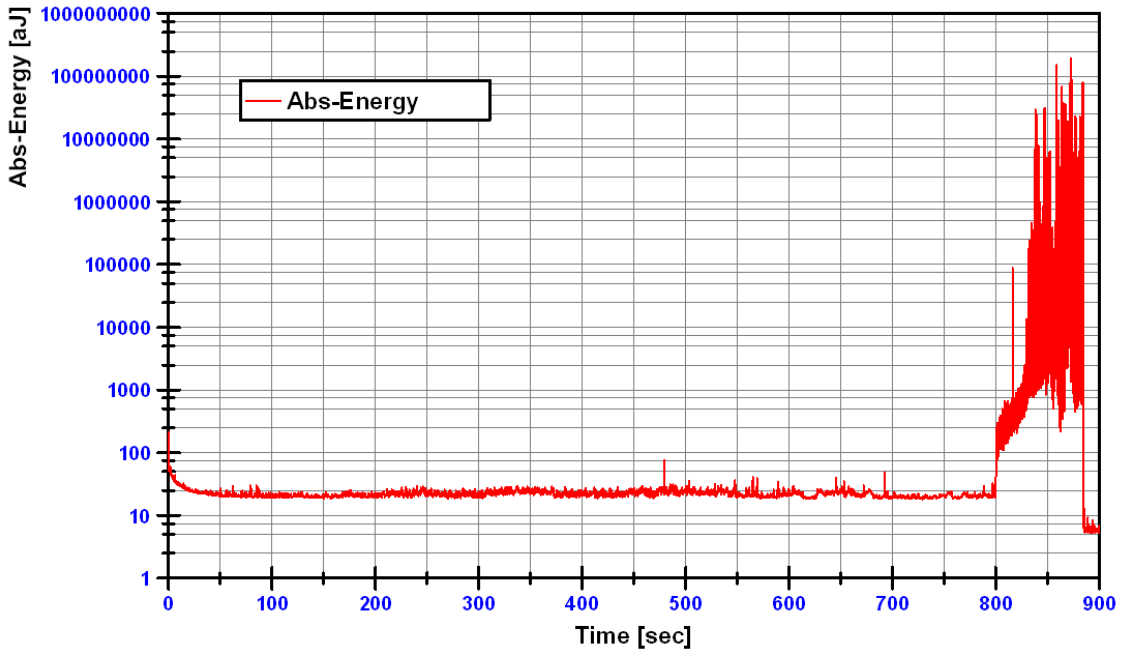

Figure 4—40 Bearing test results; run under grease starvation

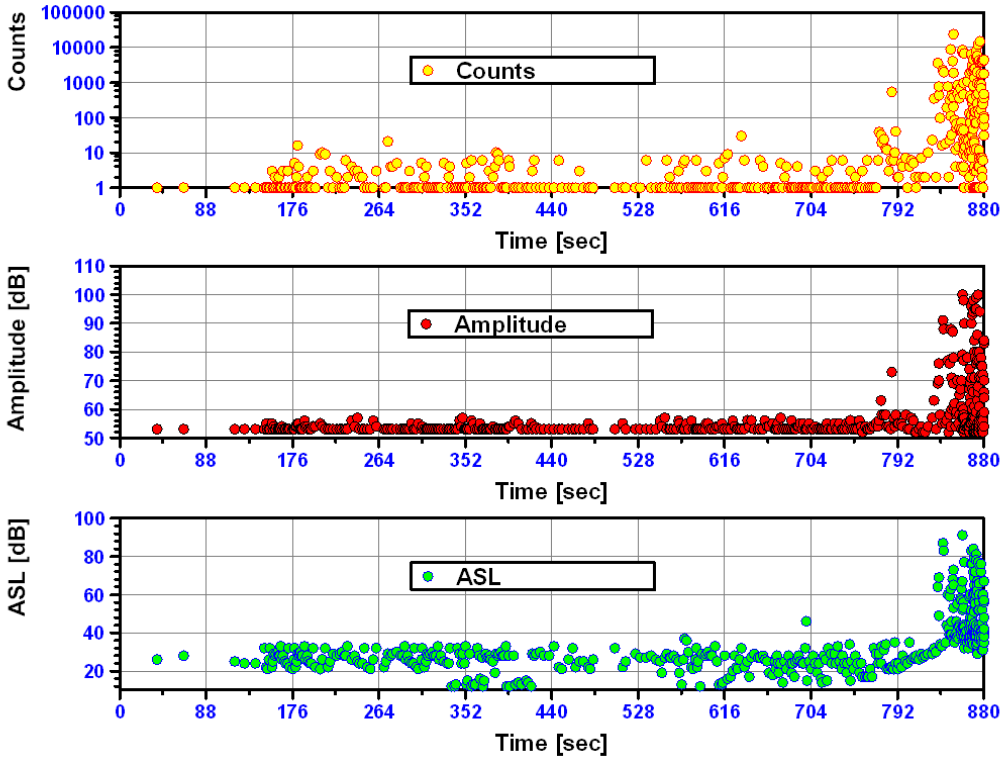

Figure 4—41 Classical AE parameters

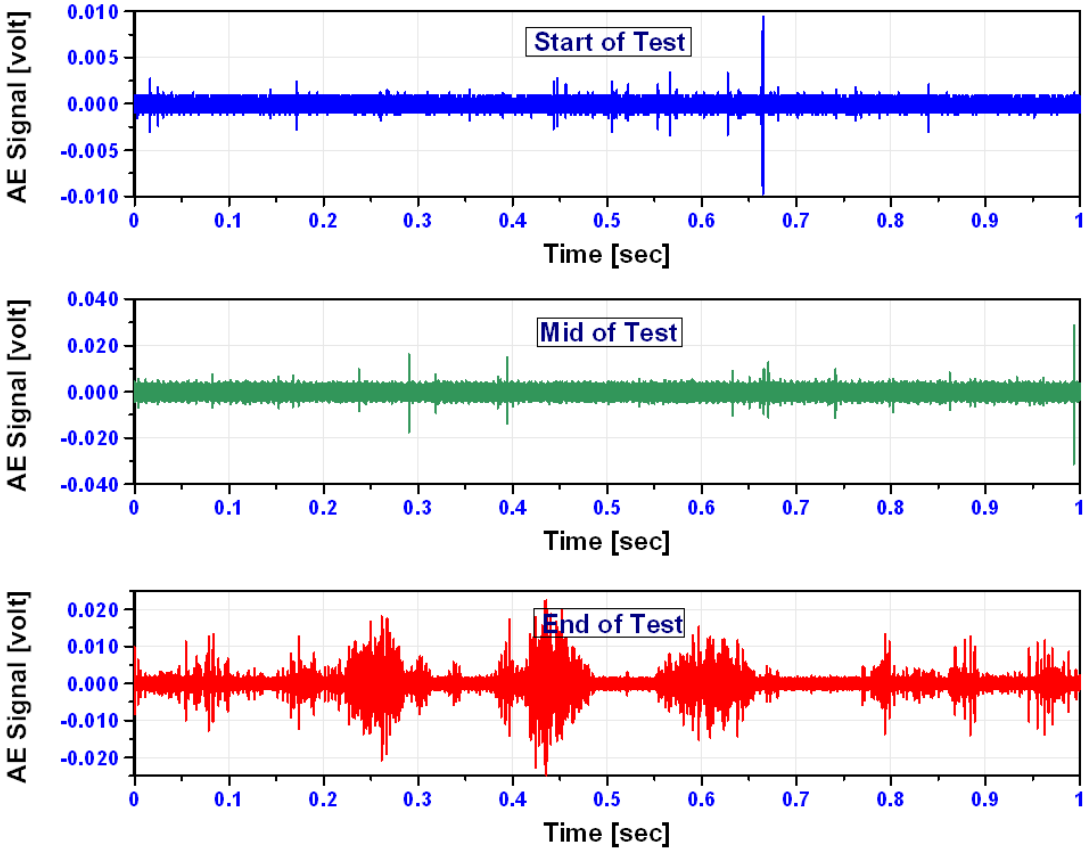

Figure 4—42 Typical AE waveforms associated with case-IV

Figure 4—43 Damage on the bearing cage

5 AE Source Location Analysis

In addition to continuous observations of AE recorded throughout the bearing tests, time domain analysis and frequency domain analysis were discussed in the preceding chapter. In this chapter the linear source location technique developed in this research program and used for all bearing tests is presented.

The capability of AE to determine source locations of signals emanating in real time from materials under load is one of the significant advantages AE offers over other non-destructive test (NDT) technologies. In application the AE signals travelling through the medium are attenuated and arrive at different sensors with a time delay. This delay can be attributed to the distance between the source (defect) and AE sensors, and, with knowledge of the signal velocity the location of the AE source can be identified.

5.1 Bearing Tests

The source location analysis for the three experimental cases of the first bearing test approach, presented in the preceding chapter, is here discussed. For this particular investigation efforts were made to identify the defect location (AE source location) in real-time. This was accomplished by identifying the wave velocity on the bearing flat ring experimentally. At a threshold of 52 dB and with known distances between the AE sensors, the velocity of the AE waveform under such conditions was experimentally determined at 4,000 m/sec. Interestingly, the dominant frequency content of AE's recorded was approximately 300 kHz, see figure (5-1), and the wave velocity of 4,000 m/sec corresponds to the symmetric zeroth Lamb wave mode (S_o) for steel at 1.8 mm-MHz (0.3 MHz * 6 mm thickness).

The propagation velocity (4,000 m/sec) was used for all source location investigations and prior to the onset of testing several Hsu-Nielsen sources were made at various positions on the flat ring surface to establish the accuracy at this velocity and specific threshold level. Results were within 4% of the exact geometric location of the Hsu-Nielsen sources. Figure (5-2) shows the source

location layout used which essentially 'unwrapped' the bearing race for linear location.

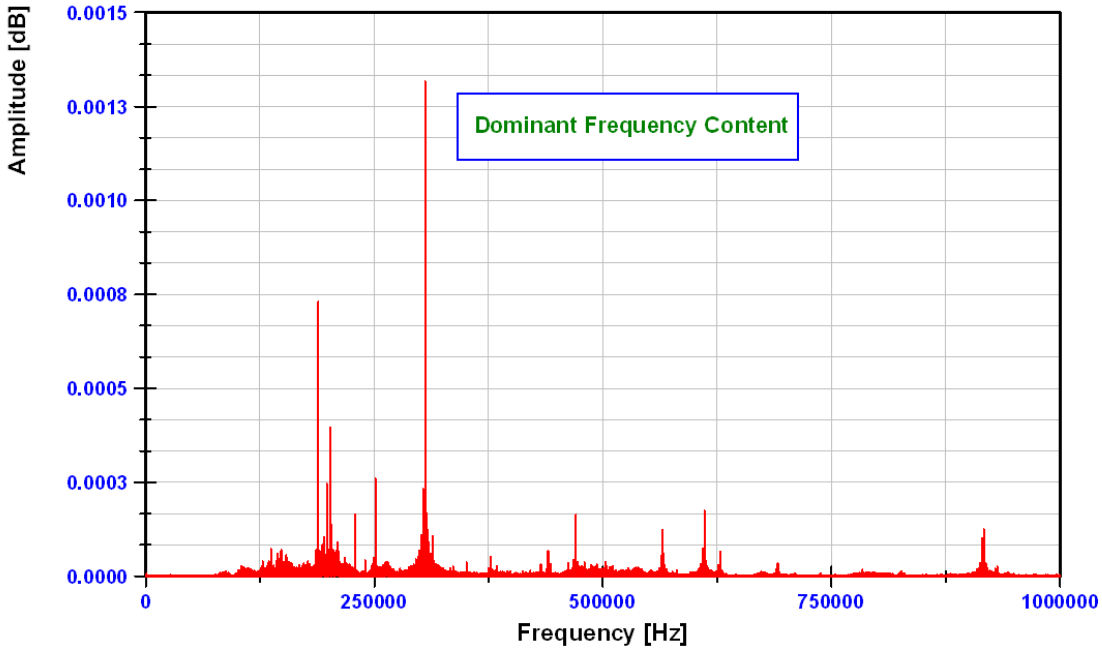

Figure 5—1 Dominant frequency content of AE's

The location plots show cumulative energy over the test simulation. It is worth mentioning that only AE events above a threshold of 52 dB contribute to the source location. Whenever the threshold is exceeded, the location of the source is computed and identified. The AE energy is assigned to the geometric position (source); this is a cumulative process and as such a fixed source will have the largest contributory energy in a cumulative plot.

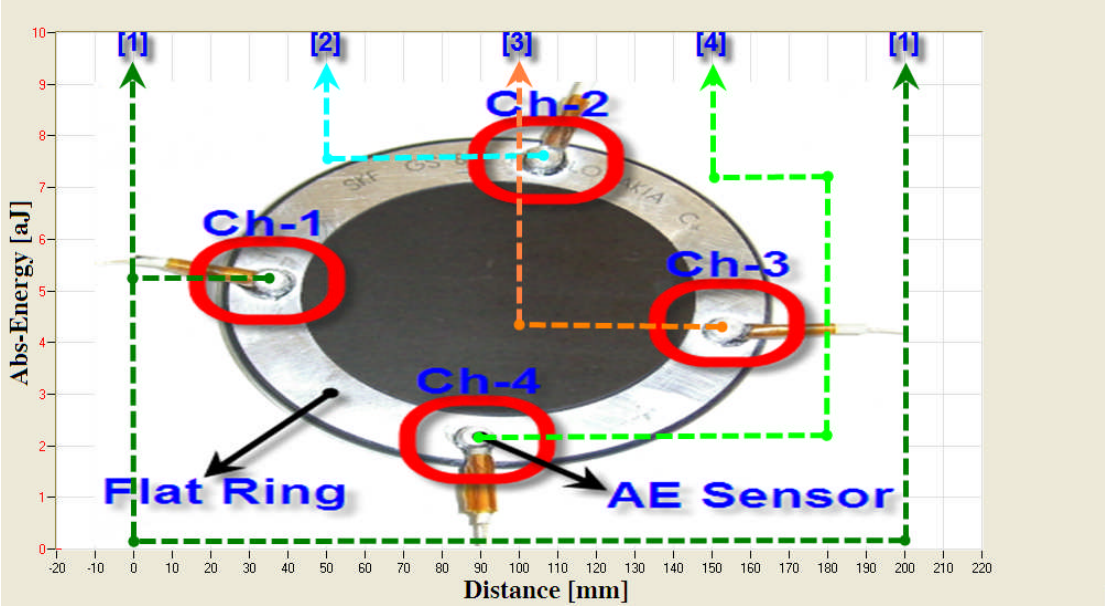

Figure 5—2 Source location layout for linear detection

5.1.1 Case I

Chapter 4 has shown the observations of AE when monitoring the degradation of an accelerated bearing test; the next phase of analysis involved source identification of AE activity during the test duration. Figures (5-3) to (5-6) highlight the trends in source location throughout the test period. These results are associated with the bearing test presented in figure (4-11).

Source location estimations employed in the bearing test provided another simple and rapid means to identify and locate the crack initiation and propagation to surface spall. The regions where the surface damage occurred are highlighted by the 'box' section termed 'zones'. Evident from these figures was that at the start of the test (run-in), an AE activity was distributed across a very broad circumferential position on the bearing ring. This is not surprising as the run-in period is associated with considerable AE events whilst the bearing dynamics stabilize, see figure (5-3). After 4- to 10-hrs geometric concentrations of AE activity in the eventual defect zones became evident with values of 4×10^4 atto-Joules (zone1), 3.4×10^5 atto-Joules (zone 2) and 5×10^4 atto-Joules (zone 3), noted at 10-hrs operation, see figures (5-4) and (5-5). On the termination of the test (16-hrs), the concentration of the AE sources was clearly

located in the highlighted damage region, see figure (5-6); maximum energy values of 5 x 10^7 atto-Joules (zone1), 52 x 10^7 atto-Joules (zone 2) and 89 x 10^7 atto-Joules (zone 3) were noted.

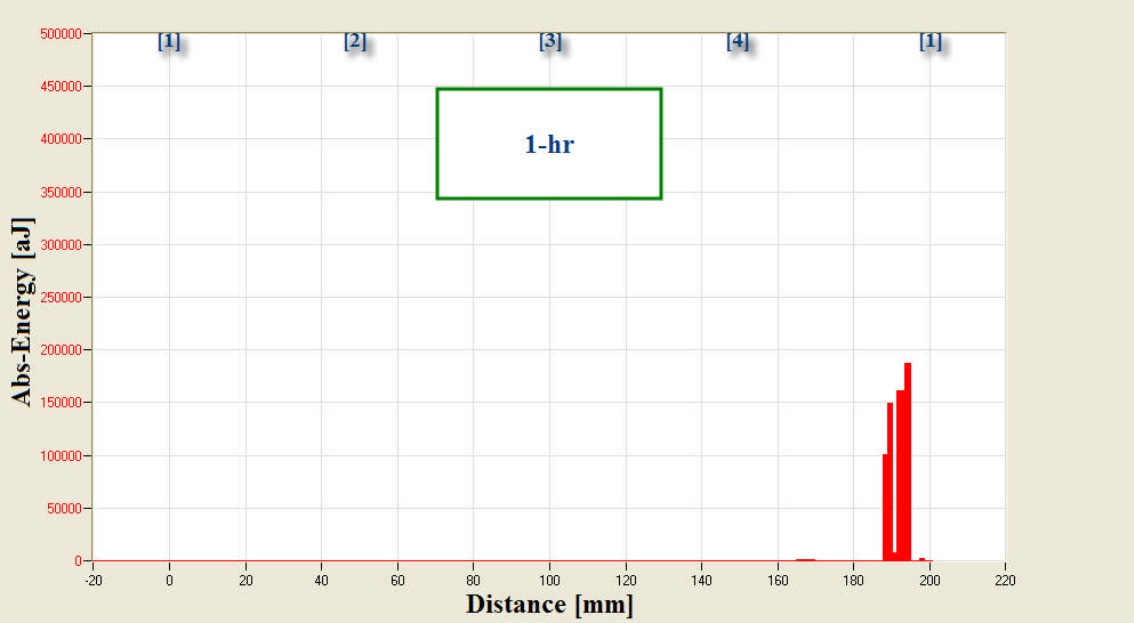

Figure 5—3 Source location estimates of AE events at 1-hr operation

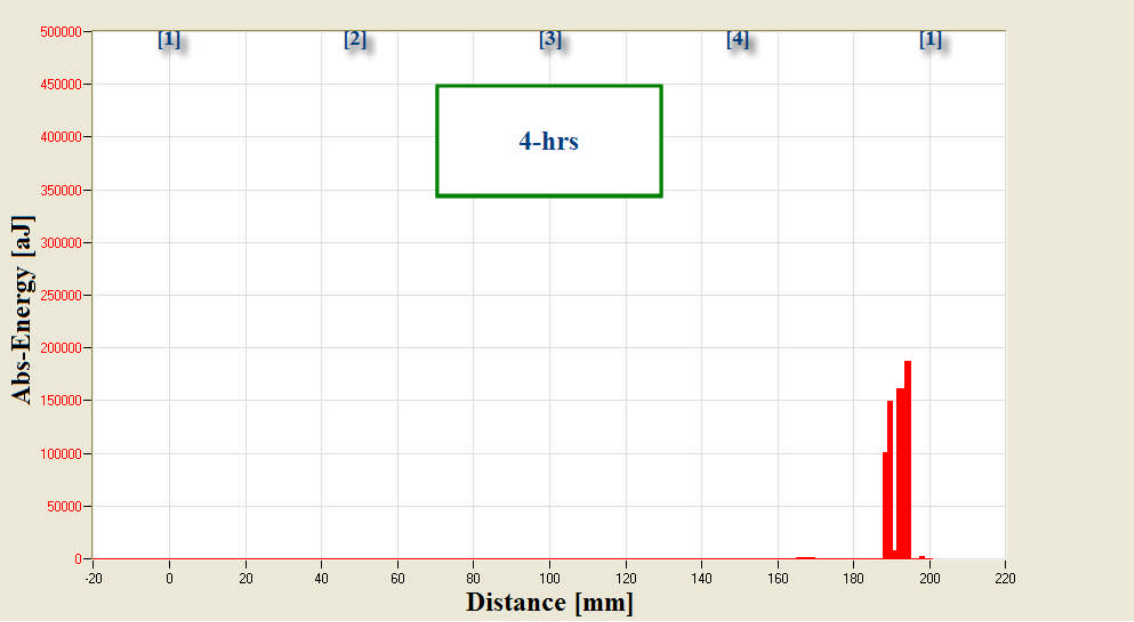

Figure 5—4 Source location estimates of AE events at 4-hrs operation

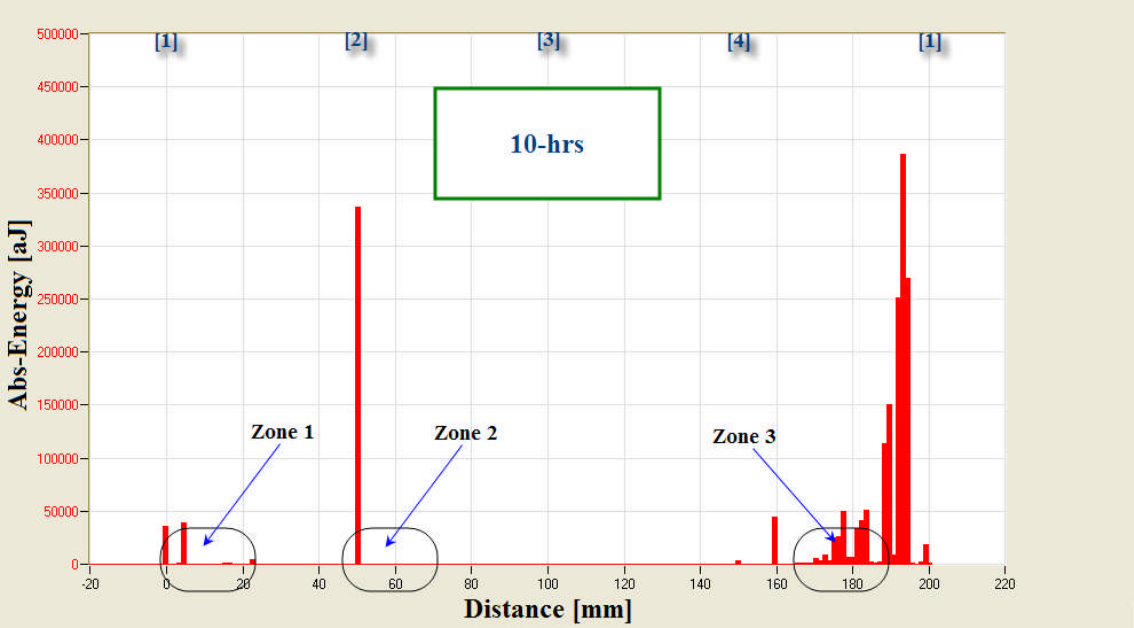

Figure 5—5 Source location estimates of AE events at 10-hrs operation

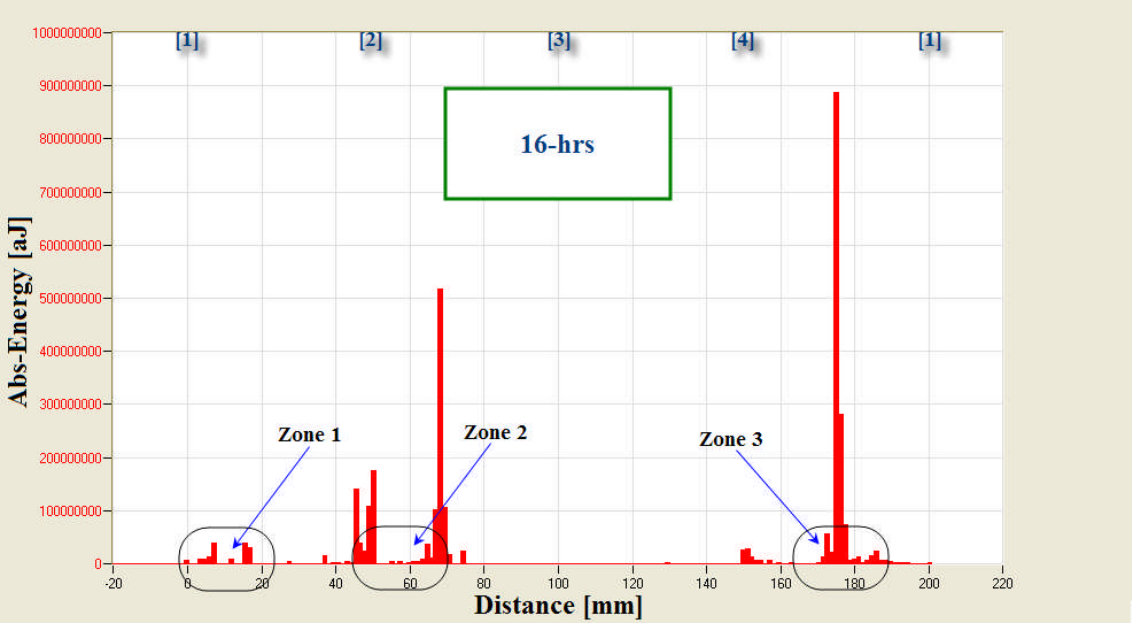

Figure 5—6 Source location estimates of AE events at 16-hrs operation

5.1.2 Case II

As in the previous case the source location over the duration of the test case, associated with the bearing test shown in figure (4-19), is presented in figures (5-7) to (5-10). At the start of the test, geometric concentrations of AE activity were distributed across the circumferential length of the bearing and this is

attributed to the run-in condition, see figure (5-7). Evident from these figures was also that after running from 1-hr to 13-hrs, the contributory AE activity to the location plots were not observed, see figures (5-7) and (5-8). At 14-hrs relatively early signs of concentrated AE source activity of the highlighted zones began to appear, see figure (5-9); geometric concentrations of AE activity in the eventual defect zones became evident with values of 105 x 10^3 atto-Joules (zone 1) and 22 x 10^3 atto-Joules (zone 2). Figure (5-10) shows the growing concentration of AE energy from the defect locations; after 20-hrs operation the concentration of the AE source was clearly located at the two highlighted regions and the maximum energy values of 40 x 10^5 atto-Joules (zone 1) and 42 x 10^5 atto-Joules (zone 2) were noted. These locations corresponded to the actual defects visually observed at the end of the test, see figure (4-22).

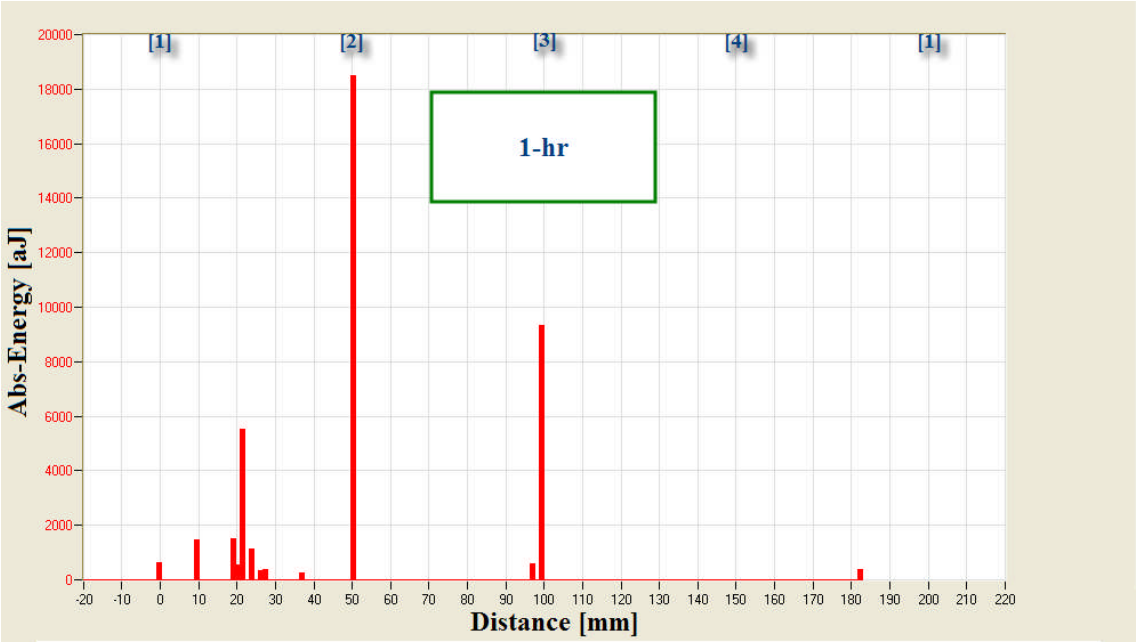

Figure 5—7 Source location estimates of AE events at 1-hr operation

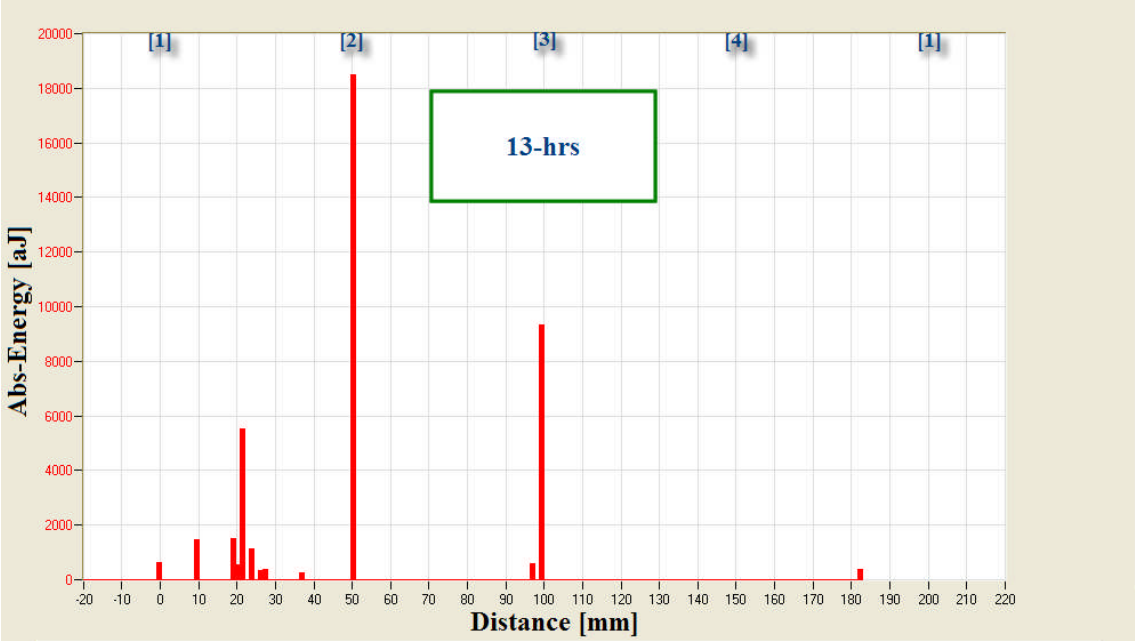

Figure 5—8 Source location estimates of AE events at 13-hrs operation

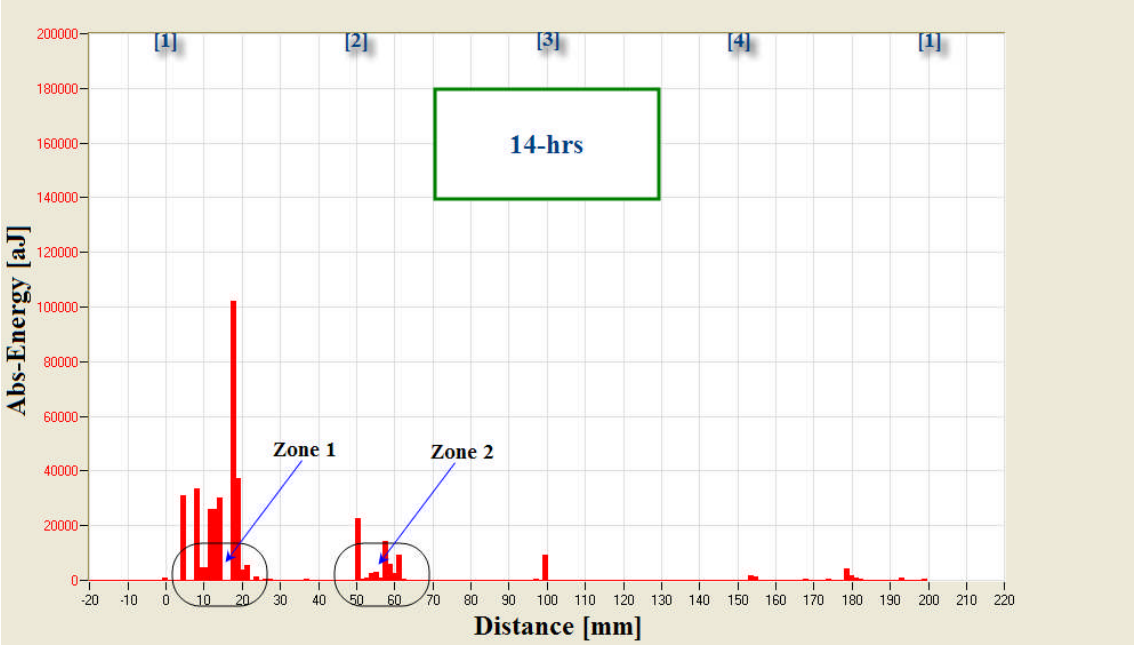

Figure 5—9 Source location estimates of AE events at 14-hrs operation

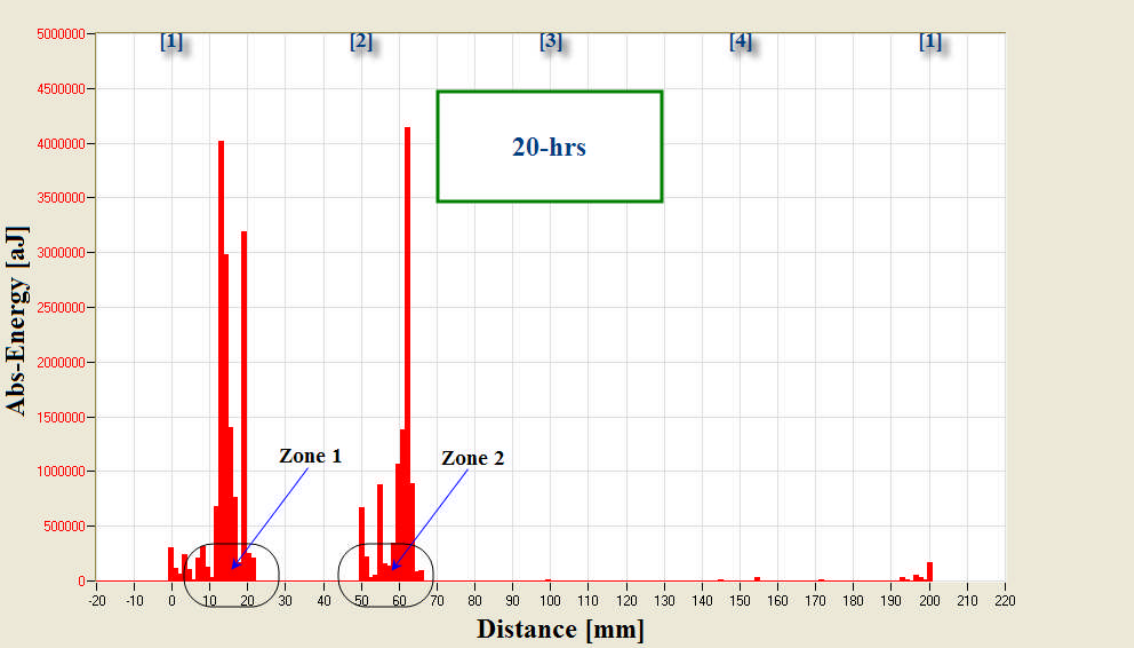

Figure 5—10 Source location estimates of AE events at 20-hrs operation

It is worth mentioning that the crack initiated at 14-hrs of operation on the basis that a broad scatter of AE sources noted at the start of the test (run-in) in the source location plots remained constant from 1– to 13-hrs operation, see figures (5-7) and (5-8); no contributory energy to the location plots was observed, but at 14-hrs of operation the concentration of AE events was from the defect regions and started to increase steadily until the test was terminated (20-hrs). Moreover, the continuous monitoring of AE activity, presented in figure (4-19), showed that from 14-hrs until the termination of the test (20-hrs) significant increase in the AE levels was observed.

5.1.3 Case III

In contrast to the previous cases, a geometric concentration of the AE source, associated with the case presented in figure (4-27), was not noted until approximately 40-hrs; this can be attributed to the low load (20 kN) applied in this test; see figures (5-11) and (5-12). Furthermore, these cumulative plots compute and identify only AE events above the defined threshold (52 dB). It is particularly interesting to note that the onset of crack development could have been identified as early as 45-hrs into the operation of the test bearing, as

shown in figure (5-13). From 45-hrs of operation a specific geometric AE source was noted which approximated to a surface damage of 20 mm in circumferential length in the vicinity of channel-2, see figures (5-13) and (5-14). This reinforces the observations of continuous monitoring of AE energy presented in figure (4-27).

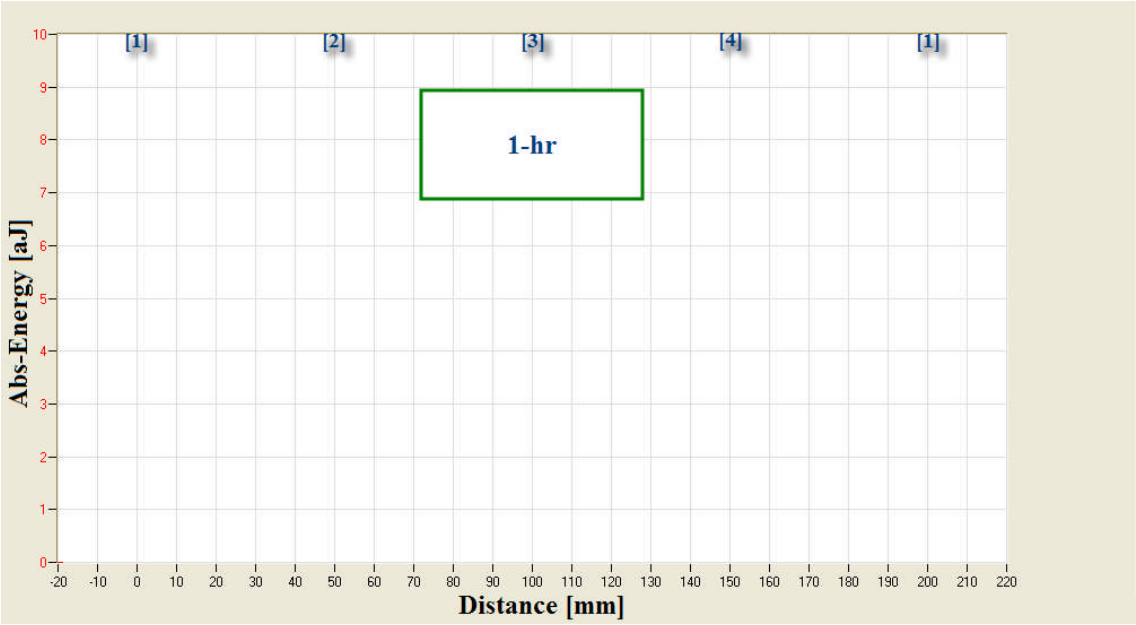

Figure 5—11 Source location estimates of AE events at 1-hr operation

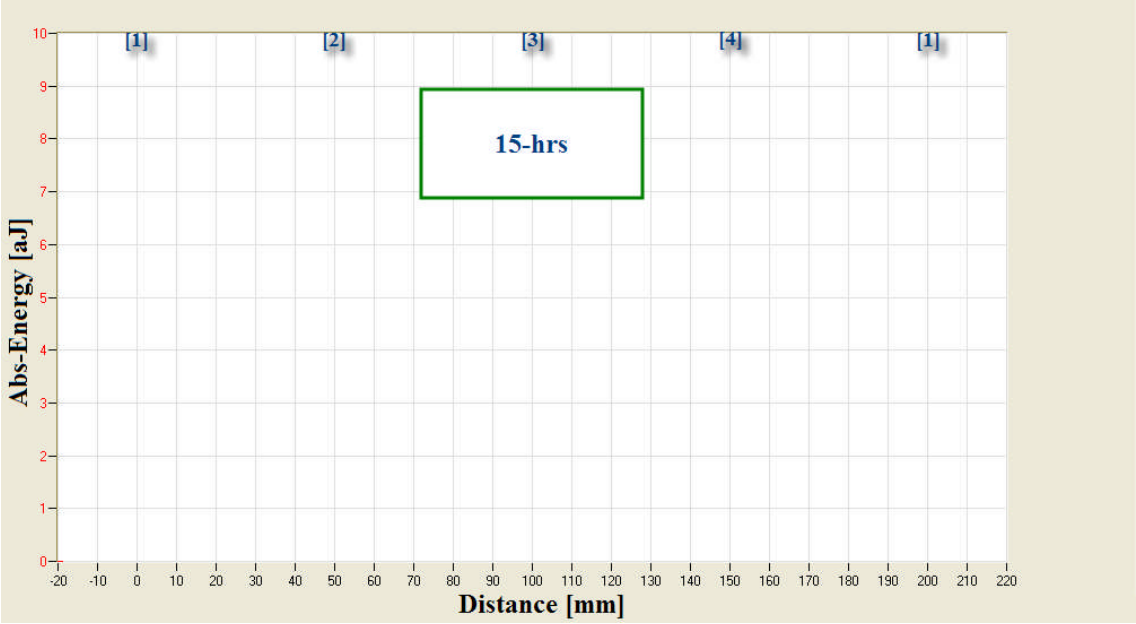

Figure 5—12 Source location estimates of AE events at 15-hrs operation

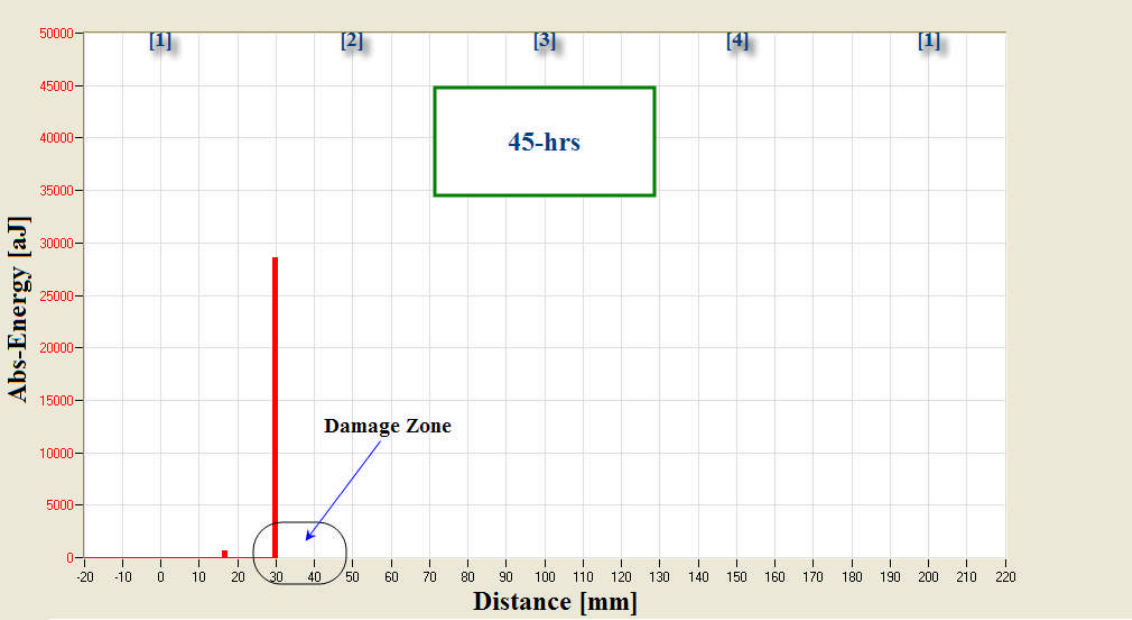

Figure 5—13 Source location estimates of AE events at 45-hrs operation

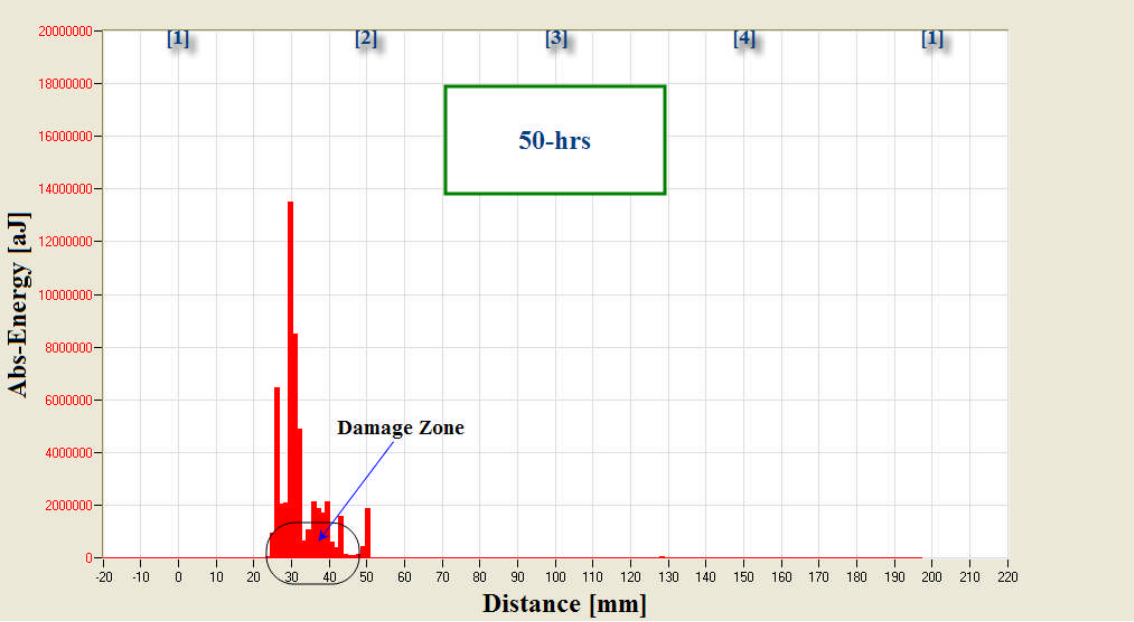

Figure 5—14 Source location estimates of AE events at 50-hrs operation

6 Shaft Condition Monitoring

In this chapter, details of shaft test rig design, laboratory experiments, results and observation are discussed. Figure (6-1) depicts the detailed steps followed from the basic design of the shaft test rig until the results interpretation.

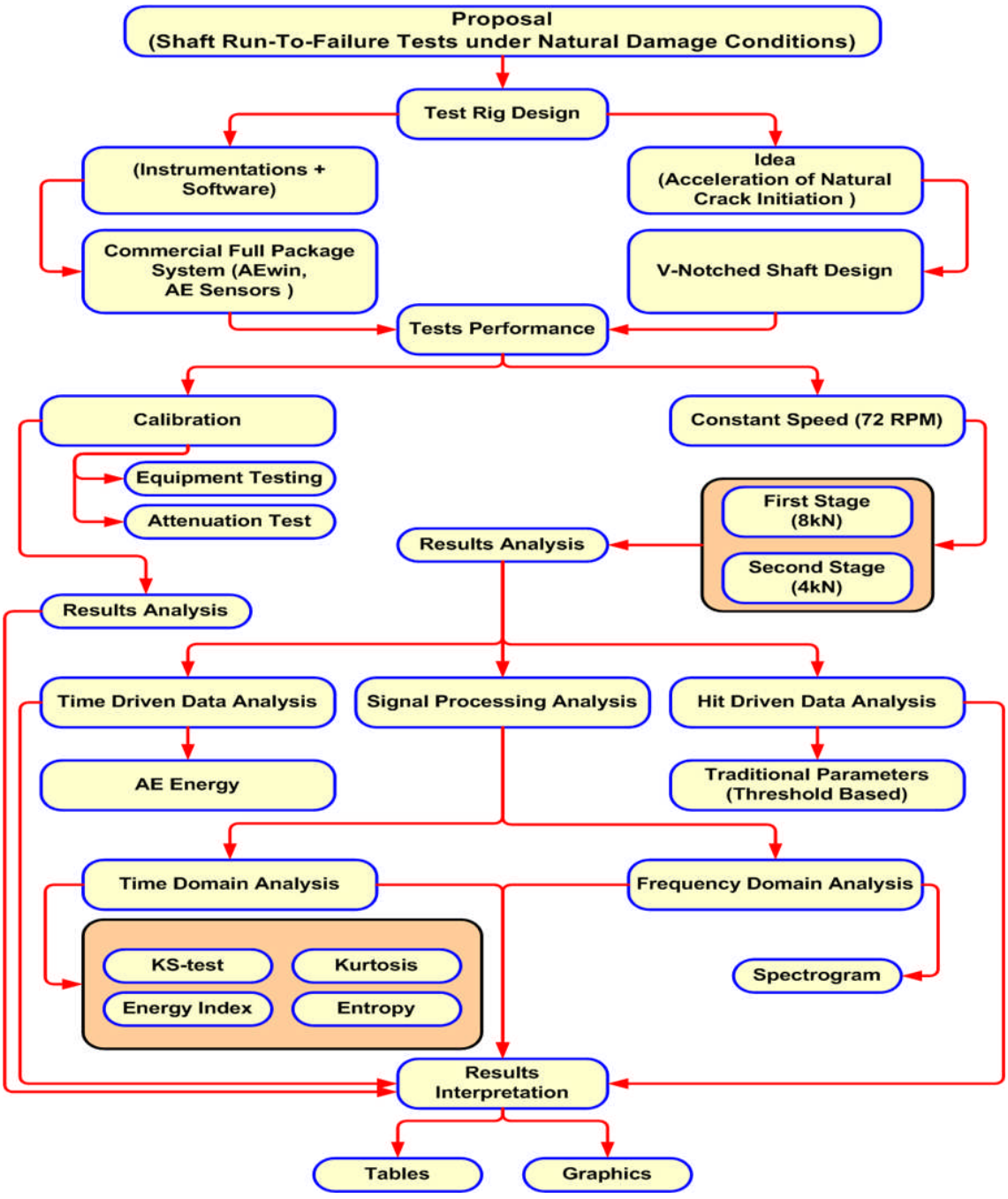

Figure 6—1 Steps of shaft test from basic design to results interpretation

6.1 Test-Rig Design and Layout

The experimental test rig, shown in figure (6-2), was built to investigate shaft failure and associated AE characteristics. The shaft is driven by an electrical geared motor (MOTOVARIO-Type HA52 B3-B6-B7 j20, 46-Lubricated: AGIP). Two taper bearings (SKF 30207 J2/Q) were employed to support the shaft and positioned on its end. An overhang thrust bearing (SKF NU 1007 ECP) was used to locate the hydraulic load shaft onto the shaft. To accelerate crack initiation and growth, a V-Notched shaft of 390 mm length and 35 mm main diameter was designed. A radial load was applied to the shaft through the overhang bearing by a hydraulic system (Hi-Force HYDRAULICS-MODEL No: HP110-HAND PUMP-SINGLE SPEED-WORKING PRESSURE: 700 BAR). The author employed [107-109] for designing the shaft test rig. Shaft design procedures are presented in appendix B. The test rig rotational speed was kept constant at 72 RPM. A flexible coupling was employed to absorb any vibration as a result of attaching the shaft to the geared motor. With AE measurements, it is vitally important to place the AE sensors as close to the source as possible. As such the AE sensor was placed on the shaft. Under such arrangements a slip ring may be employed to connect the rotating sensor to a data acquisition system. In a rotating mechanical system it is significantly important to transmit signals from sensors on a rotating shaft to an exterior stationary part (Data Processing System), and several conventional methods exist to achieve signal transmission. A slip ring, which is a method of making an electrical connection, has been generally used as a means of observing signals of a rotating machinery component. However, there is a difficulty that special machining of a rotating shaft is needed to accommodate a slip-ring in general. Thus, the author has proposed an alternative method using a specifically designed oil-filled cylinder for this investigation. This is similar to a hydrodynamic bearing but in this case the cylinder is completely filled with oil, see figures (6-2) and (6-3). A flat surface was machined on the outer periphery of the enclosing cylinder for placement of the AE sensor. A rubber seal at both sides of the cylinder end ensured no leakage and consequently there was no mechanical contact between the shaft and oil-bath that could result in generation of AE noise. This

enclosed circular bath allowed for direct contact between the rotating shaft and the oil (CASTROL, Alpha, SP, 460, 3186DM).

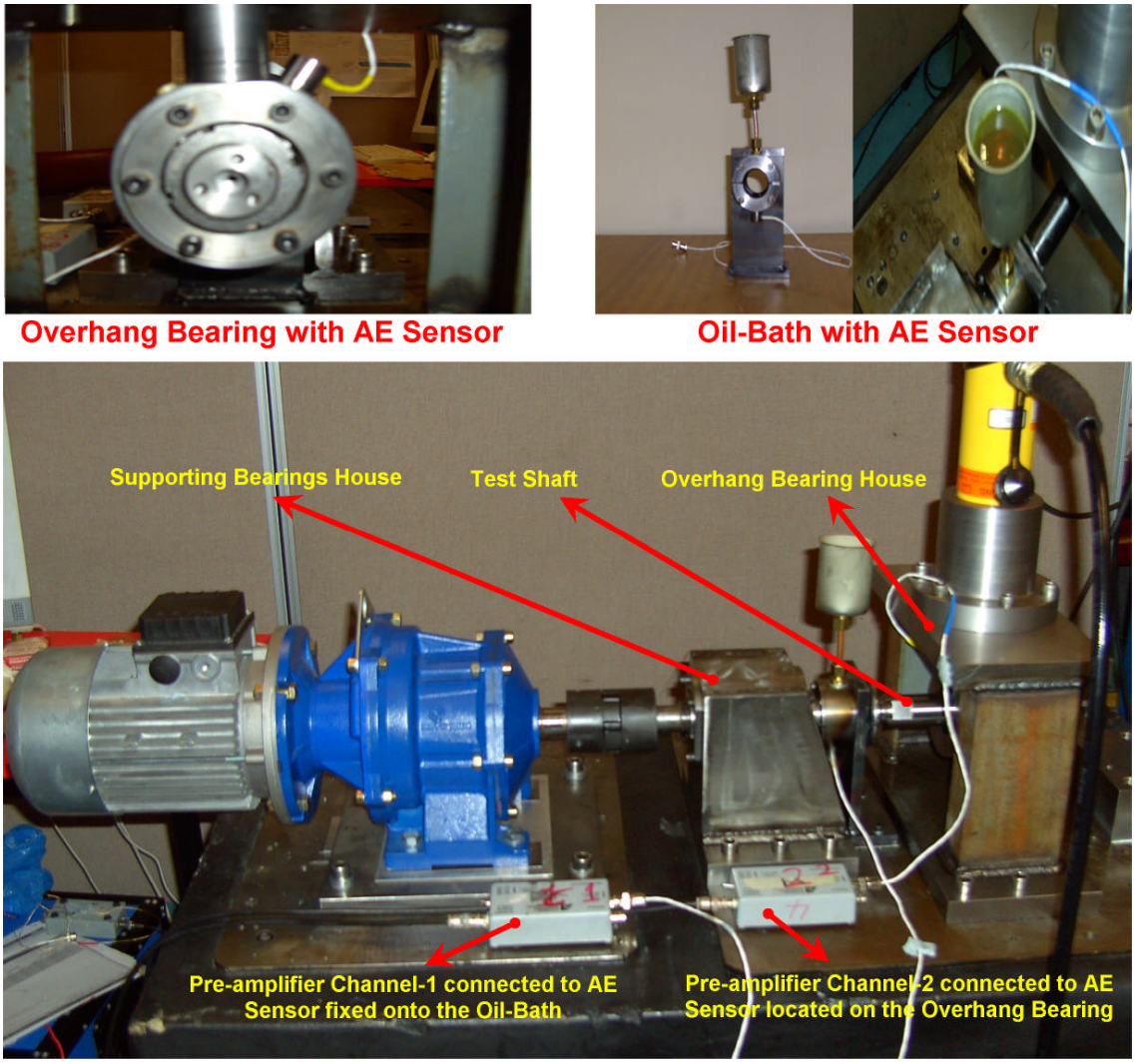

Figure 6—2 Test-Rig layout

6.2 Instrumentation and Acquisition System Calibration

Two Physical Acoustics Corporation WD transducers were employed. These are piezoelectric sensors with a bandwidth of 200-750 kHz at temperatures ranging from -65 to 177 ^{o}C. The AE sensors were attached to the overhang bearing and the oil filled cylinder using superglue and connected to variable gain preamplifiers 20, 40, and 60 dB which were in turn connected to a ruggedized PC, containing Physical Acoustics Corporation PCI-2 acquisition

cards, see figure (6-2). The preamplifiers were set at a gain of 40 dB. The software (signal processing package “AEWIN”) was incorporated within the PC to monitor AE parameters such as counts, amplitude and absolute energy (recorded at a time constant of 10 ms and sampling rate of 100 Hz). The absolute energy (atto-Joules = 10^{-18} Joules), is a measure of the true energy and is derived from the integral of the squared voltage signal divided by the reference resistance (10 k-ohms) over the duration of the AE signal. In addition, traditional AE parameters such as counts, amplitude and ASL were also measured. The ASL is a measure of the continuously varying and averaged value of the amplitude of the AE signal in decibels (dB). The ASL is calculated from the RMS measurement using the equation [4-1]. The traditional parameters were calculated over an AE event duration of 1500 µsec and a threshold of 40 dB. The threshold value was set at approximately 3 dB above the operational background noise of the shaft. The system was also continuously set to acquire AE waveforms at a sampling rate of 2 MHz.

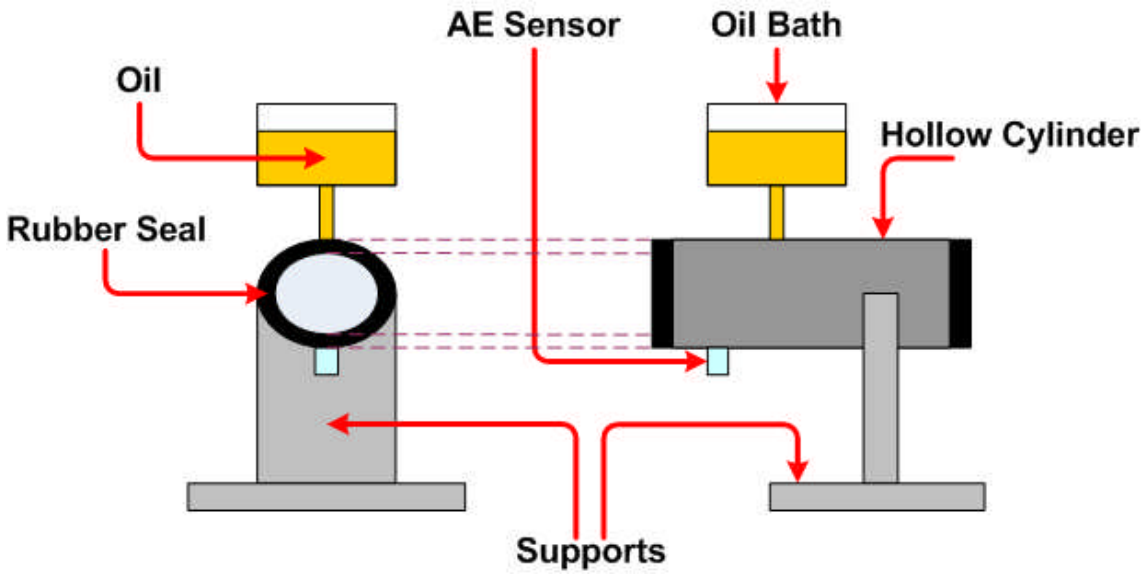

Figure 6—3 Schematic of oil-filled cylinder

6.3 Shaft Tests

Shafts were tested until complete fracture prior to which the crack was visually observable. The shaft material properties, the stress range and the crack size

govern the crack propagation rate. One of the key factors that can affect the crack growth rate is the stress at the crack tip. It should be noted that at the lower stress levels crack initiation constitutes the majority of the life time before fracture whilst higher stress levels tend to favour a much shorter initiation period but longer crack propagation duration. Under normal conditions of load, shaft material properties, rotational speed and good alignment, it is expected that cracks will be initiated in the vicinity of the notch, where a sharp change in cross-sectional area of the shaft was designed, due to the high stress concentration on that site.

The anticipated life for the defined stress levels was calculated and the results clearly illustrate that the fatigue could be ascertained within a few hours depending on the load condition. For this particular thesis two experimental cases are presented that reflect the general observations associated with other experimental tests at loads 4 kN and 8 kN. Case I is for a load condition of 4 kN whilst Case II presents results for a test load of 8 kN.

To determine the signal strength as a function of distance and assess the viability of monitoring cracked shafts by taking measurements from a bearing casing, AE measurements were taken simultaneously from both AE sensors for all tests. The results of measured AE data from channel-1 (the oil-filled cylinder channel) were compared with measured AE data from channel-2 (the overhang rolling element bearing channel).

6.3.1 Case I

The test rig rotational speed was 72 rpm and a radial load of 4 kN was employed for this particular test. Observations of continuous monitoring of the AE levels, in addition to traditional AE parameters, for 513-mins of shaft operation are presented in figures (6-4) and (6-5). The test terminated on fracture of the shaft (513-mins). Relatively high levels of measured AE activity from channel-1 were noted between 95- and 130-mins of operation. This was not observed from channel-2 though AE levels from this channel relatively increased before the final fracture; much later that was detected by channel-1. It

is clear that AE measurements from channel-2 have more AE background noise than channel-1 due to the contribution of the friction of the rolling elements, see figure (6-4). Further, the position of channel-1 has shown an advantage over channel-2 on the basis that it could produce a clear indication of steadily increased AE emission levels noted at the end of tests, see figure (6-4). After 130-mins operation the level of AE reduced to that prior to the increased AE activity at 95-mins, see figure (6-4). It was also observed that at approximately 440-mins into the test measured AE activity from channel-1 showed significant increase in AE energy levels until the test was terminated (513-mins).

Figure (6-5) shows trends of traditional AE parameters all of which show significant increase in AE activity from 430-mins of operation. It is also worth noting that relatively high levels of AE parameters (Counts, ASL and Amplitude) at 95-mins of operation were noted, particularly the activity associated with AE counts. Interestingly observations of the AE waveform, sampled at 2 MHz showed changing characteristics as a function of time. This is presented in figures (6-6) and (6-7) where a typical high transient nature of the waveform of AE events was noted after 100-mins of operation. It is also particularly interesting to note that the AE waveforms after 130-mins of operation did not show any high amplitude transient AE activity. Between 400- to 500-mins of operation high AE transient bursts were again noted until the test was terminated, see figure (6-7). On termination of the test (513-mins), a visual examination of the fractured surfaces revealed that the fatigue crack had propagated along the circumference of the shaft. Moreover, the fractured surfaces had been rubbing during rotation of the shaft, see figure (6-16). Also visually observed was the opening and closing of the crack prior to fracture. This movement, which also causes rubbing of the cracked face, results in high AE activity as noted after 456-mins of testing. The author believes that increased AE activity between 95- to 130-mins is attributed to crack initiation and the large transient AE events towards the end of the tests are due to the rapid propagation, shearing and rubbing of the cracked face.

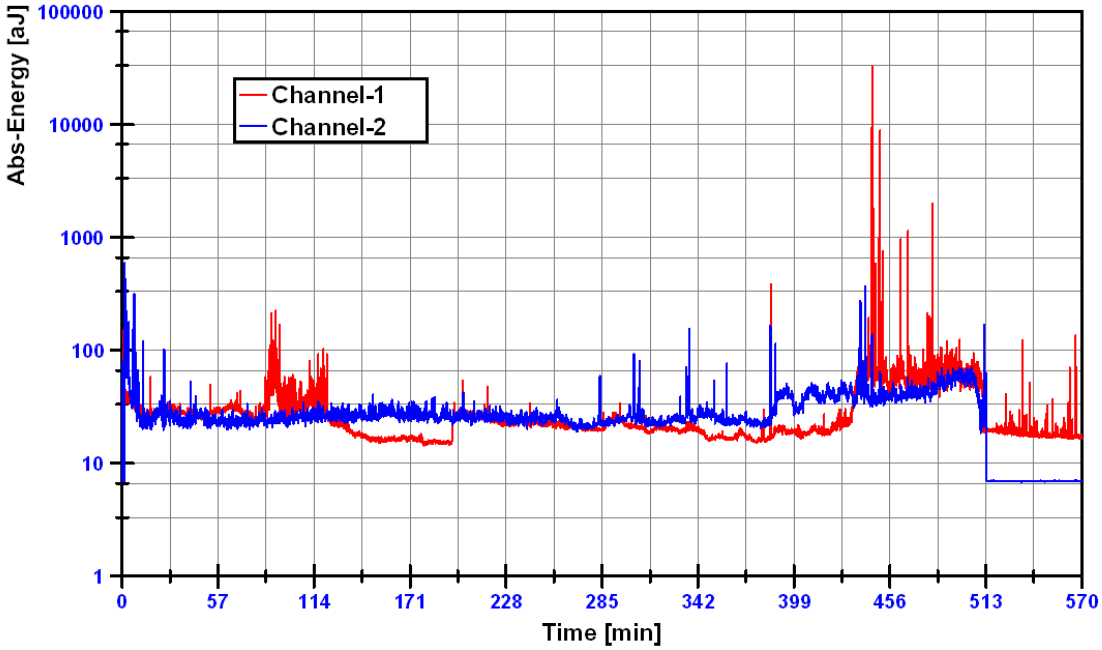

Figure 6—4 Observations of a run-to–failure shaft test

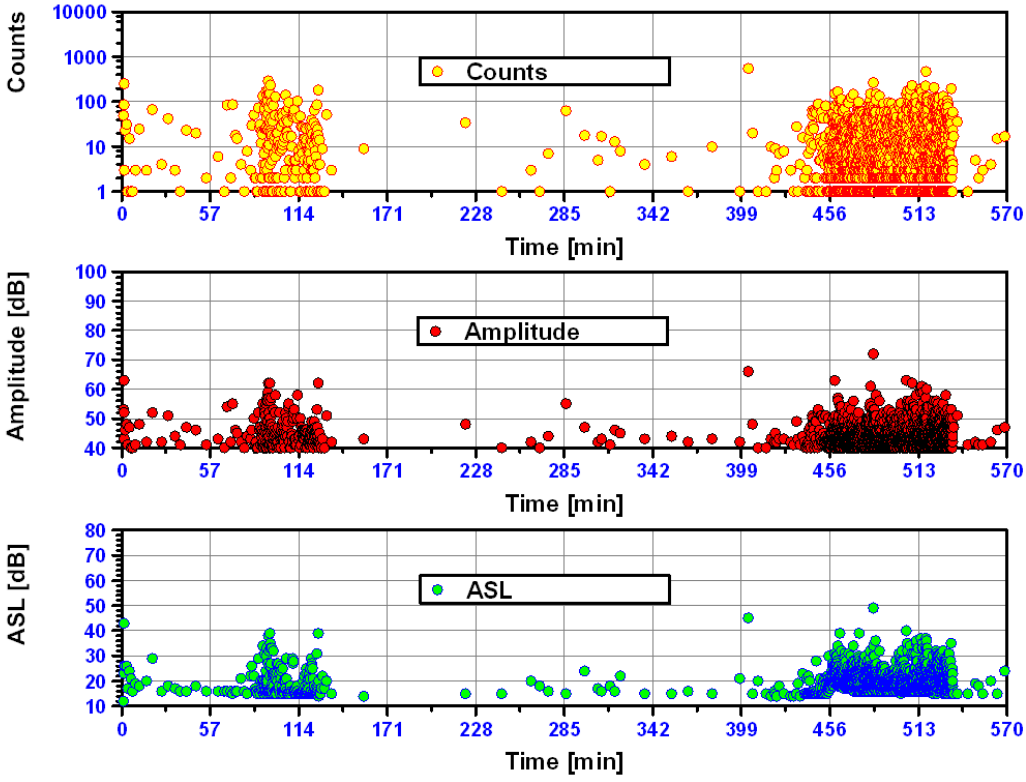

Figure 6—5 Classical AE parameters of counts, amplitude and ASL, (AE measurements from channel-1)

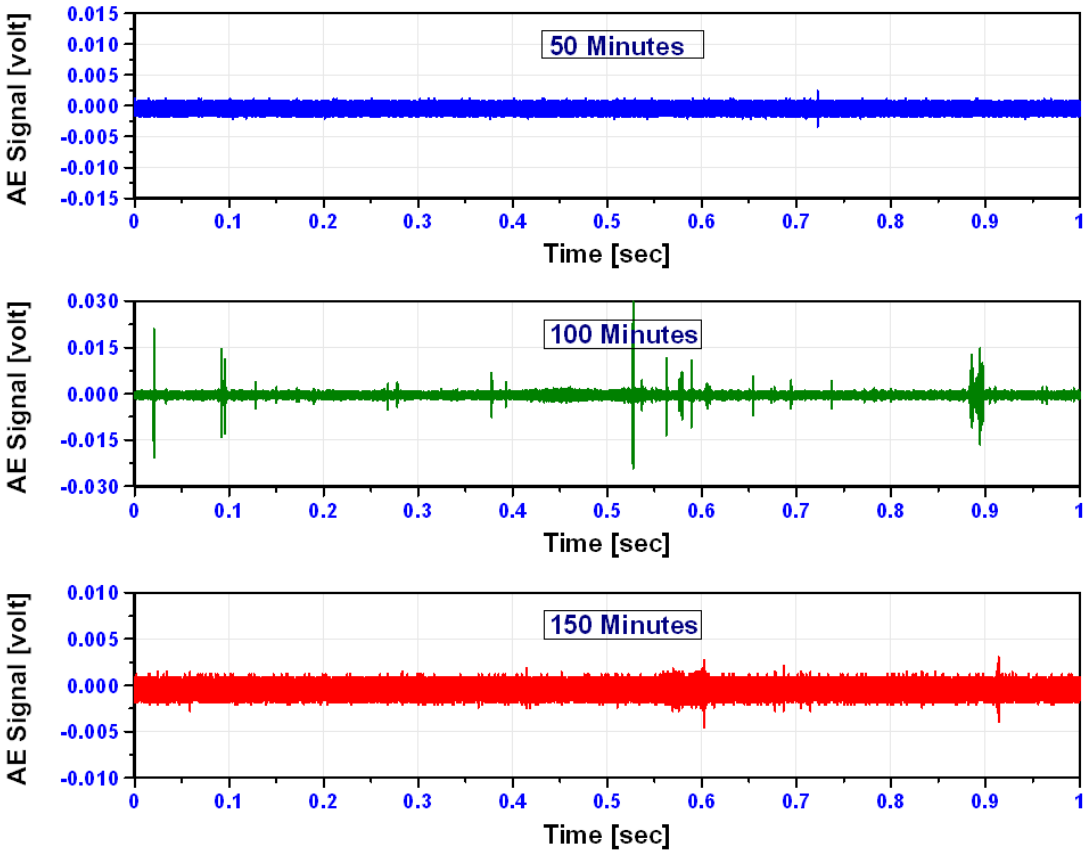

Figure 6—6 AE waveforms associated with results in figure (6-4), (AE measurements from channel-1)

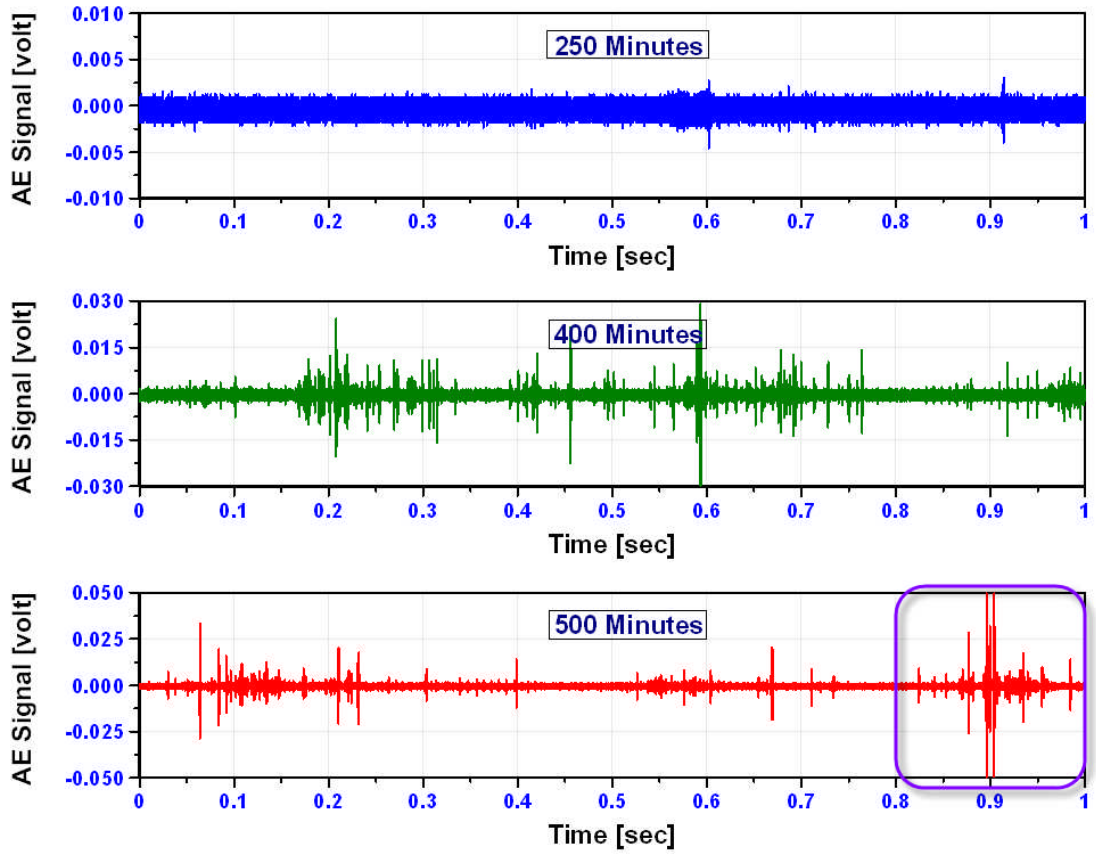

Figure 6—7 AE waveforms associated with results in figure (6-4), (AE measurements from channel-1)

Having established that tradition AE parameters such as counts, etc, showed sensitivity to changes in AE activity it was thought prudent to ascertain which other processing techniques could employ the transient characteristics noted thus far in determining the shaft conditions. The techniques employed for this assessment included the Energy Index (EI), Kurtosis (KU), Information Entropy (IE) and Kolmogorov-Smirnov Test (KS-test).

While the test passed 100-mins operation results indicated that all indicators IE, KS-test, KU and EI have relatively high values of about 0.020, 0.042, 158.2 and 4.0 respectively. It is worth stating that after 150- to 350-mins all calculated IE and KS-test values remained almost constant whilst KU and EI values showed an unsteady trend. As the test progressed with time (350- to 450-mins) all indicator values were very sensitive to the variation in shaft signals, see figure (6-8). After running 350- to 550-mins IE and KS-test started to increase steadily

while the sensitivity of KU and EI decreased with the size of localized fatigue; at 550-mins of operation IE and KS-test recorded their maximum values of 0.132 and 0.171 respectively whereas KU and EI recorded values of 250.40 and 5.13 respectively, shown in figure (6-8).

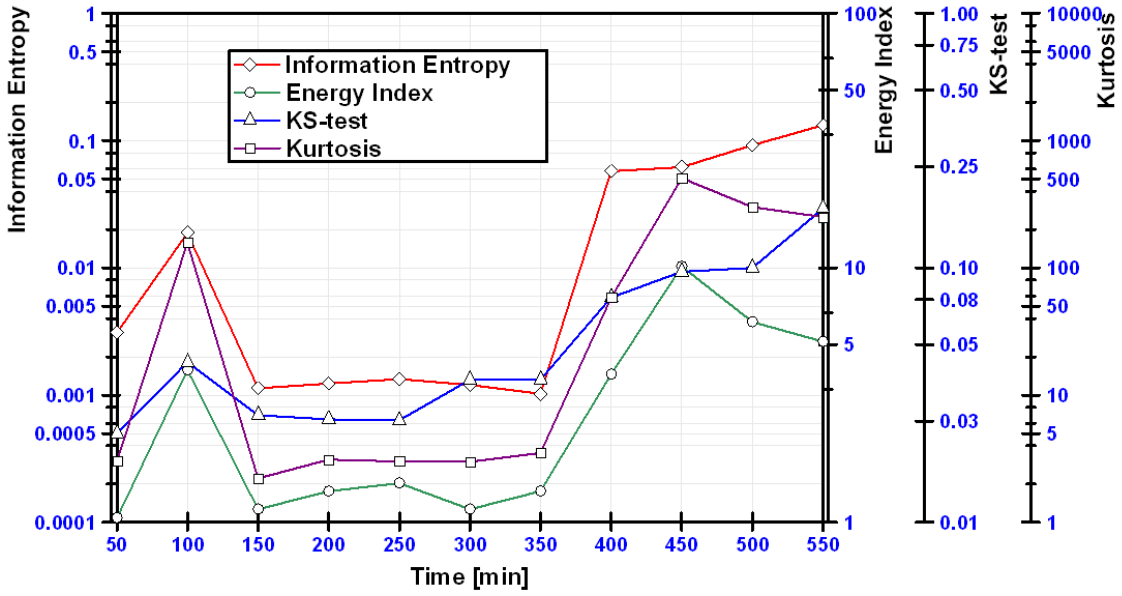

Figure 6—8 IE, KU, EI and KS-test results

The AE waveforms recorded throughout the test period was further evaluated using the spectrogram analysis. The use of the spectrogram is particularly appropriate as it gives information about the measured AE signals both in the frequency and time domain. A spectrogram was undertaken on part of the AE waveform recorded at 500-mins into operation, presented in figure (6-7). The spectrogram is presented in figure (6-9). It was evident that the large transient AE burst contained frequency ranging from 200 kHz to 1 MHz whilst continuous type of AE contained frequencies between 200 to 400 kHz. The author believes that high frequency components are attributed to the release of elastic waves particularly attributed to the propagating crack in the shaft whilst low frequency components are due to shearing and rubbing of the cracked face noted at the end of the test.

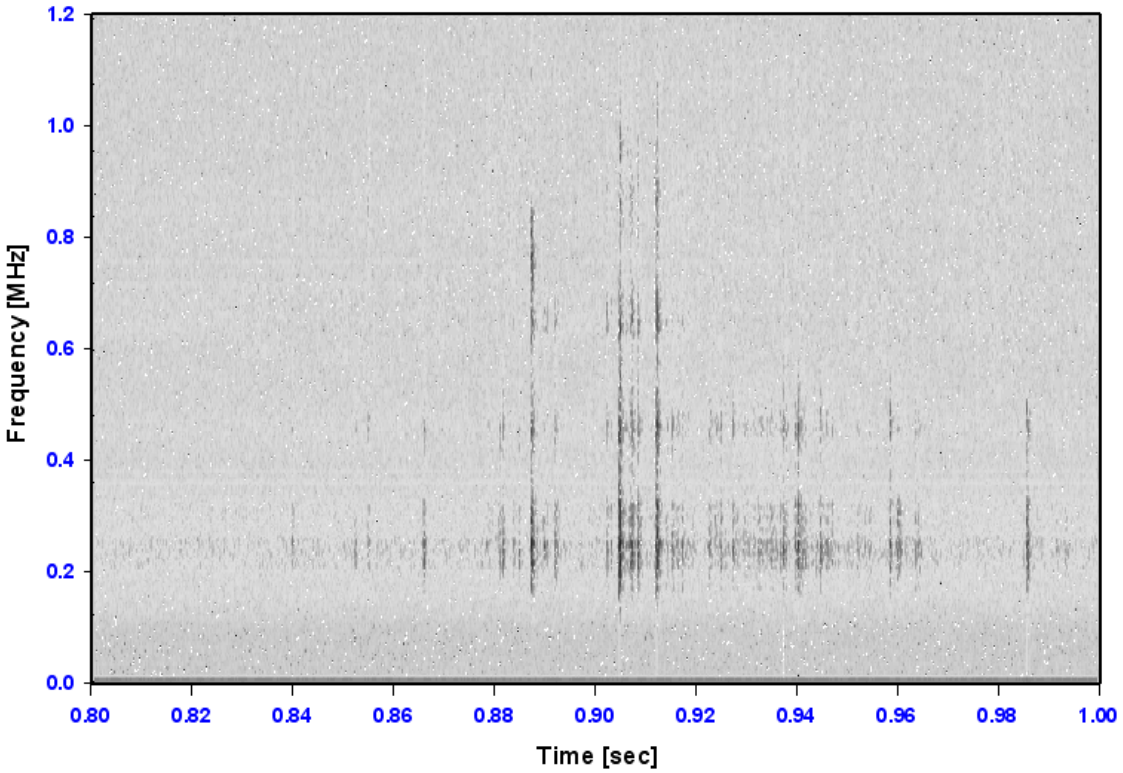

Figure 6—9 Spectrogram results associated with Case I (highlighted region of waveform in figure (6-7), 500-mins of operation)

6.3.2 Case II

The applied load on this test shaft was 8 kN. It is worth mentioning that this case presents different trends to that noted in the earlier case. Observations of continuous monitoring of the AE levels for 130-min of shaft operation is presented in figure (6-10). During the start of the test steady AE activity was noted and after approximately 80-mins a large transient rise in AE energy level was observed and this AE activity gradually increased further from 90-mins until the test was terminated, see figure (6-10). The increase in AE energy levels from earlier in the test to the condition of the observable damage was in the order of 34,900%. Again as in the previous case, channel-1 has shown an advantage over channel-2 on the basis that it could produce a clear indication of steadily increased AE emission levels noted at the end of test. Prior to the final fracture the opening and closing of the crack was also visibly observed and final fracture occurred before 130-mins. This supported earlier assumptions that the opening and closing of the crack will cause rubbing of the cracked face.

The classical AE parameters recorded over the duration of the test are detailed in figure (6-11), where it was noted that high levels of AE activity were observed at the end of the test. Also noted on the AE waveforms at 100-mins operation was the high transient nature of the waveform. Again clearly showing AE transient events, which grew in amplitude as the test progressed with time, eventually developing very high transient nature of AE events at the end of the test (130-mins), see figures (6-12) and (6-13). A very interesting observation of the AE waveform (figure 6-13, 120-mins) shows much larger duration AE signals which are typically associated with rubbing of mating components. The damage observed for this test conditions is presented in figure (6-16).

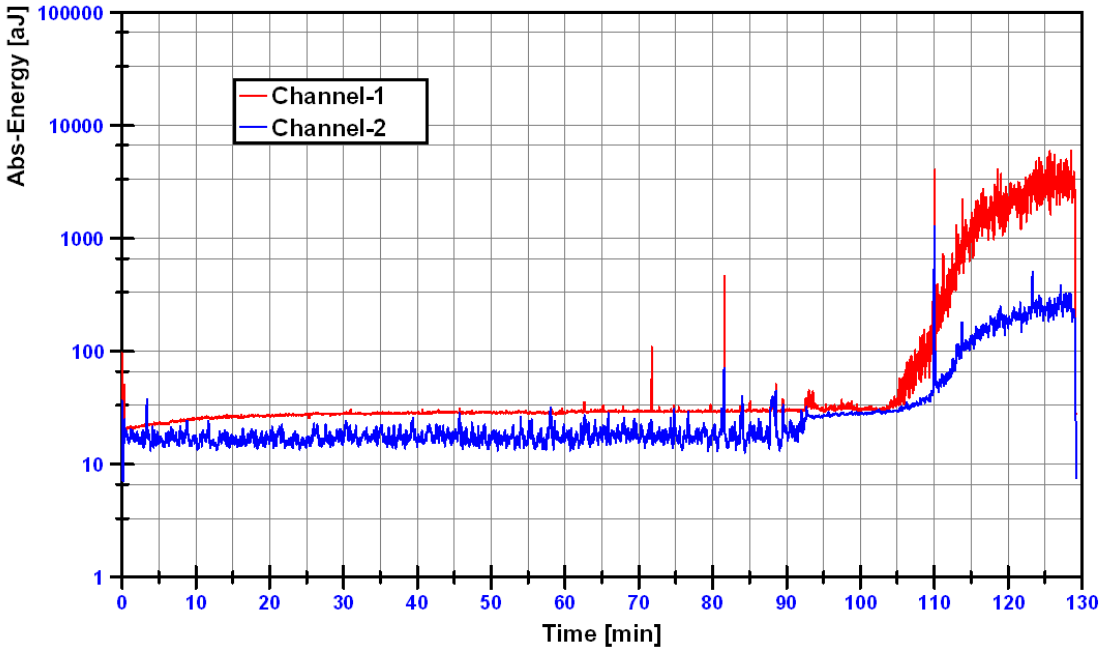

Figure 6—10 Observations of a run-to–failure shaft test

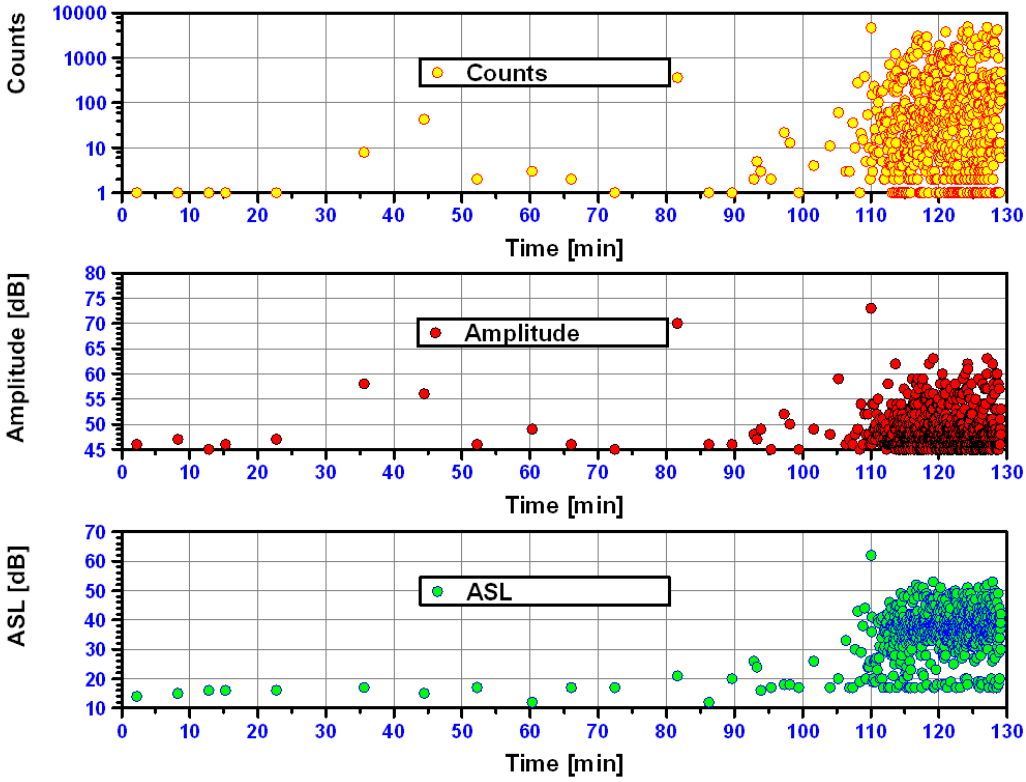

Figure 6—11 Classical AE parameters of counts, amplitude and ASL, (AE measurements from channel-1)

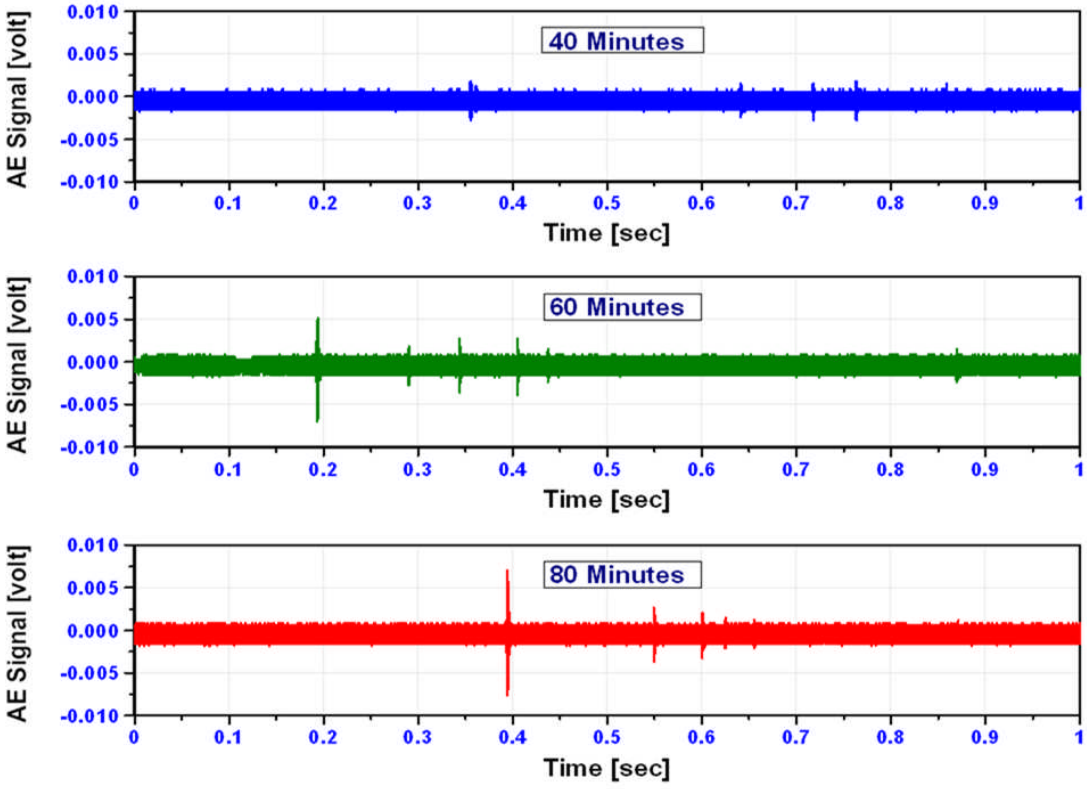

Figure 6—12 AE waveforms associated with results in figure (6-10), (AE measurements from channel-1)

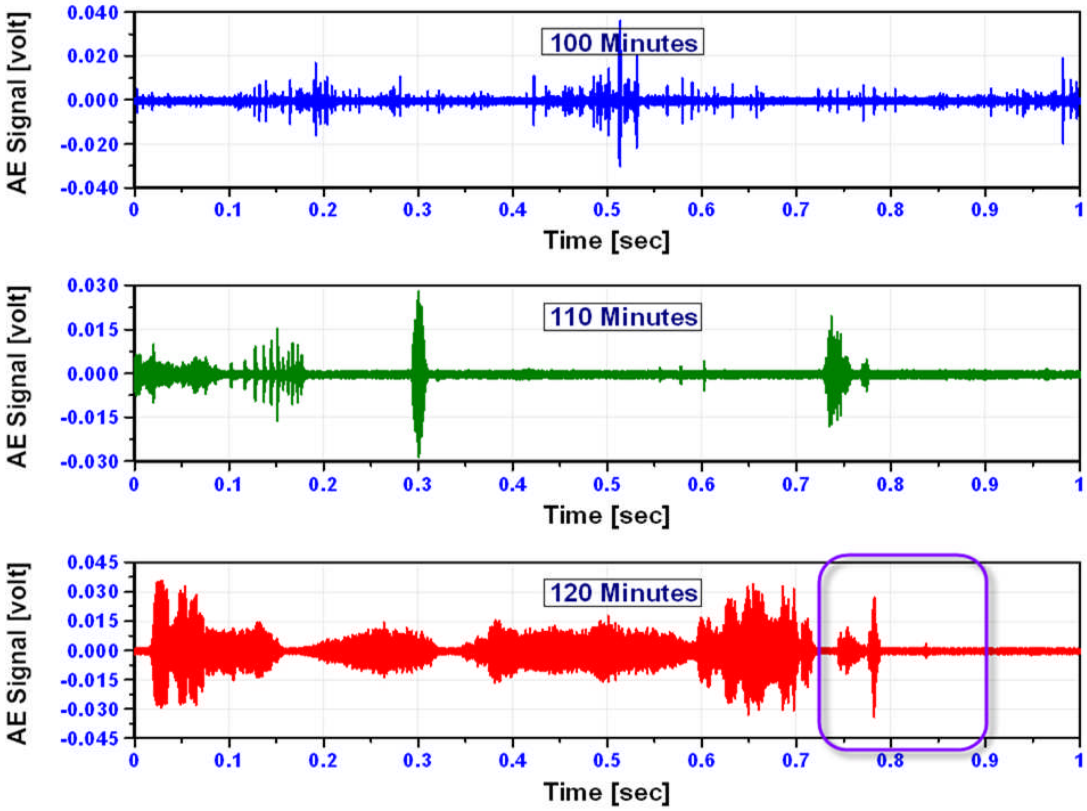

Figure 6—13 AE waveforms associated with results in figure (6-10), (AE measurements from channel-1)

Thus far the observations have shown AE to be monitoring the degradation of an accelerated shaft test; the next phase of analysis also involved the time domain analysis of AE activity throughout the test duration. Figure (6-14) highlights the trends in the Energy Index (EI), Kurtosis (KU), Information Entropy (IE) and Kolmogorov-Smirnov Test (KS-test) throughout the test period, associated with the shaft test presented in figure (6-10).

Results showed that as early as 80-mins into the operation of the shaft test, a relative high IE, KU and EI values was noted whilst the KS-test value remained almost constant, see figure (6-14). It is also worth mentioning that KS-test and IE values began to increase steadily as the test passed 100-mins of operation, reinforcing the previous observations of continuous monitoring of AE activity, as shown in figure (6-10). At 120-mins of testing, maximum KS-test and IE values of 0.23 and 0.82 were recorded respectively, see figure (6-14). It is particularly interesting to note that although these factors become very sensitive indicators as the presence of the shaft defect was pronounced, KU and EI values reduced

with increased shaft damage; KU and EI are reliable indicators only in the presence of incipient defects while they did not respond enough to the significantly increasing damage in the shaft, see figure (6-14).

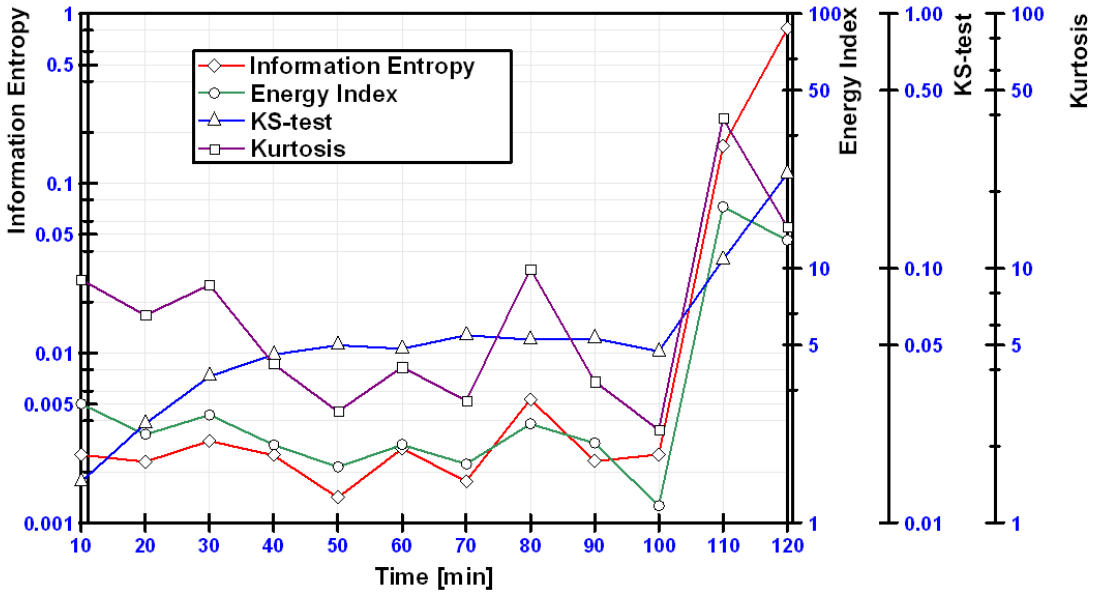

Figure 6—14 IE, KU, EI and KS-test results

A spectrogram was also undertaken on part of the AE waveform recorded at 120-mins into operation, presented in figure (6-13). From the spectrogram presented in figure (6-15), it was that evident the large transient AE burst contained frequencies of up to of 600 kHz whilst continuous type of AE contained frequencies between 100 to 150 kHz. The author also postulates that this high AE transient (high frequency components) is associated with the rapid propagation of the crack on the shaft whilst the continuous type waveform (low frequency components) is attributed to shearing and rubbing of the cracked face noted at the end of the test, see figure (6-13), 100-mins. This notion is reinforced by the relatively higher frequency content of the transient burst in comparison to the continuous emission which is attributed to the rubbing of the cracked faces;

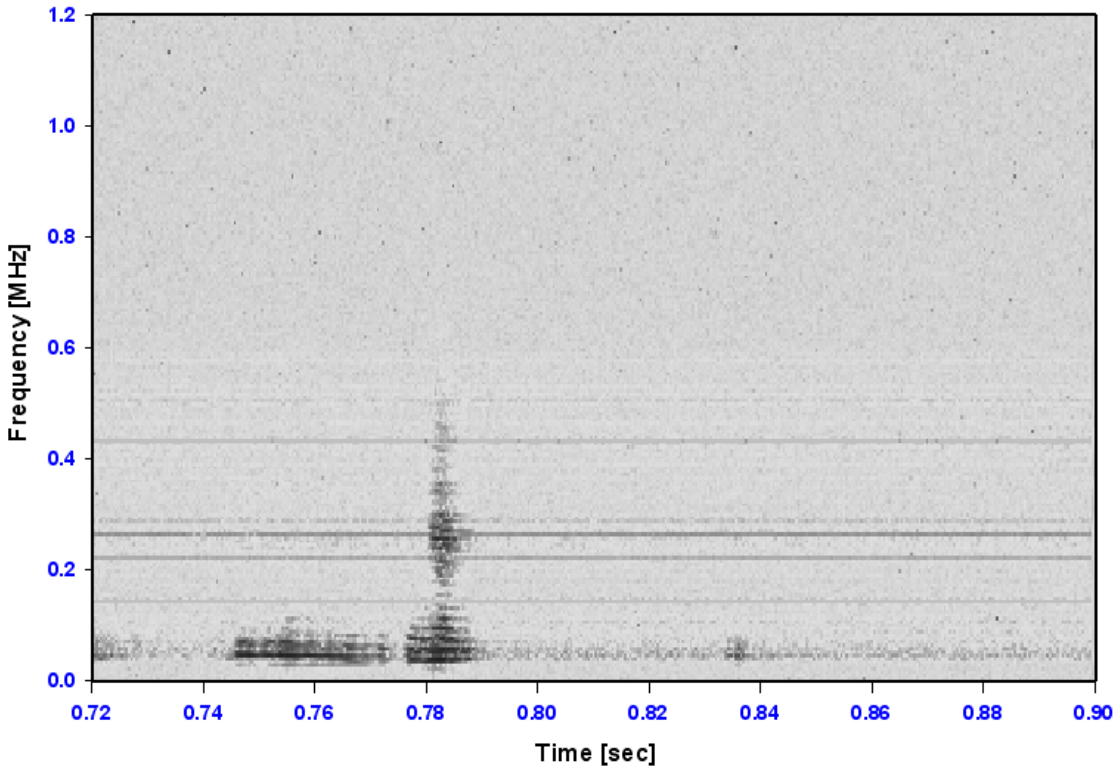

Figure 6—15 Spectrogram results associated with Case II (highlighted region of waveform in figure (6-13), 120-mins of operation)

Figure 6—16 Observed fatigue associated with case I and case II

7 Discussion

7.1 On Existing Knowledge

Operating and maintenance (O&M) aspects play an important role in the cost of productivity in industrial the world. They may well influence production rates and even cause safety concerns and therefore it is important to find ways to reduce the O&M part of the cost of these projects.

In industrial applications, minimum downtime is one of the most wanted specifications in maintenance procedures. Thus, failure to monitor the condition of machine components is not only intolerable but will also cause unnecessary maintenance costs. Therefore, it is important to understand defect development stages and the prediction of the lifetime of machine components. There are three critical states in the condition monitoring of machine components; the detection of the fault, the determination of the severity of the fault and its remaining useful life.

Rotating machinery are fatigue loaded machines and operational experience has shown that their components (e.g. bearings and shafts) fail at abrupt high rates which influences the normal operating conditions. The primary causes of damages are misalignment, impacting, and cyclic fatigue.

Bearings are vital components in rotating machinery. As failures associated with bearings represent the cause of extended outages and are typically caused by gradual deterioration and wear. Rolling element bearings are the most common cause of rotating machinery failure. Bearings are adapted to carry high and low pressure loading for supporting an end of a shaft for rotation about its longitudinal axis. Sooner or later wear, fatigue or lubricant deterioration will ultimately destroy the bearings capability to function appropriately. Fatigue is playing a major role in the bearing lifetime.

Shafts are critical components in rotating machines and are often expected to carry heavy loads and operate reliably. Further, shafts experience cyclic load

conditions, are difficult to access for maintenance and are vulnerable to crack nucleation and growth. Predicting and preventing the crack phenomenon has attracted the attention of many researchers and has continued to provide a large incentive for the use of condition monitoring techniques to detect the earliest stages of cracks. Undetected shaft failure can cause significant damage for machinery, influence production rates and even cause safety concerns. Generally, the shafts are designed to have an infinite life. This will be the case unless the shaft is overloaded or damaged. Fatigue is almost certainly the major cause of a broken shaft.

Most failures are due to unpredictable factors and the cure is to employ a robust, reliable and effective monitoring technique that can cope with the unknown. Traditional proactive maintenance not only leads to wasteful machine downtime but also untimely replacement of components. Indeed, the costs of component downtime to a machine can be very significant, therefore preventing equipment failures and minimizing stoppages due to servicing and maintenance are key priorities that can be reduced by using condition monitoring.

Slow speed rotating machines are the mainstay of several industrial applications worldwide. They can be found in paper and steel mills, water industry, wind turbines etc. Operational experience of such machinery has not only revealed challenging design issues but has also presented opportunities for further significant improvements in the technology and economics of such machines.

Predicting and preventing the crack phenomenon has attracted the attention of many researchers and has continued to provide a large incentive for the use of condition monitoring techniques to detect the earliest stages of cracks. Condition monitoring for rotating machinery applications is becoming more and more common practice. Especially for slow speed rotating components such as bearing, shafts and gears, a lot of experience is available from other applications and these offer a wide variety of selection of the relevant technologies. Conventional technologies such as thermography, oil analysis,

strain, vibration and acoustic technologies have been researched widely over the past years by a number of researchers and organizations involved.

Slow speed rotating machinery results in reduced energy loss rates from damage related processes and therefore condition monitoring technologies (e.g. vibration analysis), which detect energy loss, tend to be more difficult if not impossible to apply. It was reported that the conventional condition monitoring of slow-speed machinery using vibration analysis is fraught with difficulties. Further, where there have been claims of success, the period between detection and failure was very short. This will often progress to more serious damage affecting the operational performance of the machine. However, this is not the case for Acoustic Emission (AE) technology which is well suited to detecting very small incipient failures at low speed. Consequently, there was a considerable success in the development and application of AE to monitoring slow speed machinery components (e.g. bearings). Furthermore, one of the major advantages of the AE technique as an on-line monitoring tool over other non-destructive test methods is its capability to detect signals in real-time that are emanating from the structure under test. AE can also locate active defects in larger structural components without having to physically scan them. Determination of the AE source location is an extremely powerful tool in AE analysis and can be used to monitor a relatively large structure with a minimum number of sensors. Nonetheless these qualities are certainly not yet demonstrated in many slow speed rotating machinery applications, the availability of acoustic emission sensors offers good scenarios.

For various rotating machinery applications, condition monitoring using high frequency Acoustic Emission (AE) technology has remained a subject of intense study since the late 1960's. Although many studies on condition monitoring of rotating machinery components are presented in the literature, there are few publications that address natural mechanical degradation on rotating machine components (bearings) using AE technology. To date few publications that address natural mechanical degradation on rotating machine components have been reported. Most published work on the application of the AE to monitoring

(e.g. bearing) mechanical integrity have been conducted on artificially or 'seeded' damage which are generally induced with an electrical discharge system, engraving machine or by introducing debris into the lubricant.

Applications of condition monitoring to low speed rotating shafts showed that there are no off the-shelf technologies and there are no similar applications. In order to develop a very robust and reliable condition monitoring system for rotating machinery applications, further work should be extended to comprehend monitoring of low speed shafts. However up to now, there are not really systems available and suitable for on-line monitoring. Important reasons for this are the need of similar applications, the poor viability for reliable measurements, technology limitations and the large costs.

For analyzing the machine component's signals and measuring deviations from the normal conditions, various fault index extraction and signal processing techniques were widely applied to the measured data. They include information entropy (IE), signal shape factor (SHF), enveloping, and spectrum analysis (Fast Fourier Transform (FFT), Auto-regressive, Prony's Energy Method and Wavelet Transform).

Statistically tools such as the mean (μ), standard deviation (σ), root mean square (RMS), crest factor (CF), kurtosis (KU), shape factor (SHF) and impulse factor (IF) have also been employed for bearing defect detection.

7.2 On Results of This Research

For this research work, a specially designed test rig that encouraged the natural damage condition of a test bearing was employed. One of the challenges was to accelerate and enhance the natural crack signatures at the early stage of defect development. To implement this, a combination of a thrust ball bearing and a thrust roller bearing was selected for the first three cases at loads ranging from 20, 35 and 50 kN. One race of the thrust ball bearing (SKF 51210) was replaced with a flat race taken from thrust roller bearing (SKF 81210 TN) of the same size. As a consequence, this arrangement caused higher contact

pressure on a flat track relative to the grooved track due to the reduced contact area between the ball elements and the flat race. In the fourth case, attempts were made to generate a natural defect on the bearing components by allowing the conventional thrust roller bearing (SKF 51210) to operate under conditions of grease starvation.

These four experimental cases reflect the general observations associated with over a dozen experimental tests. Two different approaches to ascertaining the applicability of the AE technology for monitoring cracks on slow speed bearings were undertaken. The first programme involved acceleratory crack/spalls on the test bearing at three load conditions, 20, 35 and 50 kN whilst the second program involved running the bearing test under conditions of grease starvation at two different load conditions, 20 and 50 kN. It is worth stating that for the lubricated test cases, the test bearing was lubricated during the testing with Castrol, Moly Grease (650-EL).

Observations of AE energy monitored continuously for all three load conditions showed that during the first hour of the test, an increase in AE activity levels and temperature was noted. This was attributed to the 'run-in' phase, as after this period (1-hr) the measured AE energy remained relatively constant. It was observed that for all tests AE energy levels started to rise approximately a few hours before the termination. This was noted for the measurement of classical AE parameters (e.g. counts) as well. Also it was noted that AE energy levels were higher during the final stages of the bearing life for the higher load conditions. Interestingly the AE waveforms of damage showed high rise times for the AE bursts associated with the higher test loads.

To ensure a consistent lubricant viscosity throughout the test period, the measurement of temperature was undertaken. The significance of this is to ensure that friction properties of the lubricant between the bearing elements were relatively constant. It is worth stating that following the run-in (0- to 1-hr) the bearing temperature stabilized at 35 ^{o}C and a maximum temperature of 40 ^{o}C was recorded at the end of the three tests.

With knowledge of the signal velocity, the location of the AE source can be identified. For this investigation, at a threshold of 52 dB and with known distances between the AE sensors, the velocity of the AE waveform under such conditions was experimentally determined at 4,000 m/sec. The dominant frequency content of AE's recorded was approximately 300 kHz and the wave velocity of 4,000 m/sec corresponds to the symmetric zeroth lamb wave mode (S_o) for steel at 1.8 mm-MHz (0.3 MHz * 6 mm thk). This velocity was used for all source location investigations and prior to the onset of testing several Hsu-Nielsen sources were made at various positions on the surface to establish the accuracy at this velocity and specific threshold level. Results were within 4% of the exact geometric location of the Hsu-Nielsen sources. The source location layout, employed for this investigation, essentially unwrapped the bearing race for linear location. Only AE events above a threshold of 52 dB contribute to the source location. Whenever the threshold is exceeded, the location of the source is computed and identified. Further, the AE energy is assigned to the geometric position (source); a fixed source will have the largest contributory energy in a source location plot.

The second program (Grease Starvation Test) presents different trends to that noted in the previous cases. During the start of the test, steady AE activity was noted; observations of continuous monitoring of the AE levels of bearing operation did not show any considerable rise at the start of testing. A significant rise in AE energy levels gradually increased with time until the test was terminated. The increase in AE energy levels from the start of the test to the termination was in the order of 36,937%. This significant rise in AE energy levels also suggested that damage, visually observable, had occurred on the bearing. Waveforms of AE recorded throughout the test duration provided another simple and rapid means to verify damage on the test bearing. They clearly show AE transient events, which grow in amplitude as the test progressed with time and eventually develop a high transient nature of AE events at the end of the test.

Another test rig was built to investigate failure and AE characteristics of rotating shafts. To accelerate crack initiation and growth, a V-Notched shaft of 235.5 mm length and 35 mm diameter was designed. A radial load, which was imposed on the shaft to initiate a natural crack, was applied to the shaft through the overhang bearing. In a rotating mechanical system it is significantly important to transmit signals from sensors on a rotating shaft to an exterior stationary part (Data Processing System), and there exist several conventional methods to achieve signal transmission. A slip ring, which is a method of making an electrical connection, has been traditionally used as a means of observing signals from a rotating machinery component. There also remains the difficulty that special machining of a rotating shaft is generally needed to accommodate a slip-ring. Thus the author has proposed an alternative effective method using a specifically designed oil-filled cylinder. This is similar to a hydrodynamic bearing but in this case the cylinder is completely filled with oil. A flat was machined on the outer periphery of the cylinder which was for placement of the AE sensor. A rubber seal on both cylinder sides ensured no leakage and consequently there was no mechanical contact between the shaft and oil-bath that could result in AE noise generation. This enclosed circular bath allowed for direct contact between the rotating shaft and the oil. The enclosed bath was completely filled with oil.

Shaft tests were undertaken until complete fracture. The shaft material properties, the stress range, and the crack size govern the crack propagation rate. One of the key factors that can affect the crack growth rate is the stress at the crack tip. When fracture occurs, the crack will initiate and propagate through the material. It should be noted that at the lower stress levels crack initiation constitutes the majority of the life time before fracture whilst higher stress tends to favour a much shorter initiation period but a longer crack propagation duration. Under normal conditions of load, shaft material properties, rotational speed and good alignment, it is expected that cracks will be initiated in the vicinity of the notch, where sharp change in cross-sectional area of the shaft was designed, due to the high stress concentration on that site. These cracks were detected by the AE sensors. For this particular thesis two experimental

cases were discussed that reflect the general observations associated with other experimental tests at loads of 4 kN and 8 kN. Case I is for a load condition of 4 kN whilst Case II presents results for a test load of 8 kN.

The observations of AE for Cases I and II show very different characteristics. Firstly, in Case I, where the load is half that applied in Case II, the relatively early AE activity (95–130 mins) was attributed to crack initiation. As the crack propagates immediately after initiation, it is very plausible that AE would have been generated but not at the same intensity and energy levels as noted at the initiation stage. As such the observations of AE between 130-mins and 450-mins were of relatively low level until the crack propagation accelerated to final fracture. In Case I, the crack had initiated at the V-Notch edges (after 95-mins into testing) eventually leading to a rapid rise in AE until failure of the shaft (456–513 mins); the duration between initiation to the final crack propagation lasted approximately 320-mins. In Case II where a relatively higher load was applied there was not a clearly defined region where crack initiation could be identified and related to AE activity. This is attributed to the fact that the time between initiation and accelerated crack propagation is much less than at the lower loads, explaining the AE observations noted for Case II.

To determine the signal strength as a function of distance and authenticate the locations of AE sensors for the purposes of identifying sources of AE events, AE measurements were taken simultaneously from all 2 AE sensors in all cases. The results of measured AE data from channel-1 (the oil-filled cylinder channel) were compared with measured AE data from channel-2 (the overhang bearing channel). It is clear that AE measurements form channel-2 had more AE background noise than channel-1 due to the contribution of the friction of the rolling elements. Further, channel-1 has shown an advantage over channel-2 on the basis that it could produce a clear indication of steadily increased AE emission levels noted at the end of tests; thereby authenticating the oil-filled cylinder design.

The author also postulates that this high AE transient (high frequency components) is associated with the rapid propagation of the crack on the shaft

whilst the continuous type waveform (low frequency components) is attributed to shearing and rubbing of the cracked face noted at the end of the test. This action is reinforced by the relatively higher frequency content of the transient burst in comparison to the continuous emission which is attributed to the rubbing of the cracked faces. A spectrogram was undertaken on part of the AE waveform recorded throughout the tests. From the spectrograms presented in figures (6-8) and (6-14), it was evident that the large transient AE burst contained high frequency amplitudes whilst continuous type of AE contained low frequency components.

8 Conclusion

Bearing run-to-failure tests were performed under natural damage conditions on a specially designed test rig. Natural crack initiation was accelerated by using a combination of a thrust ball bearing and a thrust roller bearing. It can be concluded that this study demonstrated the applicability of AE in detecting and locating crack initiation and propagation on bearing races whilst in operation. The cases presented are representative of other tests performed in this study and show that there is a clear correlation between increasing AE energy levels and the natural propagation and formation of bearing defects. The results showed that AE parameters such as energy are reliable, robust and sensitive to the detection of incipient cracks and surface spalls in slow speed bearing. Classical AE parameters, recorded during bearing tests, were analyzed and presented graphically. Results indicated that analysis of traditional AE parameters also provided a simple, rapid and robust means that reinforced the findings of a signal based AE technique (Time Driven Data Measurements) of inspecting bearings defects and failure.

It was also demonstrated that by employing a linear source location technique, adapted for this study, the presence of a defect and its subsequent development can be detected and located by AE measurements. This study also successfully demonstrated the ability to determine the size of natural defects on bearings using AE technology.

It was shown that by employing a range of data analysis techniques, the presence of a crack onset and its propagation can be detected by the AE technique. Comprehensive signal processing analysis was conducted using most representative techniques. Time domain analysis techniques such as Kolmogorov-Smirnov Test (KS-test), Energy Index (EI) Information Entropy (IE) and Kurtosis (KU) were performed. The KS-test could efficiently distinguish AE signatures by comparing their CDF's with the AE signals in normal operation. Furthermore, the IE technique could successfully identify the crack onset and

growth by discriminating and enhancing the masked AE signatures, which were associated with the changes in the bearing structure (flat ring).

It can be concluded that KU and EI are reliable indicators only in the presence of incipient defects while they were less sensitive to increasing damage in the bearing; as the damage increased KU and EI values reduced to the undamaged levels. The observations from the results show that the IE and KS-test are more sensitive and representative to periods of high transient AE activity, typical for natural degrading bearings, than KU and EI. Hence the continuous monitoring of bearings employing techniques such as the IE and KS-test would offer the operator a relatively more sensitive tool for observing high transient type activity.

Results also revealed that the use of enveloping and FFT analysis provided a successful combination to describe whether the AE signals have interesting periodicity components or not. Hence it led to a high sensitivity of identifying the presence of bearing defects. Results of frequency domain analysis could show a clear periodicity of AE activity at 9 Hz associated with the bearing defects.

Investigations into the application of the Acoustic Emission technique to condition monitoring of slow speed shafts have also been presented. It can also be concluded that AE parameters such as energy, amplitude, counts and ASL have been validated as reliable, robust and sensitive to the detection of crack propagation and rubbing between cracked surfaces in a slow speed shaft. This highlighted the fact that traditional AE events are just as sensitive to changes in bearing mechanical state as the continuous measurement of AE energy. A correlation between the increasing AE levels and the natural degradation of the shaft was observed. This work also discussed the applicability of some statistical indicators such as information entropy (IE) and KS-test which can offer more sensitivity to the transient type activity associated with the naturally degrading shaft. It was also suggested that AE associated with crack propagation contains higher frequency components than AE associated with rubbing of cracked faces.

Results clearly illustrated that surface fatigue, such as flaking, could be initiated on the bearing flat race within a few days depending on the load condition thereby authenticating the test-rig design. It should be noted that the theoretical estimation of rolling contact fatigue is known to be subject to variability or scatter when compared to experimental results and this has been attributed to the probability of inclusions in the steel material located in the highest load zones of the race. It is also worth noting that the actual test period leading to visual damage on the race was much faster than the theoretical calculations. This variation was random but always earlier than predicted. This is attributed to issues such as misalignment, unbalance, etc, which are not incorporated in theoretical estimates; however, best efforts were undertaken to minimize this. Furthermore, the anticipated life for a defined stress was computed for a shaft and the results clearly illustrated that fatigue could be ascertained on the shaft within a few hours depending on the load condition; thereby supporting the test-rig design.

There are significant contributions of this work in the area of condition monitoring of slow speed rotating machinery. Firstly, the establishment of a correlation between Acoustic Emission activity and natural initiation and propagation of defects in low speed rotating machinery components (bearings and shafts); at the rotational speed on which these tests were employed, this is the first known attempt at correlating AE and natural defect generation in slow speed rotating shafts. Secondly, in addition to verifying the applicability of AE in detecting and locating crack initiation and propagation on bearings races whilst in operation, an estimation of the location of the AE sources was undertaken continuously throughout the test period in an attempt to correlate the eventual surface defect to the identified sources of AE; this study is the first of its kind to date. Thirdly, this study also attempted to identify the size of a natural defect on bearings using AE technology. Fourthly, this research programme can be considered as one of few publications that involved running bearing tests under conditions of grease starvation and investigated the effects of this on AE signals associated with the natural initiation and propagation of cracks on thrust bearing races whilst in operation. Finally, the results from this investigation show that

whilst measurements on operational bearings and shafts cannot be achieved as described in this study, the method of identifying the onset of crack propagation can be employed as a quality control tool for bearing and shaft manufacturers particularly for testing bearings and shafts material homogeneity. These findings were published in several international journals

9 Recommendations

The author has defined his investigations concerning a new method for detecting and locating the onset of crack propagation in bearings. The possibility of undertaking numerous tests on varying materials, etc, is essential and it will be dependent on the adoption of this method by industry, and here lies the basic premise of the research.

The modifications made to the support of the flat bearing race so as to allow positioning of the AE sensors will influence the support stiffness though the author cannot comment on the exact influence. This would probably have influence on the degradation of the bearings and therefore this influence should further be investigated although the same arrangement was applied to all test conditions. Furthermore, concerning this issue an investigation of how and where the AE sensors could be located in the case of a real thrust bearing application should be undertaken.

At the rotational speed on which shaft tests were employed, this is the first known attempt at correlating AE and natural defect generation. Hence, further experimental tests on shafts are required to validate the findings of this research. Moreover, a thorough investigation of the 'Oil-Filled Cylinder' proposed and designed by the author is essential, as this has enormous potential in improving, and increasing, the applicability of Acoustic Emission detection to the monitoring of all types of rotating shafts.

As the testing equipment and tools were specifically designed for these Acoustic Emission tests (bearings and shafts), it would be necessary to further investigate and analyze what could be the influence of the structural noise in an actual application.

Finally, this study can be considered as the first investigative step since it concerns a single application of the method to specific test rigs and to unique specimens and therefore its effectiveness, both technically and economically, has to be proved with further investigations.

REFERENCES

1. Danish Wind Industry Association, Wind Turbine Design: Basic Load Considerations, Fatigue Loads (Forces), September 19, 2003, Site of Danish Wind Industry Association, http://www.windpower.org/en/tour/design/index.htm. 2006.

Ref Type: Online Source

2. Teoh PC, Keith PC. An Evaluation of Failure Modes and Effects Analysis Generation Method for Conceptual Design, Case Study. International Journal of Computer Integrated Manufacturing 18[4], 279-293. 2005.

Ref Type: Journal

3. Daniel JI, Charles RF, Vicente LJ, Valder SJ. Damage Prognosis, for Aerospace, Civil and Mechanical Systems. West Sussex PO19 8SQ, England: John Wiley & Sons Ltd, 2005.

Ref Type: Book, Whole

4. Failure Analysis, Gears-Shafts-Bearings-Seals, Publictaions of Rexnord Industries, LLC, Gear Group, Site of Rexnord Industries, LLC, Gear Group, www.rexnord.com. 2006.

Ref Type: Online Source

5. Ian Howard. A Review of Rolling Element Bearing Vibration "Detection, Diagnosis and Prognosis". 1994. Melbourne Victoria 3001, Australia, DSTO Aeronautical and Maritime Research Laboratory.

Ref Type: Report

6. Shahab HG. A Fault Diagnosis System for Rotary Machinery Supported by Rolling Element Bearings. 2007. University of Waterloo, Ontario, Canada, University of Waterloo.

Ref Type: Thesis/Dissertation

7. McFarlane C. Stress Analysis for Machine Components, Lecture Notes, School of Engineering, Cranfield University, UK. 2010.

Ref Type: Unpublished Work

8. Harris C.M., Piersol AG. Shock and Vibration Handbook . New York, USA: McGraw-Hill, 2002.

Ref Type: Book, Whole

9. Mba D. Condition Monitoring & Vibration Diagnosis of Rotating Machines, Lecture Notes, School of Engineering, Cranfield University, UK. 2005.

Ref Type: Unpublished Work

10. Verbruggen TW. Wind Turbine Operation & Maintenance Based on Condition Monitoring. ECN-C-03-047. 2003. WT-OMEGA, ECN Wind Energy.

Ref Type: Report

11. Mba D. Condition Monitoring of Slow Speed Rotating Machinery Using Stress Waves. 1998. Cranfield University, UK, Cranfield University.

Ref Type: Thesis/Dissertation

12. Peter JS. Non-destructive Evaluation, Theory, Technique and Applications. Second Series. 2002. New York, USA, Marcel Dekker, Inc.

Ref Type: Report

13. Miller RK, McIntire P. Non-destructive Testing Handbook. American Society for Non-destructive Testing, USA, 1987.

Ref Type: Book, Whole

14. Daniel P. Oil Analysis 101, Part 1 of 2, Artical, ORBIT Magazine, Bently Nevada Publications, 2ndQuarter, 2005, Site of Bently Nevada, http://www.bently.com/articles/2Q04orbit-.htm. 2006.

Ref Type: Online Source

15. Norton MP, Karczub DG. Fundamentals of Noise and Vibration Analysis for Engineers. Cambridge, UK: Cambridge University Press, 2003.

Ref Type: Book, Whole

16. Stephen B, Ruth B. SCHAUM'S OUTLINE OF THEORY AND PROBLEMS OF ELEMENTS OF STATISTICS, Descriptive Statistics and Probability. New York, USA: McGraw-Hill, 1999.

Ref Type: Book, Whole

17. National Institute of Standards and Technology. NIST/SEMATECH e-Handbook of Statistical Methods, U.S. Commerce Department's, Technology Administration, http://www.itl.nist.gov/div898/handbook/. 2006.

Ref Type: Online Source

18. Steven F. ENCYCLOPEDIA of MATHEMATICS and ITS APPLICATIONS, Mathematical Constants, Cambridge University Press. Cambridge, United Kingdom: The Press Syndicate of the University of Cambridge, 2003.

Ref Type: Book, Whole

19. Wikipedia, The Free Encyclopedia, Root Mean Square, http://en.wikipedia.org/wiki/Root_mean_square. 2006.

Ref Type: Online Source

20. Lihui W, Robert XG, Pham DT. Condition Monitoringand Control for Intelligent Manufacturing, (Springer Series in Advanced Manufacturing). London, UK: Springer-Verlag London Limited, 2006.

Ref Type: Book, Whole

21. Mulukutla S. Introduction to Electrical Engineering, Oxford University Press. New York, USA: Oxford University Press, Inc., 2001.
Ref Type: Book, Whole

22. Al-Balushi KR. The Use of High Stress Waves for Monitoring Gears. 1995. Cranfield University, Cranfield University.
Ref Type: Thesis/Dissertation

23. Al-Balushi KR, Mba D. Energy Index Technique for Early Detection of Incipient Bearing Failures. WCEAM CM 2007. The Second World Congress on Engineering Asset Management (EAM) and the Forth International Conference on Condition Monitoring [First Edition], 991-999. 2007. UK, Coxmoor Publishing Company.
Ref Type: Conference Proceeding

24. Al-Balushi R, Samanta B. Gear fault diagnosis using energy-based features of acoustic emission signals. Proceedings of the Institution of Mechanical Engineers Part I-Journal of Systems and Control Engineering 2002; 216: 249-263.
Ref Type: Journal

25. Hall LD, Mba D. Acoustic emissions diagnosis of rotor-stator rubs using the KS statistic. Mechanical Systems and Signal Processing 2004; 18: 849-868.
Ref Type: Journal

26. Hall LD, Mba D. Diagnosis of continuous rotor-stator rubbing in large scale turbine units using acoustic emiissions. Ultrasonics 2004; 41: 765-773.
Ref Type: Journal

27. Andrade FA, Esat II, Badi MNM. Gear condition monitoring by a new application of the Kolmogorov-Smirnov test. Proceedings of the Institution of Mechanical Engineers Part C-Journal of Mechanical Engineering Science 2001; 215: 653-661.
Ref Type: Journal

28. Andrade FA, Esat I, Badi MNM. A new approach to time-domain vibration condition monitoring: Gear tooth fatigue crack detection and identification by the Kolmogorov-Smirnov test. Journal of Sound and Vibration 2001; 240: 909-919.
Ref Type: Journal

29. Kar C, Mohanty AR. Multistage gearbox condition monitoring using motor current signature analysis and Kolmogorov-Smirnov test. Journal of Sound and Vibration 2006; 290: 337-368.
Ref Type: Journal

30. Kar C, Mohanty AR. Application of KS test in ball bearing fault diagnosis. Journal of Sound and Vibration 2004; 269: 439-454.
Ref Type: Journal

31. James PS. Statistical Mechanics: Entropy, Order Parameters and Complexity. Oxford University Press, USA, 2006.
Ref Type: Book, Whole

32. Athanasios P. Probability, Random Variables and Stochastic Processes. McGraw-Hill Companies, New York, USA, 1991.
Ref Type: Book, Whole

33. Ziha K. Event oriented system analysis. Probabilistic Engineering Mechanics 2000; 15: 261-275.
Ref Type: Journal

34. Ozdemir S. Measures of uncertainty in power split systems. Mechanism and Machine Theory 2007; 42: 159-167.
Ref Type: Journal

35. Nanda AK, Maiti SS. Renyi information measure for a used item. Information Sciences 2007; 177: 4161-4175.
Ref Type: Journal

36. Qu LS, Li LM, Lee J. Enhanced diagnostic certainty using information entropy theory. Advanced Engineering Informatics 2003; 17: 141-150.
Ref Type: Journal

37. Tse PW, Peng YH, Yam R. Wavelet analysis and envelope detection for rolling element bearing fault diagnosis - Their effectiveness and flexibilities. Journal of Vibration and Acoustics-Transactions of the Asme 2001; 123: 303-310.
Ref Type: Journal

38. Tom S. Envelope Signal Processing (ESP), Application Note EP1, Diagnostic Solutions Ltd Publications, http://www.diagsol.co.uk/wp-content/uploads. 2007.
Ref Type: Online Source

39. Natan W. Acceleration Enveloping - Higher Sensitivity, Earlier Detection, Artical, ORBIT Magazine, Bently Nevada Publications, 2nd Quarter, 2005, Site of Bently Nevada, http://www.bently.com/articles/2Q04orbit-.htm. 2007.
Ref Type: Online Source

40. Smith JO. Mathematics of the Discrete Fourier Transform (DFT) with Audio Applications. USA: W3K Publishing, 2007.
Ref Type: Book, Whole

41. National Instruments Developer Zone. FFT Analysis, Tutorials, NI Publications, Feb1, 2006, Site of National Instruments, http://zone.ni.com/devzone/cda/tut/p/-id/3342. 2007.
Ref Type: Online Source

42. Tandon N, Choudhury A. A review of vibration and acoustic measurement methods for the detection of defects in rolling element bearings. Tribology International 1999; 32: 469-480.
Ref Type: Journal

43. Kay SM, Marple SL. Spectrum Analysis - A Modern Perspective. Proceedings of the Ieee 1981; 69: 1380-1419.
Ref Type: Journal

44. Suguna T., Fernando S. Autoregressive Based Diagnostics Scheme for Detection of Bearing Faults. Proceedings of ISMA . 2006.
Ref Type: Conference Proceeding

45. Baillie DC, Mathew J. A comparison of autoregressive modeling techniques for fault diagnosis of rolling element bearings. Mechanical Systems and Signal Processing 1996; 10: 1-17.
Ref Type: Journal

46. Dron JP, Rasolofondraibe L, Bolaers F, Pavan A. High-resolution methods in vibratory analysis: application to ball bearing monitoring and production machine. International Journal of Solids and Structures 2001; 38: 4293-4313.
Ref Type: Journal

47. Dron JP, Rasolofondraibe L, Couet C, Pavan A. Fault detection and monitoring of a ball bearing benchtest and a production machine via autoregressive spectrum analysis. Journal of Sound and Vibration 1998; 218: 501-525.
Ref Type: Journal

48. Mechefske C. K, Mathew J. Parametric Spectral Estimation to Detect and Diagnosis Faults in Low Speed Rolling Element Bearings: Preliminary Investigation. Mechanical System and Signal Processing 1993; 7.
Ref Type: Journal

49. Mechefske C. K. Machine Condition Monitoring: Part 1 - Optimum Vibration Signal Lengths. British Journal of NDT 1993; 35: 503-507.
Ref Type: Journal

50. Chen ZD, Mechefske CK. Diagnosis of machinery fault status using transient vibration signal parameters. Journal of Vibration and Control 2002; 8: 321-335.
Ref Type: Journal

51. Wikipedia, The Free Encyclopedia, Prony analysis (Prony's method), http://en.wikipedia.org/wiki/Prony's_method. 2008.
Ref Type: Online Source

52. Lobos T, Rezmer J, Schegner P. Parameter Estimation of Distorted Signals Using Prony Method. Power Tech Conference IEEE. Proceedings of Power Tech Conference IEEE . 2003.
Ref Type: Conference Proceeding

53. Tse PW, Yang WX, Tam HY. Machine fault diagnosis through an effective exact wavelet analysis. Journal of Sound and Vibration 2004; 277: 1005-1024.
Ref Type: Journal

54. GABERSON HA. The Use of Wavelets for Analyzing Transient Machinery Vibration. S.V.Sound and Vibration 2002; 36: 12-17.
Ref Type: Journal

55. Wikipedia, The Free Encyclopedia, What is the Spectrogram, http://en.wikipedia.org/wiki/Spectrogram. 2008.
Ref Type: Online Source

56. Knowledgerush , Encyclopedia, What is the Spectrogram, http://www.knowledgerush.com/kr/encyclopedia/Spectrogram. 2008.
Ref Type: Online Source

57. Timothy JC, Richard FB, James RR. Wind Power Comes of Age, Artical, ORBIT Magazine, Bently Nevada Publications, 2nd Quarter, 2004, Site of Bently Nevada, http://www.bently.com/articles/2Q04orbit.htm. 2006.
Ref Type: Online Source

58. Jamaludin N, Mba D, Bannister RH. Monitoring the lubricant condition in a low-speed rolling element bearing using high frequency stress waves. Proceedings of the Institution of Mechanical Engineers Part E-Journal of Process Mechanical Engineering 2002; 216: 73-88.
Ref Type: Journal

59. Jamaludin N, Mba D, Bannister RH. Condition monitoring of slow-speed rolling element bearings using stress waves. Proceedings of the Institution of Mechanical Engineers Part E-Journal of Process Mechanical Engineering 2001; 215: 245-271.
Ref Type: Journal

60. Kuboyama K. Development of Low Speed Bearing Diagnosis Technique, (NKK Fukuyama Works, Fukuyama City, Hiroshima, Japan).
Ref Type: Generic

61. Canada RG, Robinson JC. Vibration Measurements on Slow Speed Machinery. In Predictive Maintenance Technology National Conference,

Indianapolis, Indiana. Proceedings of In Predictive Maintenance Technology National Conference 8[6], 33-37. 1995.
Ref Type: Conference Proceeding

62. Robinson JC, Canada RG, Piety RG. Vibration Monitoring on Slow Speed Machinery: New Methodologies Covering Machinery from 0.5 to 600 Rpm. Fifth International Conference on Profitable Condition Monitoring-Fluids and Machinery Performance Monitoring. Proceedings of Fifth International Conference on Profitable Condition Monitoring-Fluids and Machinery Performance Monitoring . 1996.
Ref Type: Conference Proceeding

63. Mechefskse CF, Mathew J. Fault Detection and Diagnosis in Low Speed Rolling Element Bearings, Part II: The Use of Parametric Spectra. Mechanical Systems and Signal Processing 1992; 6: 297-307.
Ref Type: Journal

64. Szrom DB. Low Speed Bearing Analysis. The Tenth Annual Meeting of Vibration Institute. Proceedings of the Tenth Annual Meeting of Vibration Institute, Las Vegas, USA , 183-188. 1986.
Ref Type: Conference Proceeding

65. Holroyd JT, Holroyd Instruments Ltd. Condition Monitoring of very Slowly Rotating Machinery Using AE Techniques. COMADEM 2001. 14th International congress on Condition monitoring and Diagnostic engineering management . 2001.
Ref Type: Conference Proceeding

66. Mba D, Rao RBKN. Development of Acoustic Emission Technology for Condition Monitoring and Diagnosis of Rotating Machines: Bearings, Pumps, Gearboxes, Engines, and Rotating Structures. The Shock and Vibration Digest 2006; 38 (1): 3-16.
Ref Type: Journal

67. Holroyd TJ, Randall N. Use of Acoustic-Emission for Machine Condition Monitoring. British Journal of Non-Destructive Testing 1993; 35: 75-83.
Ref Type: Journal

68. Holroyd TJ. The application of AE in condition monitoring. Insight 2005; 47: 481-484.
Ref Type: Journal

69. Mba D, Bannister RH, Findlay GE. Condition monitoring of low-speed rotating machinery using stress waves - Part 1. Proceedings of the Institution of Mechanical Engineers Part E-Journal of Process Mechanical Engineering 1999; 213: 153-170.
Ref Type: Journal

70. Mba D, Bannister RH, Findlay GE. Condition monitoring of low-speed rotating machinery using stress waves - Part 2. Proceedings of the Institution of Mechanical Engineers Part E-Journal of Process Mechanical Engineering 1999; 213: 171-185.
Ref Type: Journal

71. Mba D. Applicability of acoustic emissions to monitoring the mechanical integrity of bolted structures in low speed rotating machinery: case study. Ndt & e International 2002; 35: 293-300.
Ref Type: Journal

72. SWANTECH Inc., Health Monitoring for Wind Turbines, SWANTECH (Stress Wave Analysi Technology Company), http://www.swantech.com/about.html. 2006.
Ref Type: Online Source

73. Morhain A, Mba D. Bearing defect diagnosis and acoustic emission. Proceedings of the Institution of Mechanical Engineers Part J-Journal of Engineering Tribology 2003; 217: 257-272.
Ref Type: Journal

74. Al-Ghamd AM, Mba D. A comparative experimental study on the use of acoustic emission and vibration analysis for bearing defect identification and estimation of defect size. Mechanical Systems and Signal Processing 2006; 20: 1537-1571.
Ref Type: Journal

75. Stresswave Technology Ltd. Method and Apparatus for detecting Variation in a Process by Processing emitted Acoustic Signals, USA Patent No. 5005415, Final. 1991.
Ref Type: Patent

76. Holroyd Instruments Ltd. Enhanced Means of Processing Signals used to interpret the Condition of Machinery, USA Patent No. 5473315, Final. 1995.
Ref Type: Patent

77. Miettinen JPP. Acoustic Emission in Monitoring Extremely Slowly Rotating Rolling Bearing. COMADEM 99. The Twelfth International Congress on Condition Monitoring and Diagnostic Engineering Management . 1999. UK.
Ref Type: Conference Proceeding

78. Choudhury A, Tandon N. Application of acoustic emission technique for the detection of defects in rolling element bearings. Tribology International 2000; 33: 39-45.
Ref Type: Journal

79. Price ED, Lees AW, Friswell I. Detection of severe sliding and pitting fatigue wear regimes through the use of broadband acoustic emission. Proceedings of the Institution of Mechanical Engineers Part J-Journal of Engineering Tribology 2005; 219: 85-98.
Ref Type: Journal

80. Yoshioka T. Detection of Rolling-Contact Subsurface Fatigue Cracks Using Acoustic-Emission Technique. Lubrication Engineering 1993; 49: 303-308.
Ref Type: Journal

81. FDIS ISO (International Standards Organization Documents) 22096. Condition monitoring and diagnosis of machines – Acoustic Emission. [22096]. 2007. International Standards Organization Documents.
Ref Type: Generic

82. Holroyd T. The Acoustic Emission & Ultrasonic Monitoring. Oxford, OX7 6UP, UK: Coxmoor Publishing Company, 2000.
Ref Type: Book, Whole

83. TWI, World Centre for Materials Joining Technology, Acousteic Emission, TWI Company, http://www.twi.co.uk/content/main_home_index.html. 2008.
Ref Type: Online Source

84. Capgo Pty Ltd, Fatigue Detection by Acoustic Emissions, Capgo Pty Ltd, http://www.capgo.com/Resources/ConditionMonitoring/Acoustic.html. 2009.
Ref Type: Online Source

85. Envirocoustics S. A., Acoustic Emission Theory, Envirocoustics S. A. Publications, http://www.envirocoustics.gr/acoustic_emission_theory_eng.htm. 2007.
Ref Type: Online Source

86. Hartmut V. AE Testing Fundamentals,Equipment, Applications. The e-Journal of Nondestructive Testing 2002; 7.
Ref Type: Journal

87. Scruby CB. An Introduction to Acoustic-Emission. Journal of Physics E-Scientific Instruments 1987; 20: 947-953.
Ref Type: Journal

88. Chen X, Zeng H, Dietmar W. In-Process Tool Monitoring through Acoustic Emission Sensing, Publications of Automated Material Processing Group, Automation Technology Division. 2001.
Ref Type: Report

89. Esward TJ, Theobald PD, Dowson SP, Preston RC. An Investigation into the Establishment and Assessment of a Test Facility for the Calibration of Acoustic Emission Sensors, National Physical Laboratory Publications. 2002. National Physical Laboratory, Queens Road, Teddington, Middlesex, TW11 0LW.
Ref Type: Report

90. Physical Acoustics Corporation, Acoustic Emission Sensor, Calibration Certificate, http://www.pacndt.com/downloads/Sensors/Integral%20Preamp/WDI%20Rev%2009.07.pdf . 2008.
Ref Type: Online Source

91. NDT, Resource Center, Partial List of ASTM Specifications, http://www.ndted.org/GeneralResources/Standards/ASTMStandards.htm . 2010.
Ref Type: Online Source

92. ASTM E 976, Standard Guide for Determining the Reproducibility of Acoustic Emission Sensor Response, American Society for Testing and Materials, West Conshohocken, USA. 1945.
Ref Type: Catalog

93. Grosse, U., C., Hsu-Nielsen Source, Nondestructive Testing Encyclopedia (NDT.net) Publications, Acoustic Emission (AE), Site of Nondestructive Testing Encyclopedia (NDT.net), http://www.ndt.net/ndtaz/ndtaz.php. 2007.
Ref Type: Online Source

94. Li XL. A brief review: acoustic emission method for tool wear monitoring during turning. International Journal of Machine Tools & Manufacture 2002; 42: 157-165.
Ref Type: Journal

95. Christian UG. NDT.net - Editorial: Special Issue on Acoustic Emission. The e-Journal of Nondestructive Testing 2002; 7.
Ref Type: Journal

96. Mark F. C. Acoustic Emission: Heeding the Warning Sounds from Materials, ASTM Publications, http://www.astm.org/SNEWS/OCTOBER_2003/carlos_oct03.html. 2007.
Ref Type: Online Source

97. Physical Acoustics Corporation, PCI-2 Based AE System, User's Manual, Rev 2, Part No: 6301-1000, Associated with AEWin, Version 1.30 or Higher. 2004.
Ref Type: Unpublished Work

98. Harris TA. Rolling Bearing Analysis. New York, USA: John Wiley & Sons, Inc., 2001.
Ref Type: Book, Whole

99. Palmgren A. Ball and Roller Bearing Engineering. Philadelphia, USA: SKF Industries, S. H. Burbank & CO., INC., 1959.
Ref Type: Book, Whole

100. British Standard, Method of Calculating Dynamic Load Ratings and Rating Life of Rolling Bearings, BS 5512:1991, ISBN 0 580 19517 1. 1991.
Ref Type: Catalog

101. SKF Products, Interactive Engineering Catalogue, Rolling Bearings, SKF, http://www.skf.com/portal/skf/home/products?maincatalogue=1&lang=en&newlink=1_8_1. 2005.
Ref Type: Online Source

102. Tobin P. PSpice for Digital Signal Processing. www.morganclaypool.com [Ebook, First Edition]. 2007. Morgan & Claypool.
Ref Type: Electronic Citation

103. Duoandikoetxea J. Fourier Analysis (Graduate Studies in Mathematics). USA: American Mathematical Society, 2000.
Ref Type: Book, Whole

104. Al-Ghamdi AM, Cole P, Such R, Mba D. Estimation of Bearing Defect Size with Acoustic Emission. Insight 2004; 46: 758-761.
Ref Type: Journal

105. Al-Ghamd AM, Mba D. A Comparative Experimental Study on the Use of Acoustic Emission and Vibration Analysis for Bearing Defect Identification and Estimation of Defect Size. Mechanical Systems and Signal Processing 2006; 20: 1537-1571.
Ref Type: Journal

106. Al-Dossary S, Hamzah RIR, Mba D. Observations of Changes in Acoustic Emission Waveform for Varying Seeded Defect Sizes in a Rolling Element Bearing. Applied Acoustics 2009; 70: 58-81.
Ref Type: Journal

107. Joseph ES, Charles RM. Mechanical Engineering Design, Fifth Edition (International Edition). McGraw-Hill Book Co., Singapore, 1989.
Ref Type: Book, Whole

108. Peter RNC. Mechanical Design. Eastbourne,UK: Antony Rowe Ltd, 1998.
Ref Type: Book, Whole

109. Walter DP. Peterson's Stress Concentration Factors. New Yorl, USA: John Wiley & Sons, Inc., 1997.

Ref Type: Book, Whole

APPENDICES

Appendix A Bearing Test Rig Design

Bearing Life Calculations for Case I

INPUT DATA		
Load applied	50000	N
number of balls	14	
balls' radious	5.75	mm
race groove radious	5.8	mm
mean bearing diameter	64	mm
rotational speed	72	rpm

SURFACE STRESS AND DEFORMATION	FLAT RACE	GROOVE RACE	
semimajor axis of the ellipse contact	0.513	4.093	mm
semiminor axis of the ellipse contact	0.513	0.205	mm
deformation	0.046	0.016	mm
maximum pressure stress	6484	2035	N/mm2
permanent deformation	0.0044	0.0000	mm
0.0001D	0.0012	0.0012	mm
permanent deformation / 0.0001D	379%	3%	
plastic / elastic deformation	9.5%	0.2%	

SUBSURFACE STRESSES				
max shear stress	2215	626	N/mm2	Thomas & Hoersh theory
shear / pressure stresses ratio	34%	31%		
depth below the surface	0.241	0.158	mm	
depth / semiminor axis of ellipse contact	47%	77%		
max amplitude orthogonal shear stress	2774	1015	N/mm2	Lundeberg & Palmgren theory
shear / pressure stresses ratio	43%	50%		
depth below the surface	0.180	0.102	mm	
depth / semiminor axis of ellipse contact	35%	50%		
max octaedral shear stress	3696	1160	N/mm2	Von Mises distortion energy theory
shear / pressure stresses ratio	57%	57%		
depth below the surface	0.385	0.154	mm	
depth / semiminor axis of ellipse contact	75%	75%		

LIFE PREDICTION	FLAT RACE	GROOVE RACE	
basic dynamic load rating	23556	61874	N
L10	1	18	days

Bearing Life Calculations for Case II

INPUT DATA		
Load applied	35000	N
number of balls	14	
balls' radious	5.75	mm
race groove radious	5.8	mm
mean bearing diameter	64	mm
rotational speed	72	rpm

SURFACE STRESS AND DEFORMATION	FLAT RACE	GROOVE RACE	
semimajor axis of the ellipse contact	0.455	3.634	mm
semiminor axis of the ellipse contact	0.455	0.182	mm
deformation	0.036	0.013	mm
maximum pressure stress	5757	1807	N/mm2
permanent deformation	0.0021	0.0000	mm
0.0001D	0.0012	0.0012	mm
permanent deformation / 0.0001D	186%	2%	
plastic / elastic deformation	5.9%	0.1%	

SUBSURFACE STRESSES				
max shear stress	1967	556	N/mm2	Thomas & Hoersh theory
shear / pressure stresses ratio	34%	31%		
depth below the surface	0.214	0.140	mm	
depth / semiminor axis of ellipse contact	47%	77%		
max amplitude orthogonal shear stress	2463	901	N/mm2	Lundeberg & Palmgren theory
shear / pressure stresses ratio	43%	50%		
depth below the surface	0.160	0.090	mm	
depth / semiminor axis of ellipse contact	35%	50%		
max octaedral shear stress	3282	1030	N/mm2	Von Mises distortion energy theory
shear / pressure stresses ratio	57%	57%		
depth below the surface	0.342	0.136	mm	
depth / semiminor axis of ellipse contact	75%	75%		

LIFE PREDICTION	FLAT RACE	GROOVE RACE	
basic dynamic load rating	23556	61874	N
L10	3	53	days

Bearing Life Calculations for Case III

INPUT DATA		
Load applied	20000	N
number of balls	14	
balls' radious	5.75	mm
race groove radious	5.8	mm
mean bearing diameter	64	mm
rotational speed	72	rpm

SURFACE STRESS AND DEFORMATION	FLAT RACE	GROOVE RACE	
semimajor axis of the ellipse contact	0.378	3.016	mm
semiminor axis of the ellipse contact	0.378	0.151	mm
deformation	0.025	0.009	mm
maximum pressure stress	4778	1500	N/mm2
permanent deformation	0.0007	0.0000	mm
0.0001D	0.0012	0.0012	mm
permanent deformation / 0.0001D	61%	1%	
plastic / elastic deformation	2.8%	0.1%	

SUBSURFACE STRESSES				
max shear stress	1632	461	N/mm2	Thomas & Hoersh theory
shear / pressure stresses ratio	34%	31%		
depth below the surface	0.178	0.116	mm	
depth / semiminor axis of ellipse contact	47%	77%		
max amplitude orthogonal shear stress	2044	748	N/mm2	Lundeberg & Palmgren theory
shear / pressure stresses ratio	43%	50%		
depth below the surface	0.133	0.075	mm	
depth / semiminor axis of ellipse contact	35%	50%		
max octaedral shear stress	2723	855	N/mm2	Von Mises distortion energy theory
shear / pressure stresses ratio	57%	57%		
depth below the surface	0.283	0.113	mm	
depth / semiminor axis of ellipse contact	75%	75%		

LIFE PREDICTION	FLAT RACE	GROOVE RACE	
basic dynamic load rating	23556	61874	N
L10	16	286	days

ME/A1/36084	
ISSUE	MODIFICATION
A	———

ALL DIMENSIONS IN MILLIMETRES UNLESS OTHERWISE STATED

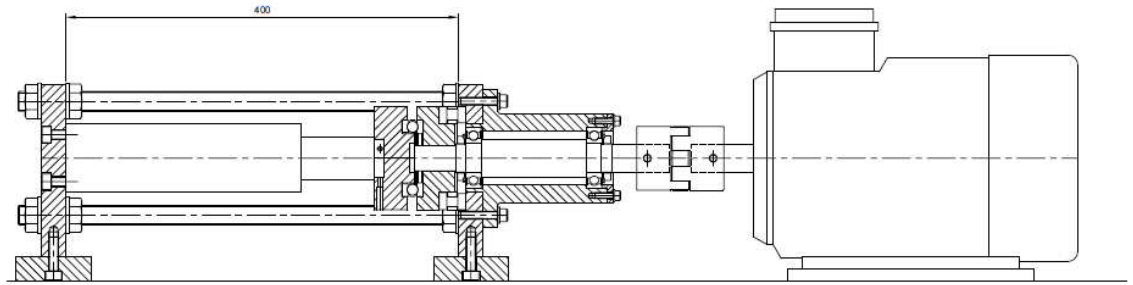

THIRD ANGLE PROJECTION			SHEET SIZE A1	1	A1/36084	ASSEMBLY		1	??	??	??		
				ITEM	PART No.	DESCRIPTION		No. OFF	MATL	SPEC.	REMARKS		
GENERAL TOLERANCE ON DIMENSIONS MACHINED ±0.2 UNMACHINED OTHER DIMENSIONS AS STATED	COST CODE	No. OF SETS REQ.	SCALE HALF SIZE	DRAWN	CHKD.	APPVD.	STRESS APPVD.	TITLE THRUST BEARING TEST RIG ASSEMBLY					
	M40395	1		A HUTCHINGS	A H								
				19/05/06	19/05/06								
WELD WHERE SHOWN THUS			FINISH SELF	SCHOOL OF ENGINEERING CRANFIELD UNIVERSITY				DRAWING No. ME/A1/36084					
MACHINE WHERE SHOWN THUS	USED ON DRG. A/??????							SHT. 1 OF 1 SHEETS					

Appendix B Shaft Test Rig Design

Equations and Factors used in the Shaft Design

Material Properties
Shaft Material Type: Low Carbon Steel
Minimum Tensile Strength (σ_{uts}) = 475 Mpa
Yield Strength (S_y) = 420 x 10^6 N/m^2
Safety Factor (n) = 2

Factors
The surface finish factor (k_a) = 0.88
The size factor (k_b) = 0.874
The load factor (k_c) =1
The temperature factor (k_d) =1
The duty cycle factor (k_e) =1
The fatigue stress concentration factor (k_f) = 0.523
The miscellaneous factors (k_g) = 1
The endurance limit of test specimen (σ'_e) = 239.4 MPa

Power = 1.5 kW
Speed = 72 rpm
Load-1 = 4kN
Load-2 = 8kN

Torque (T) = $\dfrac{\text{Power}}{\left(\frac{2\pi}{60}\right) \text{x rpm}}$
Endurance Limit $(\sigma_e)=k_a k_b k_c k_d k_e k_f k_g \sigma'_e$
$a=\dfrac{(0.9\sigma_{uts})^2}{\sigma_e}$
$b=-\dfrac{1}{3}\log\left(\dfrac{0.9\sigma_{ut}}{\sigma_e}\right)$
Bending Stress $(\sigma_a) = a*N^b$
Load (F)= $\dfrac{2M_{@Notch}}{\text{L(distance)}}$
Bending Stress at V – Notch $(\sigma_{normal@Notch}) = \dfrac{32M_{@Notch}}{\pi d^3}$
Sheer Stress at V – Notch $(\tau_{normal}) = \dfrac{16T}{\pi d^3}$
Maximum Bending Stress $(\sigma_{normal@x}) = \dfrac{32M_{max}}{\pi D^3}$
Shaft Diameter at V-Notch $(d^3_{@Notch})=\dfrac{32n}{\pi}\sqrt{\left(\dfrac{M_{@Notch}}{\sigma_e}\right)^2+\left(\dfrac{T}{S_y}\right)^2}$

Torque = 198.96 N.m
Endurance Limit = 96.26 Mpa
a = 1898.56 MPa
b = -0.2158
Fatigue Life (N) at 4 kN = 36,000 cycles
Fatigue Life (N) at 8 kN = 10,800 cycles

Results
Shaft Diameter (D) = 35 mm
Shaft Diameter at V-Notch (d) = 25 mm

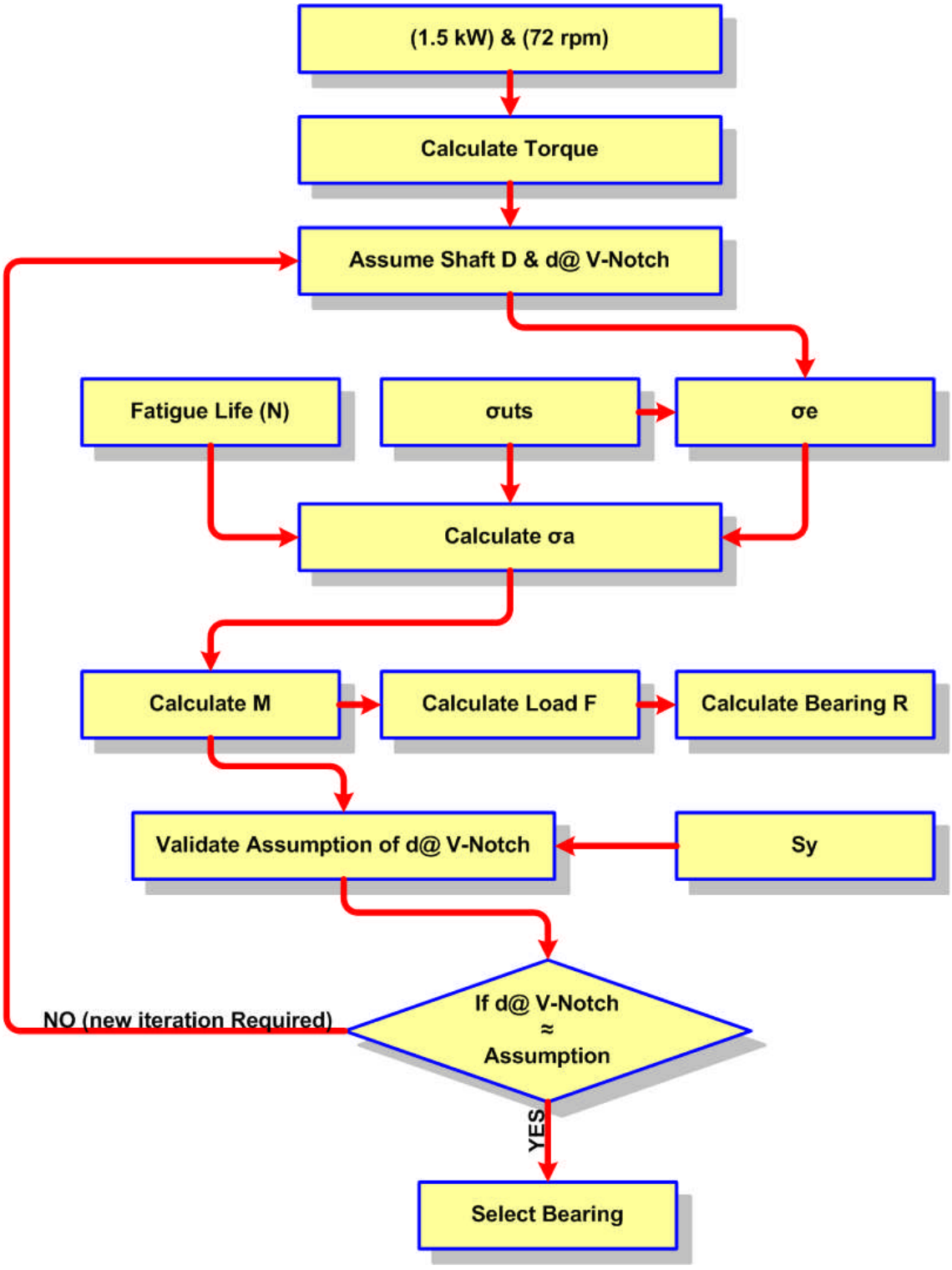

Shaft Design Flow Chart

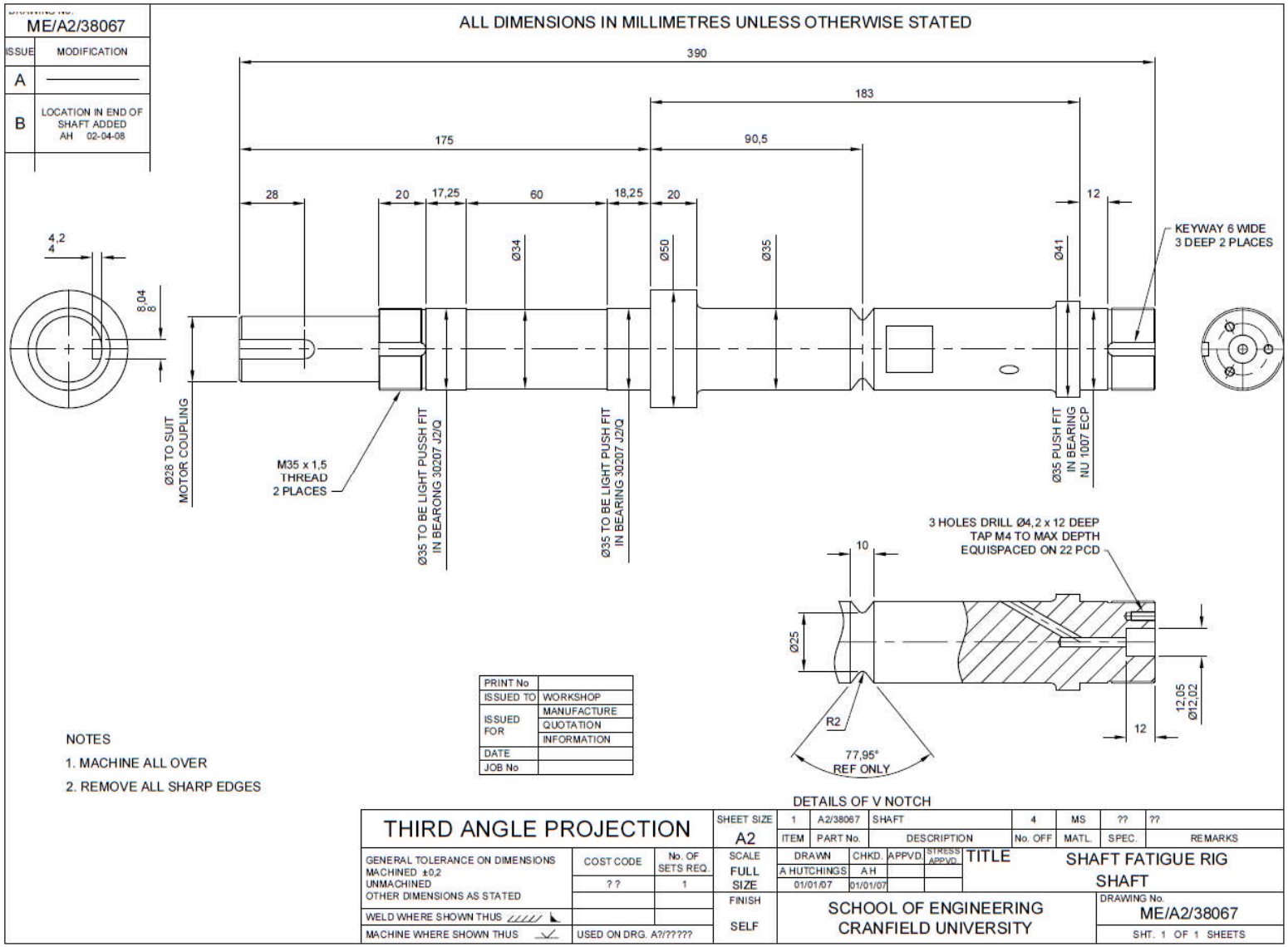
ME/A2/38067
ISSUE MODIFICATION
A —
B LOCATION IN END OF SHAFT ADDED AH 02-04-08
ALL DIMENSIONS IN MILLIMETRES UNLESS OTHERWISE STATED
390
183
175
90,5
28
20
17,25
60
18,25
20
12
4,2
4
8,04
8
Ø34
Ø50
Ø35
Ø41
KEYWAY 6 WIDE
3 DEEP 2 PLACES
Ø28 TO SUIT
MOTOR COUPLING
M35 x 1,5
THREAD
2 PLACES
Ø35 TO BE LIGHT PUSSH FIT
IN BEARONG 30207 J2/Q
Ø35 TO BE LIGHT PUSH FIT
IN BEARING 30207 J2/Q
Ø35 PUSH FIT
IN BEARING
NU 1007 ECP
3 HOLES DRILL Ø4,2 x 12 DEEP
TAP M4 TO MAX DEPTH
EQUISPACED ON 22 PCD
10
Ø25
R2
77,95°
REF ONLY
12
12,05
Ø12,02
DETAILS OF V NOTCH
PRINT No
ISSUED TO WORKSHOP
ISSUED FOR MANUFACTURE
QUOTATION
INFORMATION
DATE
JOB No
NOTES
1. MACHINE ALL OVER
2. REMOVE ALL SHARP EDGES
THIRD ANGLE PROJECTION
SHEET SIZE A2
1 A2/38067 SHAFT 4 MS ?? ??
ITEM PART No. DESCRIPTION No. OFF MATL. SPEC. REMARKS
GENERAL TOLERANCE ON DIMENSIONS
MACHINED ±0,2
UNMACHINED
OTHER DIMENSIONS AS STATED
COST CODE ??
No. OF SETS REQ. 1
WELD WHERE SHOWN THUS
MACHINE WHERE SHOWN THUS
USED ON DRG. A?/?????
SCALE FULL SIZE
FINISH SELF
DRAWN A HUTCHINGS 01/01/07
CHKD. A H 01/01/07
APPVD.
STRESS APPVD.
TITLE
SHAFT FATIGUE RIG
SHAFT
SCHOOL OF ENGINEERING
CRANFIELD UNIVERSITY
DRAWING No. ME/A2/38067
SHT. 1 OF 1 SHEETS

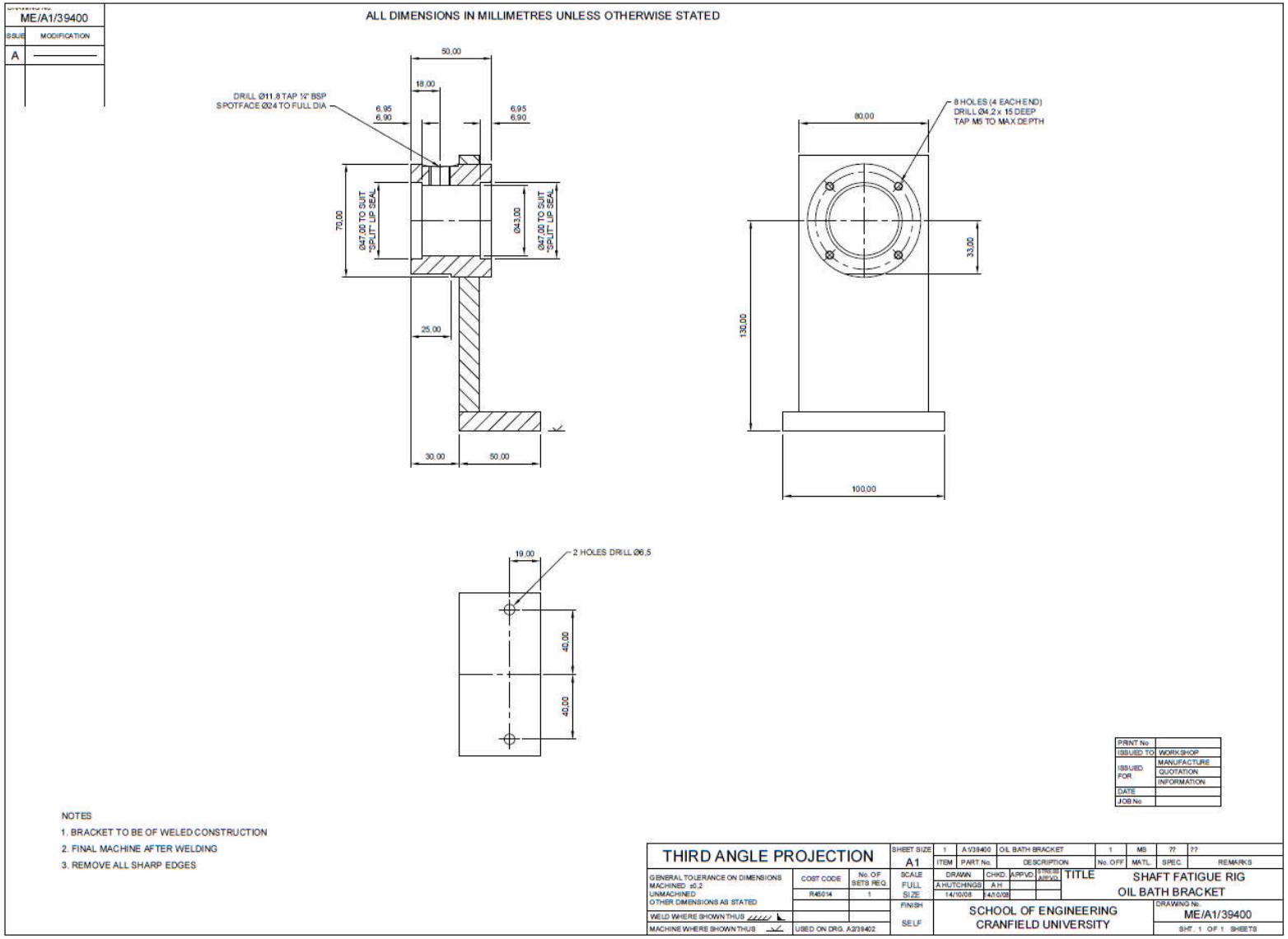
ME/A1/39400
ISSUE MODIFICATION
A
ALL DIMENSIONS IN MILLIMETRES UNLESS OTHERWISE STATED
50.00
18.00
DRILL Ø11.8 TAP ½" BSP
SPOTFACE Ø24 TO FULL DIA
6.95
6.90
6.95
6.90
70.00
Ø47.00 TO SUIT SPLIT LIP SEAL
Ø43.00
Ø47.00 TO SUIT SPLIT LIP SEAL
25.00
30.00
50.00
8 HOLES (4 EACH END)
DRILL Ø4.2 x 15 DEEP
TAP M5 TO MAX DEPTH
80.00
33.00
130.00
100.00
19.00
2 HOLES DRILL Ø6.5
40.00
40.00
PRINT No
ISSUED TO WORKSHOP
ISSUED FOR MANUFACTURE
QUOTATION
INFORMATION
DATE
JOB No
NOTES
1. BRACKET TO BE OF WELED CONSTRUCTION
2. FINAL MACHINE AFTER WELDING
3. REMOVE ALL SHARP EDGES
THIRD ANGLE PROJECTION
SHEET SIZE A1
1 A/139400 OIL BATH BRACKET 1 MS ?? ??
ITEM PART No. DESCRIPTION No. OFF MATL. SPEC. REMARKS
GENERAL TOLERANCE ON DIMENSIONS MACHINED ±0.2 UNMACHINED OTHER DIMENSIONS AS STATED
COST CODE R45014
No. OF SETS REQ. 1
SCALE FULL
SIZE
FINISH SELF
DRAWN A HUTCHINGS 14/10/08
CHKD. A H 14/10/08
APPVD.
DWG APPVD.
TITLE SHAFT FATIGUE RIG
OIL BATH BRACKET
WELD WHERE SHOWN THUS
MACHINE WHERE SHOWN THUS
USED ON DRG. A/239402
SCHOOL OF ENGINEERING
CRANFIELD UNIVERSITY
DRAWING No. ME/A1/39400
SHT. 1 OF 1 SHEETS